LUND UNIVERSITY
Faculty of Science

MASTER THESIS

Atmospheric Fate of Methyl Bromide

Author:
Lars Magnus T. JOELSSON

Supervisor:
Elna J. K. NILSSON
Department of Combustion Physics
LUND UNIVERSITY
Faculty of Engineering

Co-supervisor:
Matthew S. JOHNSON
Copenhagen Centre for
Atmospheric Research
UNIVERSITY OF COPENHAGEN
Department of Chemistry

March 29, 2012

Upptäckten av förtunningen av ozonlagret över Antarktis skakade världen även utanför de vetenskapliga kretsarna i början på 1980-talet. Läget ansågs så allvarligt att en lång lista av de antropogena ozonnedbrytande ämnena förbjöds under det internationella Montrealprotokollet. En åtgärd som verkar särskilt radikal i ljuset av de motstånd ett liknande avtal mött gällande de så kallade växthusgaserna. Ett av ämnena som bannlystes var CH_3Br. Till skillnad från de flesta övriga som nämns i dokumentet har dock CH_3Br betydande naturliga källor (haven och förbränning av biomassa för att nämna de två viktigaste). Dessa källor var vid Montrealprotokollets införande i samma storleksordning som de mänskliga utsläppen, idag dominerar de CH_3Br-budgeten. Montrealprotokollets framgång ledde till att frågan om ozonlagrets förtunnande som ett globalt miljöproblem närmast har skrivits av. Nya studier har dock visat att ozonlagret även över Arktis börjat förtunnas på ett liknande sätt. Detta tros ha en koppling till senaste tidens klimatförändring. Några av de mest kraftfulla ozonnedbrytarna är en familj radikaler som kallas BrO_x ($Br + BrO$), för vilka CH_3Br är den viktigaste källan i stratosfären.

På senare tid har kraftiga minskningar av kvicksilvernivåerna i atmosfären över Arktis observerats. Kvicksilvret tas istället upp i näringskedjan och utgör ett hot särskilt för djur i toppen av näringskedjan, såsom isbjörn. Br-radikaler misstänks ligga bakom även detta fenomen, vilket kallats *Atmospheric Mercury Depletion Events* i litteraturen. Att förbättra förståelsen för de processer som frisätter BrO_x från CH_3Br är därför viktigt för att förbättra förståelsen många delar av kemin i atmosfären.

Varje reservoar av ett särskilt ämne har en unik blandning av isotopsammansättningar. En process som fungerar som källa för ett ämne kan verka olika snabbt för molekyler med olika isotopsammansättningar, således med olika massa. En sådan effekt kallad *Kinetic Isotope Effect* (KIE) kan hjälpa till att spåra källan för en viss reservoar.

Den fotokemiska reaktorn vid *Copenhagen Centre for Atmospheric Research*, Köpenhamns universitet, har i denna studie används för att bestämma nya värden på hastighetskonstanterna $k_{(i)}$ för reaktionen:

$$CH_3Br + OH \longrightarrow \text{produkter} \tag{i}$$

och $k_{(ii)}$ för reaktionen:

$$CH_3Br + O(^1D) \longrightarrow \text{produkter}. \tag{ii}$$

Radikalerna ($O(^1D)$ och OH) framställdes i studien genom att fotolysera ozonmolekyler med UV-C-ljus. Oxidationsprocessen undersöktes genom att alternera korta fotolysperioder med mätningar av koncentrationen av de olika reaktanterna i cellen. Mätningarna urfördes med en Fourier Transfer infrarödspektrometer. Hastighetskonstanten $k_{(i)}$ bestämdes med *Relative-Rate*-metoden, vilket innebär att CH_3Br åtföljdes av och jämfördes med ett referensämne. Hastighetskonstanten $k_{(i)}$ bestämdes därför först som en faktor av hastighetskonstanten $k_{(iii)}$, som beskriver reaktionen:

$$\text{referens} + OH \longrightarrow \text{produkter}. \tag{iii}$$

Hastighetskonstanten $k_{(ii)}$ bestämdes med simuleringsprogrammet Kintecus®. En kinetisk justerades så att dess resultat överensstämmer med de uppmätta koncentrationer av CH_3Br. $k_{(i)}$ är enligt våra studier $(3.53 \pm 0.23) \times 10^{-14}{}^{\mathrm{cm}^3}/_{\mathrm{molecules}}$, vilket är högre än det för tillfället rekommenderade värdet. $k_{(ii)}$ visade sig vara i intervallet $(2.5 : 5.4) \times 10^{-10}{}^{\mathrm{cm}^3}/_{\mathrm{molecules}}$, även det högre än det enda tidigare värdet som har rapporterats. Atmosfäriska budgetmodeller kan därför behöva revideras för att erhålla bättre värden för koncentrationer på ämnen innehållande Br och även indirekt ämnen som påverkas av dessa. CH_3Br har två dominerande

isotopsammansättningar, nämligen $CH_3{}^{79}Br$ och $CH_3{}^{81}Br$. En möjlig *Kinetisk Isotopeffekt* för reaktionerna (i) och (ii) undersöktes och kvantifierades.Våra resultat tyder på att $KIE_{(i)}$ finns i intervallet 1:1.2. Reaktion (i) är därför antagligen snabbare för den lättare molekylen $CH_3{}^{79}Br$ än för den tyngre $CH_3{}^{81}Br$. Även om ett värde på $KIE_{(ii)}$ inte kunde slås fast, så gick ett troligt värde att härleda till $KIE_{(ii)} < 1$. Reaktion (ii) är därför i motsats till reaktion (i) förmodligen snabbare för $CH_3{}^{81}Br$ än för $CH_3{}^{79}Br$. Så vitt vi vet så är dessa de första försöken att bestämma $KIE_{(i)}$ och $KIE_{(ii)}$. Resultatet kan bidra till en bättre förståelse för atmosfäriska källor för Br-reservoarer.

The photochemical reactor in *Copenhagen Centre for Atmospheric Research*, University of Copenhagen, was used to determine new values for the rate constants $k_{(i)}$ and of the reaction:

$$CH_3Br + OH \longrightarrow \text{products} \tag{i}$$

and $k_{(ii)}$ for the reaction:

$$CH_3Br + O(^1D) \longrightarrow \text{products}. \tag{ii}$$

The radicals ($O(^1D)$ and OH) were produced by photolysis of ozone molecules with UV-C light. The oxidation process was monitored by alternate short photolysis periods and measurements of the concentrations of the different reactants in the cell. These measurements were conducted with a Fourier Transfer Infrared Spectrometer. To obtain concentrations from the IR spectra the iterative non linear least square fitting program MALT5 was used. The rate constant $k_{(i)}$ was determined with the *Relative Rate* method, meaning that CH_3Br was accompanied by and compared with a reference compound. The rate constant $k_{(i)}$ was therefore first obtained as a factor of the rate constant $k_{(iii)}$, describing the reaction

$$\text{reference} + OH \longrightarrow \text{products}. \tag{iii}$$

The rate constant $k_{(ii)}$ was determined with the simulation software Kintecus®. A kinetic model was first adjusted to fit measured reference compound concentration, whereupon $k_{(ii)}$ in the model was adjusted to fit measured CH_3Br concentrations. $k_{(i)}$ was found to be $(3.53 \pm 0.23) \times 10^{-14}{}^{\mathrm{cm}^3}/_{\mathrm{molecule\,s}}$, higher than the current recommended value. $k_{(ii)}$ was found to be in the range $(2.5 : 5.4) \times 10^{-10}{}^{\mathrm{cm}^3}/_{\mathrm{molecule\,s}}$, also higher than the only value previously stated in the literature. Atmospheric budget models might therefore have to be revised in order to give a better estimate of Br-containing compound concentrations and indirectly concentrations of all species affected by them. CH_3Br has two dominant isotope configurations, namely $CH_3{}^{79}Br$ and $CH_3{}^{81}Br$. A possible *Kinetic Isotope Effect* (KIE) for the reactions (i) and (ii) were examined and quantified by a method similar to the Relative Rate method described above. To quantify the amount of CH_3Br lost to reaction (i) in the system designed to seek $KIE_{(ii)}$, Kintecus® was employed. $KIE_{(i)}$ were found to be in the range 0.98:1.24. Reaction (i) is thus most likely faster for the lighter molecule $CH_3{}^{79}Br$ than the heavier $CH_3{}^{81}Br$. $KIE_{(ii)}$ could not be satisfyingly quantified, but was deduced to most likely be $KIE_{(ii)} < 1$. The reaction (ii) is therefore in contrast to reaction (i) faster for $CH_3{}^{81}Br$ than $CH_3{}^{79}Br$. To our knowledge, these are the first attempts to decide values for $KIE_{(i)}$ and $KIE_{(ii)}$. The results might contribute to a better understanding of the atmospheric sources of Br reservoirs.

Contents

List of Figures

List of Tables

List of Reactions

1. Introduction

> "Had industry used bromine instead of chlorine in the chemicals used in spray cans and as solvents and refrigerants, we would have had a catastrophic ozone hole everywhere and at all seasons by the mid 1970s. The impact on the chemistry of the atmosphere would have been profound, and the consequences for life on the surface of the planet would have been severe. We avoided such a fundamental change in Earth's chemical mode of operation by luck rather than foresight and planning."
>
> *(Paul J. Crutzen)*

Our sun emits electromagnetic radiation in a way that resembles a black body, meaning that the spectrum of light ranges over all possible wavelengths. In contrast to the visible light (the region with highest irradiance), UV radiation, which is of shorter wavelengths, carries such high amounts of energy that it causes damage to DNA molecules. Still, life on the surface of the earth is possible; as light with very short wavelengths ($\lambda \leq 242.3\,\text{nm}$) (Sander et al., 2011) travels down through the atmosphere most of its photons get absorbed by oxygen molecules. Each molecule will be split up, but instantly reformed again as the two oxygen atoms reunite (Chapman, 1930). The light is merely converted to heat. Rays with slightly longer wavelengths ($\lambda \leq 1180\,\text{nm}$) (Sander et al., 2011) will not, however, be filtered by the omnipresent oxygen, but by its a little more exotic cousin ozone (O_3). Ozone will, similarly to oxygen, be split up by the photons, into atomic (O) and molecular oxygen (O_2) and then rapidly recombined (Chapman, 1930). If the O atom is stolen by another body though, the cycle is interrupted and the ozone cannot reform. Even more troublesome from an ozone friendly point of view would be if the product from such a reaction would in turn react with an ozone molecule and thereby reform the original specie. A catalytic cycle would thus be established, where the catalyst itself would not be consumed in its destruction of ozone. Typically, Chlorine (Cl) and Chlorine oxide (ClO) could play the parts through the reactions (Seinfeld and Pandis, 2006):

$$\text{Cl} + \text{O}_3 \longrightarrow \text{ClO} + \text{O}_2 \tag{R 1a}$$

$$\text{ClO} + \text{O} \longrightarrow \text{Cl} + \text{O}_2. \tag{R 1b}$$

Cl and ClO (commonly referred to as ClO_x) will go on to deplete ozone molecules until they react with some other compound.

Free Cl radicals would not be abundant enough in the atmosphere for this to concern us if it had not been for the anthropogenic haloalkanes (Fahey and Hegglin, 2011). In the 1930's when the old toxic refrigerants, such as ammonia (NH_3) and sulfur dioxide (SO_2), were sought to be

replaced, compounds that were non-flammable, non-toxic, and in general chemically inactive were on the wish list. The idea arose to substitute the hydrogen atoms in a hydrocarbon with strong binding halogen atoms (fluorine, chlorine, bromine, iodine), such that an inert molecule meeting the criteria listed above, would be composed. Chlorine and fluorine turned out to be the most widely used choice, constituting a group of compounds named Chlorofluorcarbon (CFC). To illustrate the faith that was put to the safety of this family of chemicals it can be mentioned that the pioneer Thomas Midgley Jr., with risk for his own life and health, even blew out a candle light with a lungful of dichlorofluoromethane at the American Chemical Society in 1930 (Burton, 2000). The industry soon found a large array of applications for the CFC's and they were thus used too a large extent (Burton, 2000). When a great deficit of ozone over the Antarctic was discovered in the early 1980's it was soon connected to the emissions of CFC's (Fahey and Hegglin, 2011). The international political community acted fairly quickly and banned a long list of ozone depleting compounds in an international treaty, known as the Montreal Protocol, in 1990 (UNEP, 2000). Compared to one chlorine atom, one bromine atom is, similarly to reaction R 1, capable of destroying 40–100 times more ozone molecules (Brasseur and Holland, 1995). Clearly if brominated instead of chlorinated compounds were used to the same extent, the consequences would have been catastrophic. Being the biggest source of Br in the stratosphere (Fahey and Hegglin, 2011), the atmospheric fate of CH_3Br is thus important to investigate.

In the troposphere the most likely course for a CH_3Br molecule is to be oxidized by a hydroxyl radical (OH) (Hsu and Demore, 1994):

$$CH_3Br + OH \longrightarrow \text{products.} \qquad \text{(R 2)}$$

OH is formed by a reaction between atomic oxygen and water molecules (Seinfeld and Pandis, 2006). The stratosphere, on the other hand, is very dry and gets drier with altitude, meaning that OH concentrations will also drop with altitude (Sander et al., 2006). The CH_3Br molecule might then just as well snatch the atomic oxygen itself (Thompson and Ravishankara, 1993), especially as UV light is less attenuated for higher altitudes (Sander et al., 2006) and more atomic oxygen is therefore released. In this case, the atomic oxygen must be in the higher energy state $O(^1D)$, rather than its ground state $O(^3P)$. In other words, there is an ongoing race for CH_3Br between the OH and $O(^1D)$ radicals in the atmosphere, where OH makes a "clean sweep" in the troposphere but where $O(^1D)$ gains more and more possession the higher you go in the stratosphere. How much bromine that is found at a certain altitude, and subsequently how much ozone bromine is expected to deplete at that altitude, will therefore depend on the speed of these two reactions. Estimates of inorganic bromine concentrations in the stratosphere (e.g. Br and BrO) rely on these assumptions, since measurement coverage is quite patchy (Wayne, 1990). Now, the global budget calculations of CH_3Br do not sum up. 36.1 Gg/yr are missing (to be compared with the 42 Gg/yr CH_3Br that is produced in the ocean, which is the largest single source) (Montzka and Reimann, 2011). This can either be due to an underestimation of sources, overestimation of sinks or a combination of the two. To better determine the sinks could therefore help to solve this mystery. Since oxidation is the biggest atmospheric sink of CH_3Br, looking at reaction R 2 and R 3 is a good place to start. The speed of a reaction depends on the concentrations of the participating compounds and a rate constant k. For example, in the bimolecular reaction:

$$A + B \longrightarrow AB$$

the reaction speed is decided by:

$$\frac{d[\mathrm{AB}]}{dt} = k[\mathrm{A}][\mathrm{B}]. \tag{1.1}$$

To approximate concentrations of a compound, the rate constants for its source and sink reactions must therefore be known. The only study of the rate constant for

$$\mathrm{CH_3Br} + \mathrm{O(^1D)} \longrightarrow \text{products}, \tag{R 3}$$

which is an important source reaction for Br, listed in the literature (National Institute of Standards and Technology, 2012) is a study by Thompson and Ravishankara (1993). One reason for this deficit is the fact that it is difficult to produce large enough quantities of $\mathrm{O(^1D)}$. At the *Copenhagen Centre for Atmospheric Research* (CCAR) a photochemical reactor was constructed to offer favourable conditions for such experiments.

In this work, the photoreactor at CCAR is employed to obtain new estimates for the reaction rate constants of reaction R 3. In addition, the rate constant of the reaction R 2 will be sought. The measurements are conducted using infrared spectroscopy and the calculations of the reaction rate are performed using the relative rate method, where this is possible. A kinetic model is compiled and used in order to determine the reactions' rate constant where the relative rate method fails. The present work suggests that the reaction $R\,2$ has the reaction rate constant $k_{(\mathrm{R\,2})} = 3.53 \pm 0.23 \times 10^{-14}\mathrm{cm^3/molecules}$, which is slightly faster than the current literature value $k_{(\mathrm{R\,2})} = 3.0 \times 10^{-14}\mathrm{cm^3/molecules}$ (Atkinson et al., 2006). Also $k_{(\mathrm{R\,3})} = (2.5 : 5.4) \times 10^{-10}\mathrm{cm^3/molecules}$, is higher than the literature value $k_{(\mathrm{R\,3})} = (1.8 \pm 0.27) \times 10^{-10}\mathrm{cm^3/molecules}$ (Sander et al., 2011).

The speed of a chemical reaction can sometimes depend on the isotopes that participate in the reaction, a phenomenon called *Kinetic Isotope Effect* (KIE). Since certain reactions can be linked to certain sources of a compound, its isotopic composition in a reservoir can tell us something about the reservoir's origins. A good estimate of the Kinetic Isotope Effect can therefore be a useful tool for tracing the sources of a compound. The Br atom is curious in the sense that it has two almost equally abundant isotopes: ^{79}Br and ^{81}Br. In this thesis such an effect will be examined for both reactions R 2 and R 3. It will be shown that $\mathrm{KIE}_{(\mathrm{R\,2})}$ is in the range 1:1.2 and $\mathrm{KIE}_{(\mathrm{ii})} < 1$. This implies that reaction R 2 is most likely faster for the lighter molecule $\mathrm{CH_3}^{79}\mathrm{Br}$ than the heavier $\mathrm{CH_3}^{81}\mathrm{Br}$, while reaction R 3 instead is faster for $\mathrm{CH_3}^{81}\mathrm{Br}$ than $\mathrm{CH_3}^{79}\mathrm{Br}$. To our knowledge, these are the first attempts to decide values for $\mathrm{KIE}_{(\mathrm{R\,2})}$ and $\mathrm{KIE}_{(\mathrm{R\,3})}$.

In this thesis the reader will first be guided through ozone's crucial role in the atmosphere. $\mathrm{CH_3Br}$ will then be briefly introduced and described. We will look through the set of reactions expected to occur in the laboratory system and how the reactions studied in this work have been assessed previously. In the experimental part an overview of the entire experimental work is given, whereupon the individual parts such as laboratory set up, analysis and simulations are explained. Furthermore, the results are presented and discussed and some conclusive remarks are drawn.

2. Atmospheric chemistry

In this chapter relevant theoretical background for this work will be presented. Much of the reason why the reactions addressed in this study are interesting is due to their impact on ozone. Being the most important trace gas in the atmosphere, some facts about ozone will therefore be a good starting point for this chapter.

2.1. Ozone

2.1.1. Tropospheric ozone

If the reader were to take a stroll in summertime Los Angeles, the chances are that she would have her mood dampened a bit by a gloomy haze filling the valley. She can cleverly suspect that this phenomenon is somehow linked with the heavy traffic load of the city (CCME, n.d.). She might not guess however that this smog's main constituent is ozone (Seinfeld and Pandis, 2006), a term she has previously mostly encountered in alarming newspaper reports of high UV radiation levels. Looking out over the obscured Los Angeles skyline, she should be interested to learn that high concentrations of ozone like this are very likely to cause severe health problems to people exposed to them (Kunzli et al., 2003). Above this mist, in the free troposphere, there is a quite different view of the ozone molecule to be gained. Almost all of the trace gases in the higher troposphere have one common oxidant, namely the hydroxyl radical (OH) (Seinfeld and Pandis, 2006). Hydroxyl radicals are formed by photolysis of O_3 and subsequent reaction with water

$$O_3 + h\nu \longrightarrow O(^1D) + O_2 \tag{R 4}$$

$$O(^1D) + H_2O \longrightarrow OH + OH, \tag{R 5}$$

such that ozone plays a key part in the removal of both undesired pollutants and greenhouse gases in the troposphere. A wise man once described OH as the "garbage man" of the atmosphere, which is a quite helpful picture.

2.1.2. Stratospheric ozone

The Chapman cycle

At even higher altitudes, in the region of the atmosphere called the *stratosphere* (from 10 km – 15 km to 45 km – 55 km (Seinfeld and Pandis, 2006)), the main feature of ozone is found. And it lies hidden in the following four reactions, called the *Chapman cycle* (Chapman,

Table 2.1.: *Definitions of ultraviolet radiation used in this work*

UV-A	400 nm–315 nm
UV-B	315 nm–280 nm
UV-C	280 nm–100 nm

1930; Sander et al., 2011):

$$O_2 + h\nu(\lambda < 175\,\text{nm}) \longrightarrow O(^1D) + O(^3P) \quad \text{(R 6)}$$

$$O_2 + O(^1D) + M \longrightarrow O_3 + M \quad \text{(R 7)}$$

$$O_3 + h\nu(\lambda < 411\,\text{nm}) \longrightarrow O(^1D) + O_2 \quad \text{(R 4)}$$

$$O_3 + O(^3P) \longrightarrow O_2 + O_2 \quad \text{(R 8)}$$

When ozone and oxygen molecules absorb UV radiation by reactions R 4 and R 6, they hinder the UV rays in reaching the surface. Since both oxygen and ozone are more or less instantly reformed through reactions R 7 and R 8, their concentrations are virtually untouched by this bombardment from the sun. These species will thus constitute a kind of shield from UV radiation for the lower atmosphere. Without this shield, life as we know it would not be possible as UV radiation causes harm to DNA molecules. Another key role of ozone can be revealed giving reaction R 7 some extra attention. From an energy budget point of view, there seems to be something missing from the four reactions above. The photon brings in energy to split up the molecules in reactions R 4 and R 6, but when the same molecules are reformed via reaction R 7 this energy seems to have mysteriously vanished. To most people (except perhaps those with a degree in economics), this does not make sense. Luckily, this discrepancy is just due to sloppy writing. Reaction R 7 does actually include two steps. First, an intermediate high energy molecule is formed ($O_2 + O \longrightarrow O_3^*$). This intermediate state of the molecule is unstable and will fall apart unless it can lose its excess energy somehow. A collision with a third body M might do the job. The atmosphere's main constituents are N_2 and O_2, so one of these two would be the most likely object for such a collision. One of the reasons why N_2 and O_2 are so common is that they are both chemically inert species, and sure enough, they will remain their merry selves even after meeting O_3^*. So as a result of the collision, O_3^* will be relaxed to its stable state and the energy will merely be carried away by the third body, ending up as thermal energy. This is not only interesting as a mathematical exercise, but will have important consequences. In the troposphere most of the heat is generated by solar radiation absorbed and re-emitted by the surface. The heat is then distributed by vertical convection. In this way, the troposphere is on average warmest closest to the ground and cooler the higher you go. Now, as pointed out earlier not much UV radiation penetrates down to these lower parts of the atmosphere, meaning that the Chapman cycle will lack its driving factor. Higher up where less UV radiation has attenuated and the Chapman cycle will run more intensely, the heat generated by it will actually start to be seen on a thermometer, so to speak. At the same time you might not feel the heat from ground as much at this level. So, at a certain height temperature are steered by the Chapman cycle and beyond this point the temperature would actually start to increase for higher altitudes. This conditions defines the stratosphere. The verge between the troposphere and the stratosphere, marked by this shift in vertical temperature gradient, is called the *tropopause*. A tropospheric air parcel would have trouble crossing the tropopause since it would soon be cooler and therefore heavier than the surrounding air. So, the tropopause

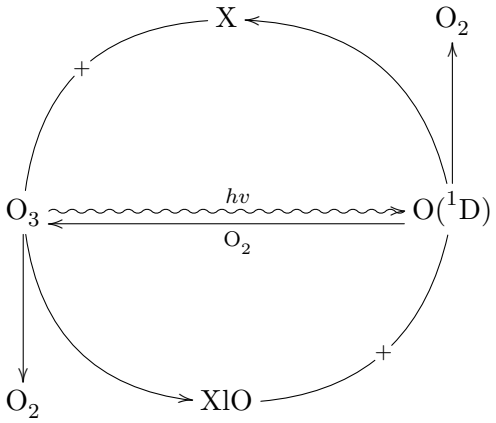

Figure 2.1.: *Chapman cycle and catalytic ozone destruction cycle*

functions as a lid on top of the troposphere, encapsulating the air below it. In conclusion, if we had no ozone, there would be no stratosphere, and the very structure of the atmosphere would be quite different. The inclusion of M in reaction R 7 also represents a pressure dependence of the reaction. From reactions R 4, R 6, R 7 and R 8, keeping in mind that pressure decreases with height while the incident UV radiation get more and more extinct as it travels down through the atmosphere, a peak of ozone production will occur at some level, namely around 40 km (Seinfeld and Pandis, 2006). The altitude with maximum ozone levels will vary both geographically and temporally. The layer is commonly referred to as the *ozone layer*. Ozone is also responsive to radiation with longer wavelengths, such as the radiation emitted by the surface of the earth. When radiation has been absorbed it is re-emitted back to the stratosphere, but then in any possible direction. In this way, portions of the heat radiation from earth are hindered in leaving the atmosphere, with an slight warming of the atmosphere as a result. This mechanism, known as the *Greenhouse effect* is almost general knowledge after the last decade's intense climate change debate. So, to complete this multifaceted picture of ozone, ozone does in addition belong to the Greenhouse gases (GHG).

Catalytic ozone destruction

Looking at reaction R 7, one can conclude that the rate limiting factor of the reaction is the supply of the free radical $O(^1D)$. Now, if $O(^1D)$ were tied up in different constellations instead, ozone could not be formed. Consequently, reaction R 4 would happily eat its way through the ozone stock. Since $O(^1D)$ is very reactive, this does happen to some extent. A radical X can intrude the Chapman cycle by the following generalized catalytic cycle:

$$X + O_3 \longrightarrow XO + O_2 \quad \text{(R 9a)}$$

$$XO + O \longrightarrow X + O_2 \quad \text{(R 9b)}$$

$$\text{Net: } O_3 + O \longrightarrow O_2 + O_2$$

see Figure 2.1. Here X is usually replaced with Cl, Br, OH or NO. The vast release of chlorofluorocarbon prior to the inuring of the Montreal Protocol injected substantial amounts of active Cl into the stratosphere, which had serious consequences for the ozone layer (Fahey and Hegglin, 2011). Molecule by molecule, Br is 40–100 more effective in destroying ozone than Cl (Brasseur

and Holland, 1995). So, even though chlorine is about 100 times as abundant in the atmosphere as bromine (Brasseur and Holland, 1995), the bromine burdens' effect on stratospheric ozone should still be the subject to some attention. The explanation for this asymmetry is as follows; most of the active chlorine in the stratosphere are actually unavailable for reactions with ozone, as they are tangled up in the stable reservoir species HCl and $ClONO_2$ (Seinfeld and Pandis, 2006). Their bromine counterparts HBr and $BrONO_2$, on the other hand, do not tie up bromine to the same degree. Why is this? While HCl is formed by the reaction $Cl + CH_4 \longrightarrow HCl + CH_3$ (Atkinson et al., 2006), the corresponding reaction $Br + CH_4 \longrightarrow HBr + CH_3$ is endothermic (consumes rather than gives away energy) and therefore virtually never occurs at atmospheric temperatures (Lorkovic et al., 2006). HBr is instead formed through a reaction with HO_2 (Atkinson et al., 2006; Bedjanian et al., 2001), of which stratospheric concentrations are substantially lower than those of CH_4 (Sander et al., 2006). Also HBr is removed by OH about 12 times faster than the removal of HCl by OH (Seinfeld and Pandis, 2006). Furthermore, $BrONO_2$ are like $ClONO_2$ removed primarily by photolysis, but the photolysis lifetime is estimated to be about 36 times shorter for $BrONO_2$ than for $ClONO_2$ (6 min compared to 10 h) (Seinfeld and Pandis, 2006). Thus, bromine will be both less likely to end up in inactive constellations (HBr, $BrONO_2$) and, if this would still be the case, much more likely to be released to its active shape again (Br, BrO).

2.1.3. The ozone hole

What happens when the mercy of reservoir species ceases can be studied wintertime over Antarctica. Due to topographical reasons the Antarctic stratosphere gets extremely cold, with temperatures well below −80 °C (15 km – 20 km) (Seinfeld and Pandis, 2006). When air is cooled it gradually loses its ability to hold water, so in these cold conditions even in the very dry stratosphere water starts to condense such that clouds can form. These clouds, called *Polar Stratospheric Clouds* (PSC) (Seinfeld and Pandis, 2006) or Mother-of-Pearl clouds, are a beautiful sight. From a molecular point of view they present a new playground; HCl is absorbed onto the crystals and suddenly, the otherwise hopeless reaction $HCl + ClONO_2 \longrightarrow Cl_2 + HNO_3$ is made possible (Seinfeld and Pandis, 2006). Active chlorine is thus released after photolysis of Cl_2 (Seinfeld and Pandis, 2006). In this way, chlorine is transferred from the reservoir species (HCl, $ClONO_2$) to the active forms (Cl, ClO). The mechanism results in an increased ozone depletion. The October average of total ozone poleward of 63°S has dropped about 37% from the years prior to ozone hole to today (Fahey and Hegglin, 2011). Even though emissions of most of the ozone depletion species has ceased, the values are not expected to recover before 2050 (Fahey and Hegglin, 2011). Paradoxically due to global warming has there even been indications that an ozone hole might be establishing also over the North pole (Manney et al., 2011). Cl is often used to explain this mechanism, but the reasoning is analogue for Br (Seinfeld and Pandis, 2006).

2.2. Atmospheric Mercury Depletion Events

Br is suspected to be involved in another process, even though more geographically confined still alarming in its own right. It concerns sudden drops of atmospheric Hg observed in the Arctic (Schroeder et al., 1998). The atmospheric mercury Hg^0 is deposited onto the snow, probably

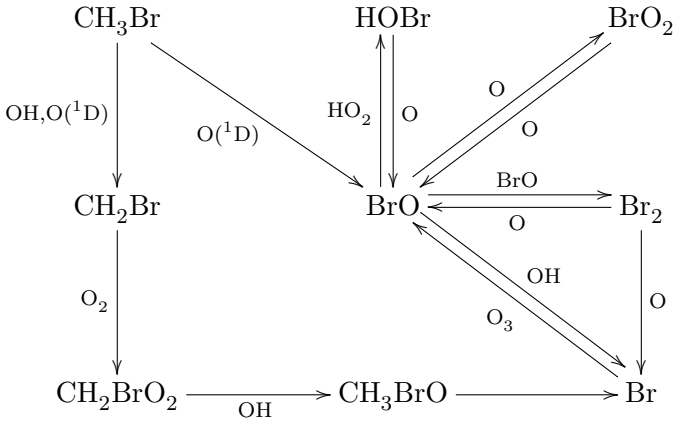

Figure 2.2.: *Oxidation chain of CH_3Br*

through reaction R 10 (Ebinghaus et al., 2004):

$$Hg^0 + BrO \longrightarrow HgO + Br. \qquad (R\,10)$$

Hg is taken up in the ecosystem and accumulates in the food chain. Hg levels in Northwest Greenland polar bears have increased greatly from supposed natural levels the last century (Dietz et al., 2011). The health effect for large animals like the polar bear is yet to be examined (Basu et al., 2009; Sonne et al., 2007).

2.3. CH_3Br

About a third of the Br atoms found in the stratosphere was transported there in the form of CH_3Br (Fahey and Hegglin, 2011). In contrast to many other molecules bringing up halogen[1] radicals to the stratosphere, the sources of CH_3Br has in addition to the anthropogenic part also an important natural contribution. Man-made CH_3Br is mostly used as a fumigant, though this burden has dropped dramatically in post-Montreal-protocol-period. Between 1996 and 1998, the source strength of fumigation in soils was in the range 28.1 Gg/yr – 55.6 Gg/yr, 2008 the value was estimated to be 4.6 Gg/yr – 9.0 Gg/yr (Montzka and Reimann, 2011). Natural CH_3Br are biologically produced in the oceans with a quite constant source strength of 42 Gg/yr and released by biomass burning with a source strength of 29 Gg/yr (Montzka and Reimann, 2011). According to Montzka and Reimann (2011), there is a 36.1 Gg/yr deficit in the global budget calculations. Br is a unusual in the sense that it has two almost equally abundant isotopes, such that CH_3Br have two dominating isotopic constellations, namely $CH_3{}^{79}Br$ and $CH_3{}^{81}Br$. These two are relatively easy to distinguish from one another in a IR spectrum and they are both included in the HITRAN molecular absorption database (Rothman, 2012). Properties of CH_3Br are tabulated in Table 2.2. The object reactions R 2 and R 3 are the starting points of an oxidation chain, see Figure 2.2. To see the full reactions see appendix E.

[1] A group of elements, all with 7 electrons in the outermost shell, including fluorine, chlorine, bromine, iodine and astatine. A single halogen atom will therefore be a radical by definition.

Table 2.2.: *Properties of CH_3Br at standard atmospheric pressure 1000 hPa*

Molar mass	94.939 g/mol[a]
Density	4.064 g/L (15 °C)[b]
Melting point	179.47 K[c]
Boiling point	276.6 K[d]
Vapour pressure	1900 hPa (20 °C)[b]
Atmospheric lifetime	0.7 years[e]
100-year Global Warming Potential	5[e]
Ozone Depletion Potential	0.39[f]
Global annual mean surface mixing ratio	7.3–7.5 ppt (2008) [g]

[a] National Institute of Standards and Technology (2011)
[b] *Air Liquide Gas Encyclopedia* (2009)
[c] Egan and Kemp (1938)
[d] *Research Chemicals Catalog* (1990)
[e] Solomon et al. (2007)
[f] Ko et al. (1998)
[g] Montzka and Reimann (2011)

2.3.1. Previous works

The only previous attempt to determine $k_{(R\,3)}$ listed in the literature (National Institute of Standards and Technology, 2012) was made by Thompson and Ravishankara (1993) as part of a larger study of $O(^1D)$ reactions with bromocarbons. The principle behind research was to produce $O(^1D)$ radicals, let them react with the bromocarbon molecule (R) and then measure the temporal evolution of the $O(^3P)$ concentration. $O(^3P)$ are produced by quenching, f.x.

$$CH_3Br + O(^1D) \longrightarrow CH_3Br + O(^3P) \qquad (R\,11)$$

Comparative measurements were made where the $O(^1D)$ radicals are just let out in a sea of N_2 and consequently all get quenched. Thompson and Ravishankara (1993) found the value to be $k_{(R\,3)}(T = 298\,K) = (1.78 \pm 0.08) \times 10^{-10}$. Sander et al. (2011) revaluates this number to $k_{(R\,3)}(T = 298\,K) = (1.8 \pm 0.27) \times 10^{-10}$. National Institute of Standards and Technology (2012) lists a number of independent values of $k_{(R\,2)}$ from publications published between 1965–2001. To these, an unpublished study by Nilsson, Joelsson, Johnson and Nielsen (n.d.), can be added. The values of $k_{(R\,2)}$ at $T = 298\,K$ range from $4.9 \times 10^{-14}\,cm^3/molecule\,s$ to $2.8 \times 10^{-14}\,cm^3/molecule\,s$. The studies are presented in Table 2.3 and in Figure 2.3.

Table 2.3.: *Present and previous works: $CH_3Br + OH \longrightarrow H_2O + CH_2Br$,*

Study	$k(T = 298\,\mathrm{K})$ $\left(\mathrm{cm}^3/\mathrm{molecule\,s}\right)$
Present work	$(3.53 \pm 0.23) \times 10^{-14}$ [a]
Review	
Sander et al. (2011)	$(3.0 \pm 0.3) \times 10^{-14}$
Atkinson et al. (2006)	2.9×10^{-14}
Experiment	
Nilsson, Joelsson, Johnson and Nielsen (n.d.)	$(4.9 \pm 0.5) \times 10^{-14}$ [b]
Hsu and Demore (1994)	2.8×10^{-14} [a]
Chichinin et al. (1994)	$(3.27 \pm 0.50) \times 10^{-14}$ [c]
Zhang et al. (1992)	$(3.08 \pm 0.46) \times 10^{-14}$ [d]
Mellouki et al. (1992)	2.96×10^{-14} [e]
Howard and Evenson (1976)	$(3.50 \pm 0.8) \times 10^{-14}$ [f]
Davis et al. (1976)	$(4.14 \pm 0.43) \times 10^{-14}$ [d]
Theory	
Chiorboli et al. (1993)	4.90×10^{-14}
Cohen and Benson (1987)	4.06×10^{-14}

[a] Relativ Rate
[b] Pulse Radiolysis -Kinetic Spectroscopy
[c] Discharge electron paramagnetic resonance
[d] Flash Photolysis -Resonance Fluorescence
[e] Laser Photolysis -laser induced fluorescence
[f] Discharge Flow -Laser Magnetic Resonance

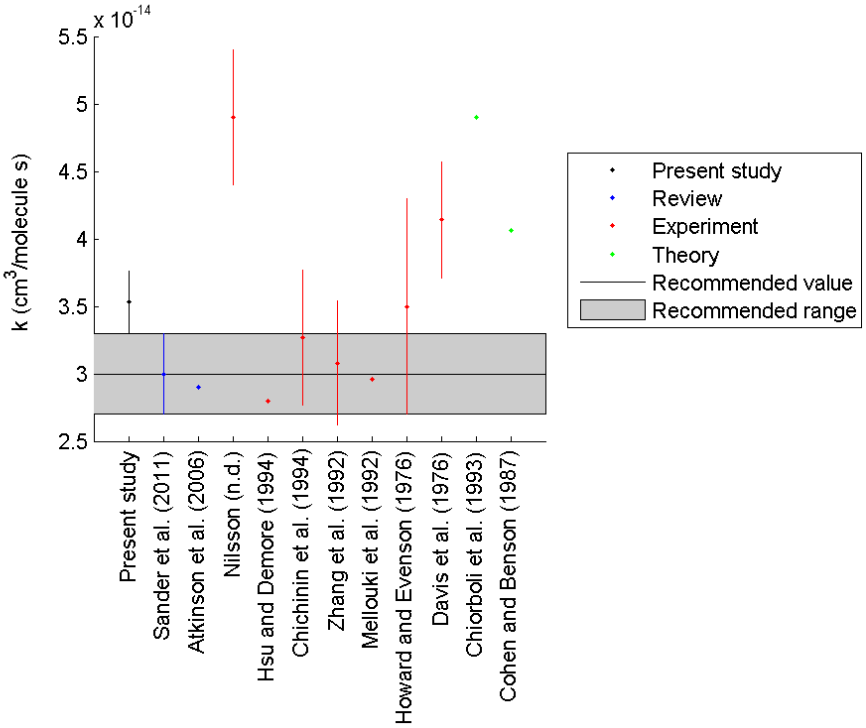

Figure 2.3.: *Comparison: present and previous works*

3. Method

In this chapter an overview of the entire method will be presented to give an idea how the different parts of the method are connected. Each part will then be described in higher detail. Last, an example of the entire procedure will be given.

3.1. Overview of the methods

The experiments were carried out in the photochemical reactor at Copenhagen Centre of Atmospheric Research. The reactor is described in detail in section 3.3. The objective of a typical experiment is to investigate the reaction rate k_A for a reaction A. The reaction A is generally the oxidation of an object compound, e.g. CH_3Br. Either $O(^1D)$- or OH-radicals are used as oxidants:

$$X + OH \longrightarrow \text{products} \tag{R 12}$$

$$X + O(^1D) \longrightarrow \text{products} \tag{R 13}$$

where X is the object compound. In order to obtain k_A, the relative rate method is utilized, see section 3.7.1. Thus, the object compound will be accompanied by a certain reference molecule in the experiments, see Table 3.1. The reference molecule is chosen so that its reaction rate corresponding to k_A is sufficiently close to k_A and well determined in the literature. Each test will therefore have a specific gas mix, including an object compound, a reference compound, O_3 and in case of a OH-experiment, water vapour introduced in the reaction chamber. A *Fourier Transform Infrared Interferometer* (FTIR), see section 3.4, is used to record an infrared spectrum of the chamber. The spectrum functions as a snapshot of the the compounds present, with each constituent leaving an unique absorption "fingerprint" in the spectrum. A set of Hg-lamps, which emit light in the UV-C region, are employed to photodissociate O_3. The photolysis is done in short time steps which transfers a small portion of O_3 to radicals enabling reactions R 12 and R 13. Spectra are recorded after each step, until about 80% of the initial concentration of O_3 is consumed. This way, the development of compound concentrations due to radical reactions is recorded as a time series of spectra. The experiment procedure is described more carefully in section 3.5. The analyses of the spectra are performed with the spectrum simulation program MALT5 (Griffith, 2008), described in section 3.6. Results from MALT5 analysis is then used in calculating Relative Rates and Kinetic Isotope Effects; the procedure is described in section 3.7. Due to the inevitable presence of water vapour in the reaction cell, there always will be a competition between reactions R 12 and R 13. To determine which of these that dominates, a model of chemical kinetics for the whole experimental system is run in the software Kintecus®, see section 3.8. From the model runs the fraction of loss of the reactants due to each of these reactions can be obtained. The model is included in appendix E.

3.2. Experimental requirements

To our knowledge the rate constant for reaction R 3 has been previously estimated only once (Thompson and Ravishankara, 1993). This is probably due the difficulties these experiments present. $O(^1D)$ is obtained by photolysis of O_3 (see reaction R 4) with light of wavelengths shorter than 320 nm (Seinfeld and Pandis, 2006). Firstly, the light source must be shielded from the ozone, such that no hot surfaces do initiate unwanted chemistry. Secondly, the cell is preferably large; a low surface to volume ratio keeps down the influence of the gas interaction with the walls. Finally, $O(^1D)$ is very reactive towards H_2O, forming strongly oxidizing OH radicals. For many compounds, there is a race between the reactions R 12 and R 13, so to be able to measure the reaction rate of one of them, its reaction rate must be much faster than the other. The partition of reactions R 12 and R 13 in the experiments are determined by the O_3 to H_2O ratio; a low water concentration will promote reaction R 13 in favour of reaction R 12. Now, it is very difficult to get a cell absolutely dry; H_2O and consequently OH will thus always be present in any $O(^1D)$ experiment. The solution is to produce a lot of $O(^1D)$, which means to fill a cell with high concentrations of ozone and then strongly illuminate a large part of its volume. A transparent cell surrounded by lamps could meets all the above mentioned criteria. The problem is that very few types of useful materials are transparent for that short wave length of light. The photoreactor at CCAR (Nilsson et al., 2009) meet these requirements.

3.3. Experimental setup

The photoreactor at CCAR is described in detail in (Nilsson et al., 2009). The cylindrical 101.4 L cell is constructed by 1 cm thick quartz glass, indeed transparent down to 190 nm. The possibilities to make high quality $O(^1D)$ experiments at CCAR are therefore excellent. An overview of the photoreactor is shown in Figure 3.1. The cylinder is 2 m long with an inner diameter 250 mm and a 10 mm thick wall, making a total volume of 101.4 L. The cylinder is surrounded by 16 58 W UV-C lamp. The UV-C lamps emit strongly in a narrow Hg line at 254 nm; the spectrum along with transmission of the cell is shown in Figure 3.2. The temperature of the system is controlled by a fan and a heat exchanger and insulated with polyurethane. When the lamps are turned on there is a small temporary increase in temperature.

3.3.1. Radical generation

The radicals used in the experiments all are made from O_3. The O_3 is generated by a ozone generator (Model AC-20, O3 Technology), whereupon ozone enriched (20 %) oxygen gas from the ozone generator is pumped through a glass flask containing silica gel, Figure 3.3. The flask is cooled with a mix of dry ice and ethanol, enabling it to cool to a minimum of $-78.5\,^{\circ}C$. The ozone is trapped in the cool silica gel and takes on a beautiful dark purple colour. The flask is then slowly warmed to room temperature and the ozone escapes into the cell.

3.4. Fourier Transform Infrared Spectroscopy

To measure the concentrations of the different compounds in the cell a Bruker IFS 66v/S spectrometer is employed. A beam from light source resembling a black radiator is split up by half transparent mirrors into two separate but identical beams. The path length of one of

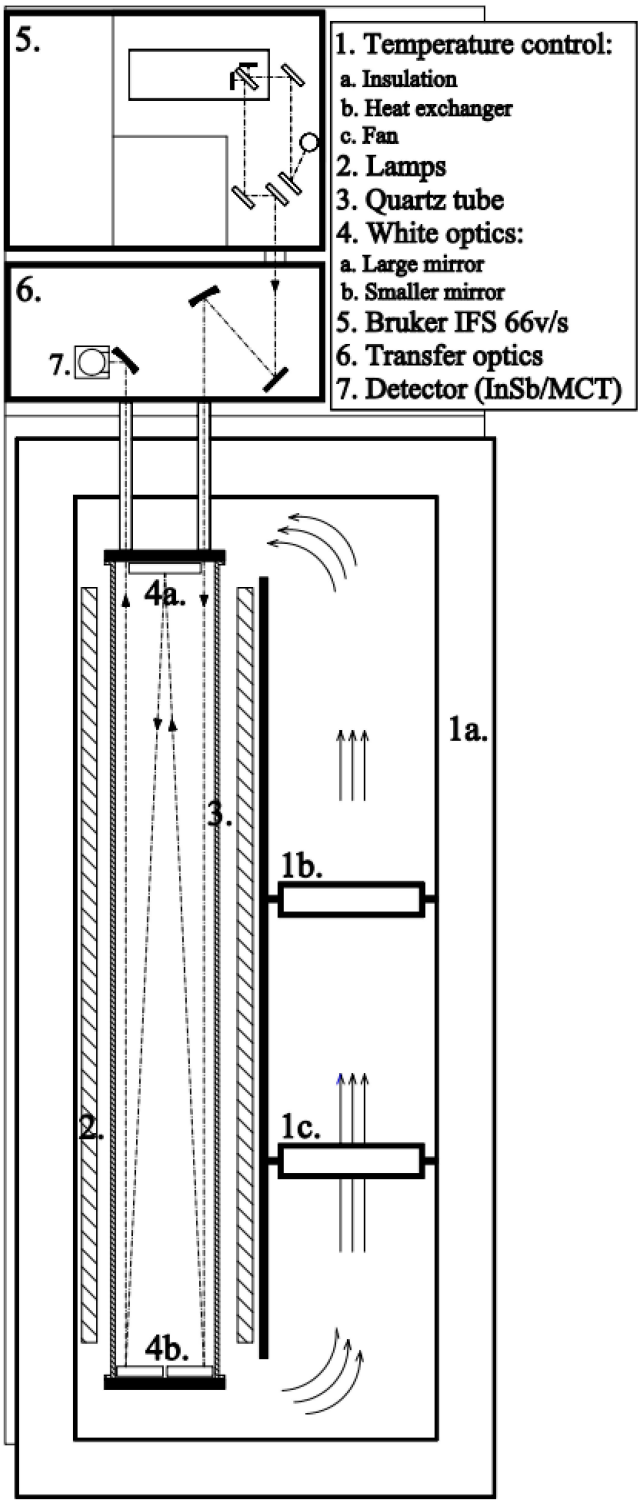

Figure 3.1.: *A sketch over the photochemical reactor, taken from Nilsson et al. (2009)*

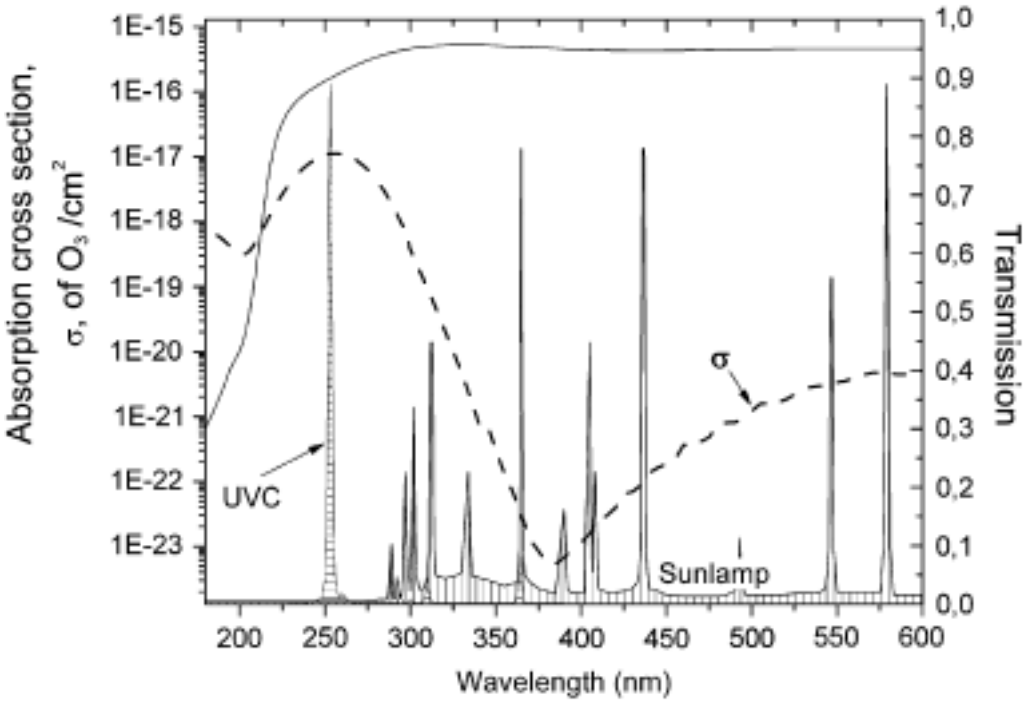

Figure 3.2.: *Absorption cross-section of ozone (dashed). The horizontally hatched area represents the UV-C lamps, photolysing ozone in the Hartley band giving $O(^1D)$. The vertically hatched area is the sun lamps which photolyse ozone in the Chappuis band giving $O(^3P)$. Full drawn line is the transmission of the quarts chamber. Figure and caption are taken from Nilsson et al. (2009)*

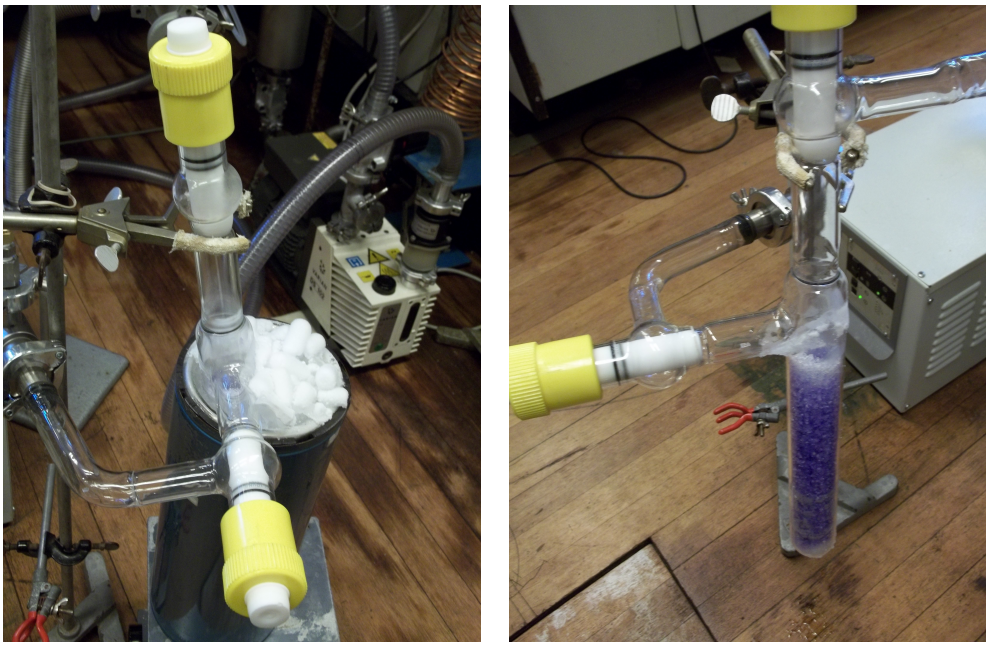

(a) Cooling with dry ice **(b)** Ozone ready

Figure 3.3.: *Ozone cold trap*

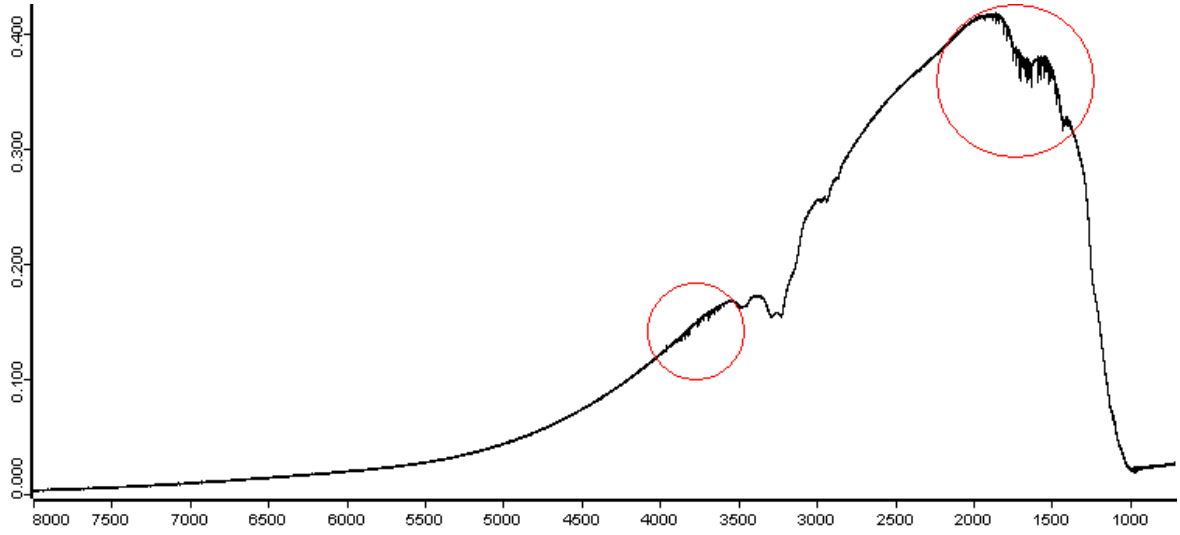

(a) Empty cell, traces of water vapour are encircled

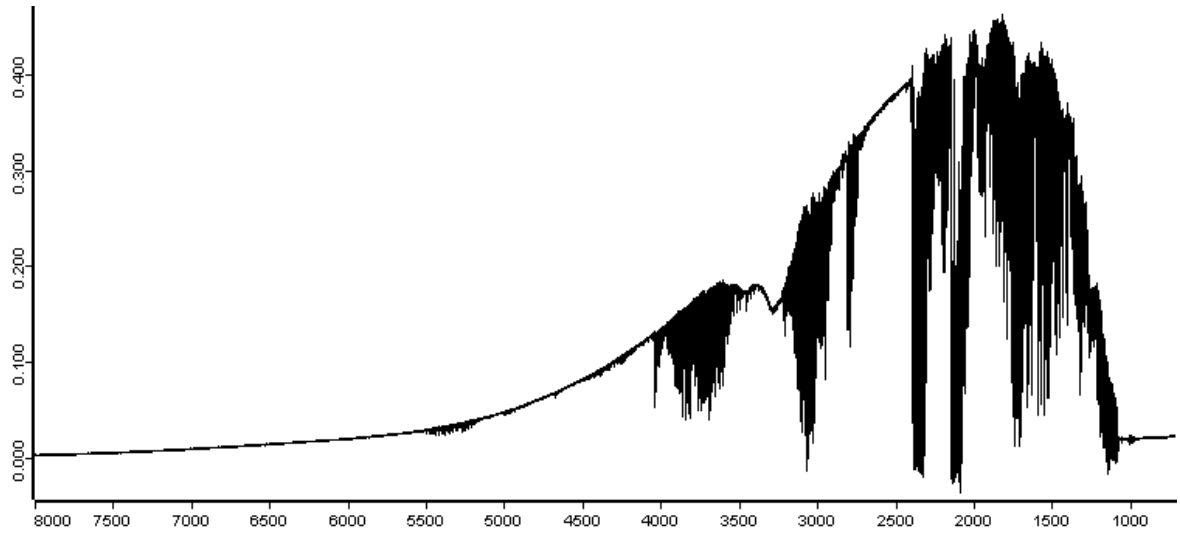

(b) Experiment 37, CH_3Br, CH_4 and O_3 are inserted

Figure 3.4.: *IR spectra of the cell, intensity of light is drawn on the ordinate, the wave number [cm^{-1}] is drawn on the abscissa*

the beams is fixed, while the other one's path length is shortened and prolonged by a moving mirror. This way, when the beams are re-combined, interference will create beat frequencies. The beam will then pass through some transfer optics to ensure the beam will have the right angle to enter the cell. Molecules rotate and vibrate in different manners, but curiously these inner movements cannot happen at any chosen intensity but only at well defined energy levels. Molecules in the cell will therefore pick up photons with frequencies which will correspond to an energy a molecule will need to change its energy to a higher level. Some frequencies in the light will therefore be weakening. Finally, the light which now contains information is collected by the detector, which throughout these experiments was a MCT-detector. Each output spectrum consists of 32 co-added spectra with a resolution of $0.125\,\mathrm{cm}^{-1}$. Examples of spectra are shown in Figure 3.4.

3.5. Experiment procedure

Each kinetic experiment begins by taking a spectrum of an empty cell, see Figure 3.4a, partly to make sure that no there is no contamination in the cell and partly to use as a background for the analysis. The background spectrum will be subtracted from the other spectra of the experiment. Some contaminations such as H_2O and CO_2, which sometimes can reside in the spectrometer rather than in the cell, will this way be cancelled and cause no further problem for the analysis. The cell will at this point have been properly vacuum pumped, preferably over night. The different compounds are first let into a vacuum pumped stainless steel gas line which is easily connected to the specific gas flask or finger bottle. The amounts are controlled by a small control volume in the gas line connected to a pressure gauge. From this control volume the gas is then flushed into to cell with N_2 via a Teflon tube. The concentration in the cell should not be too high such that the main peaks in the IR spectrum are saturated, yet high enough to get a good signal-to-noise-ratio. Around 2/3 of saturation level is sufficient. The cell is sometimes left to rest for some time before the kinetic experiment is initiated to let the system reach phase equilibrium, see Table A.2. The concentrations of the different species are monitored with the spectrometer to see whether the concentrations are stable. Ozone is prepared as described in section 3.3.1, and introduced directly into the cell via a Teflon tube, such that reactions with tube walls are minimized. This is usually done before, but sometimes after, the resting of the cell. When the mix is ready, the cell is filled with bath gas to reach the desired pressure (Table 3.1). Experiments are as a general rule preferably conducted at condition resembling those in the atmosphere, so for the OH experiments, pressures just below 1000 mbar are used. For the $O(^1D)$ experiments, on the other hand, the reaction:

$$O(^1D) + M \longrightarrow O(^3P) \qquad \text{(R 14)}$$

called quenching consumes $O(^1D)$-radicals such that the efficiency of reaction R 13 declines. Reducing quenching of oxygen atoms via reaction R 14 is done by keeping the pressure low, either around 50 mbar or without additional bath gas resulting in a pressure around 2 mbar. Too low a pressure might increase the interaction with the wall, thus are most $O(^1D)$ experiments conducted at around 50 mbar. A spectrum of the cell is taken as a starting point for the experiment. The lamps are turned on for a short time to initiate radical formation, via reactions R 4 and R 5, subsequent oxidation of the species in the cell. A spectrum of the cell will be taken and the lamps will again be turned on. This is repeated until only about 20% of the initial concentration of ozone is left. The patterns for the photolysis steps are tabulated in Table C.1.

Table 3.1.: *Experiment setup information (in the order they were conducted): type, reference compound, total pressure and temporal duration, all experiments were conducted at T=298 K*

Experiment	Type	Reference	Total pressure (mbar)	Duration (HH:MM)
1	Stability		1000	01:16
2	Photolysis		1000	00:55
3	Stability	CH_4,CH_3OH,N_2O [a]	1000	01:16
4	Photolysis	CH_4,CH_3OH,N_2O [a]	1000	01:02
5	Stability	(O_3)	1000	00:35
6	Photolysis	(O_3)	1000	00:32
7	OH	CH_4	1000	01:52
8	OH	CH_4	1000	01:21
9	$O(^1D)$	CH_4	2	01:44
10	$O(^1D)$	CH_4	2	01:22
11	OH	CH_4	1000	01:25
12	$O(^1D)$	CH_4	50	01:36
13	Stability		200	02:18
14	Dilution		200	01:12
15	Photolysis		200	00:54
16	Stability		200	18:22
17	Stability	CH_4	200	02:40
18	Dilution	CH_4	200	00:53
19	Stability	C_2H_6	200	02:34
20	Dilution	C_2H_6	200	01:27
21	Photolysis	C_2H_6	200	00:16
22	Stability	CH_4	200	64:39
23	Photolysis	CH_4	200	00:28
24	Dilution	CH_4	200	00:30
25	OH	CH_4	1000	01:03
26	OH	C_2H_6	1000	01:20
27	OH	C_2H_6	1000	01:20
28	OH	CH_4	1000	01:17
29	$O(^1D)$	CH_4	50	00:39
30	$O(^1D)$	CH_4	50	00:50
31	$O(^1D)$	CH_4	50	00:22

[a] References N_2O and CH_3OH was used in experiments finally excluded from this report

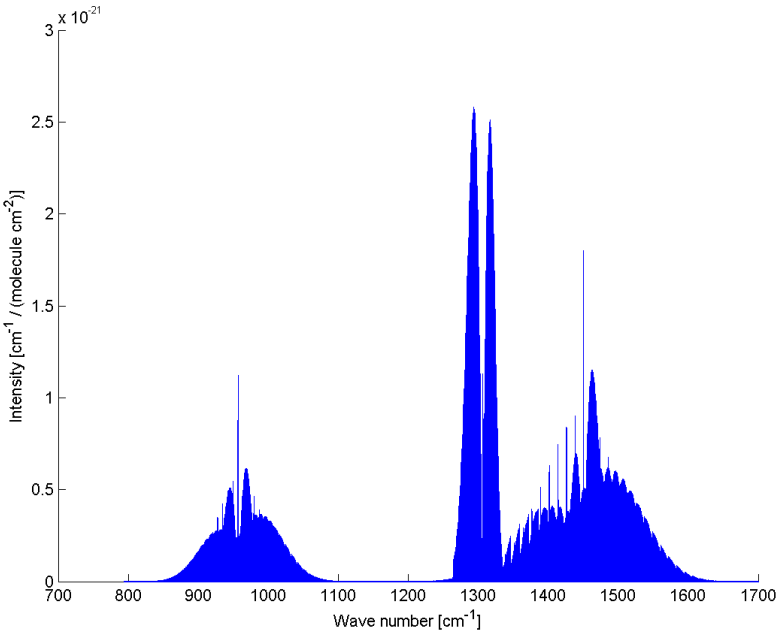

Figure 3.5.: *Example of HITRAN line by line cross sections, $CH_3{}^{79}Br$*

A list of the experiments conducted throughout the study is presented in Table 3.1. Prior to the kinetic experiments the stability towards "time", photolysis, ozone and the other constituents of the gas mix are tested for each compound. The details of these tests are described in appendix A. To verify a linear relationship between concentrations and spectral peaks, dilution experiments are performed, see appendix B. Additional experiments were conducted with CH_3OH and N_2O were conducted, but are not included in this report. The CH_3OH experiments are rejected due to analysis problems of CH_3OH and/or unknown chemistry in the systems. N_2O is a common reference compound in studies of $O(^1D)$-reactions but, since no pure $O(^1D)$ system was possible to setup a model over the kinetic system is required. No such model scheme has been developed thus far. All experiments were conducted at $T = 298\,\mathrm{K}$.

3.6. Analysis

Spectra analysis were performed by the iterative non linear least squares fitting program MALT5 (Griffith, 2008). The program uses a set of reference spectra of the compounds which are believed to constitute a measured spectrum to synthesize a simulated spectrum. The amplitudes of the reference spectra are changed to resemble the measured spectrum as closely as possible. When the fit is optimized the amplitudes of the reference spectra correspond to concentrations of the corresponding species residing in the cell for the time of the spectrum. The reference spectra are either from the HITRAN database (Rothman, 2012) (H_2O, CO_2, O_3, N_2O, CO, CH_4, HNO_3, C_2H_6, CH_3Br, $CH_3{}^{79}Br$ and $CH_3{}^{81}Br$). The HITRAN database is a collection of line by line cross sections. For each compound a small part of the full measured spectrum are selected, see Table 3.2. Error estimates of the fits are obtained automatically.

Table 3.2.: *Regions for analysis*

Compound	Range (cm^{-1})
H_2O	1270–1390
CO_2	2140–2300
O_3	2680–2820
O_3 alt.	2140–2300
N_2O	2140–2300
CO	2140–2300
CH_4	1270–1390
HNO_3	1270–1390
C_2H_6	2800–2995
CH_3Br	1270–1390

3.7. Kinetics

3.7.1. Relative Rate method

An established method to measure reaction rates is the Relative Rate method (henceforth sometimes abbreviated as RR). A benefit of the method is that the exact irradiance of the lamps and photolysis times do not necessarily have to be known, as both these factors will affect the object and the reference compound equally. A drawback is that the result will rely on the literature value of the reference reaction.

The theory behind the Relative Rate method can be described as follows. If the speed of reaction R 2, similar to equation (1.1), is considered:

$$\frac{d[CH_3Br]}{dt} = -k_{(R\,2)}[CH_3Br][OH]. \tag{3.1}$$

By first solving the differential equation (3.1), $k_{(R\,2)}$ can be solved for as:

$$k_{(R\,2)} = \frac{\ln\left({}^{[CH_3Br]_{t=0}}/_{[CH_3Br]_t}\right)}{[OH] \cdot t}. \tag{3.2}$$

The concentration of CH_3Br can be quite easly measured, whereas the concentration of the shortlived OH is more difficult to measure. Thus, equation (3.2) has two unknowns. Now, with a reference compound, a new equation can be added, e.g. one similar to equation (3.2), describing reaction:

$$CH_4 + OH \longrightarrow H_2O + CH_3, \tag{R 15}$$

namely

$$k_{(R\,15)} = \frac{\ln\left({}^{[CH_4]_{t=0}}/_{[CH_4]_t}\right)}{[OH] \cdot t}, \tag{3.3}$$

where $k_{(R\,15)}$ is known. If equations (3.2) and (3.3) are combined and $k_{(R\,2)}$ is solved for:

$$k_{(R\,2)} = \frac{\ln\left({}^{[CH_3Br]_{t=0}}/_{[CH_3Br]_t}\right)}{\ln\left({}^{[CH_4]_{t=0}}/_{[CH_4]_t}\right)} \cdot k_{(R\,15)} \tag{3.4}$$

is obtained. Generally, the data should thus obey:

$$\ln\left(\frac{[\text{object}]_{t=0}}{[\text{object}]_t}\right) = \frac{k_{\text{obj}}}{k_{\text{ref}}} \ln\left(\frac{[\text{reference}]_{t=0}}{[\text{reference}]_t}\right) \tag{3.5}$$

where $[\text{object}]_{t=0}$, $[\text{object}]_t$, $[\text{reference}]_{t=0}$ and $[\text{reference}]_t$ are the concentrations of the object and the reference compound at times $t = 0$ and t, k_{obj} and k_{ref} are the rate constants for the object and reference reactions respectively. A straight line is fitted to the measured data points using a linear weighted total least squares fit algorithm (Krystek and Anton, 2007) by which also error estimates are given. The slope of the curve will then correspond to $\frac{k_{\text{obj}}}{k_{\text{ref}}}$. If instability occurs it will be most apparent early in the experiments and will be visible as some of the first points will deviate from a straight line connecting later data points. Also in the end of the experiment deviations from the linearity can occur as secondary chemistry begins to have some significance and distorts the results. Points can be discarded for these reasons, especially if stability tests show significant instability in the test systems. Only points in the linear regions of the plots are used and these are manually chosen by examining the relative rate plots. The discarded points are tabulated in Table C.2. A weighted mean $\bar{X} \pm \sigma_{\bar{X}}$ of the experiment results is calculated as:

$$\bar{X} = \frac{\sum_{i=1}^{k} {}^{X_i}/_{\sigma_i^2}}{\sum_{i=1}^{k} {}^{1}/_{\sigma_i^2}}, \sigma_{\bar{X}} = \sqrt{\frac{\sum_{i=1}^{k} 1}{\sum_{i=1}^{k} {}^{1}/_{\sigma_i^2}}} \tag{3.6}$$

where X_i represent the measured values and σ_i their uncertainty. The relative rate method can strictly speaking be used only if the significant loss of reactants is the studied reaction only. While this very well might be the case for the OH studies, the $O(^1D)$ system will always be affected by OH reactions. The combination of the two reactions is linear:

$$\text{RR}_{\text{meas}} = c \times \text{RR}_{\text{OH}} + (1 - c) \times \text{RR}_{\text{O}(^1\text{D})} \tag{3.7}$$

where RR_{meas}, RR_{OH} and $\text{RR}_{\text{O}(^1\text{D})}$ are the measured relative reaction rate and the rates due to OH and $O(^1D)$ correspondingly, c the fraction reactant loss by OH. Since the OH reaction strongly overpowers the $O(^1D)$ reaction in the OH experiments the RR_{OH} obtained in this study can safely be used. For the $O(^1D)$ experiments instead the Kintecus® software was utilized, see section 3.8.

3.7.2. Chamber chemistry

When the reaction chamber is filled with the experiment gas mix and the UV-C lamps (with a strong peak at $\lambda = 254\,\text{nm}$) are turned on, a chain of reactions will take place. What kick starts this reaction chain is reaction R 4:

$$O_3 + h\nu(\lambda{=}254\,\text{nm}) \longrightarrow O(^1D) + O_2 \tag{R 4}$$

$O(^1D)$ is extremely reactive and will hasten to find a reaction partner. If water is present in the chamber, and it always is no matter how hard we are trying to get rid of it, reaction R 5 is a very likely fate for the $O(^1D)$:

$$O(^1D) + H_2O \longrightarrow OH + OH \tag{R 5}$$

Table 3.3.: *Literature values of the rate constants for the reactions of interest for this thesis, all at 298 K, values taken from Sander et al. (2011) except where noted otherwise*

Number	Reaction	k ($^{cm^3}/_{molecule\,s}$)
R 2	$CH_3Br + OH \longrightarrow$ products	$(3.0 \pm 0.3) \times 10^{-14}$
		$(4.9 \pm 0.5) \times 10^{-14}$ [a]
R 3	$CH_3Br + O(^1D) \longrightarrow$ products	$(1.8 \pm 0.27) \times 10^{-10}$
R 15	$CH_4 + OH \longrightarrow CH_3 + H_2O$	$(6.3 \pm 0.6) \times 10^{-15}$
R 16	$CH_4 + O(^1D) \longrightarrow$ products	$(1.75 \pm 0.26) \times 10^{-10}$
R 18	$C_2H_6 + OH \longrightarrow H_2O + C_2H_5$	$(2.5 \pm 0.2) \times 10^{-13}$

[a] Nilsson, Joelsson, Johnson and Nielsen (n.d.)

$O(^1D)$ might also react with whatever compounds inserted into the cell. In case of the object compound this reaction read:

$$CH_3Br + O(^1D) \longrightarrow \text{products} \tag{R 3}$$

Whereas, the reactions involving the reference compounds read:

$$CH_4 + O(^1D) \longrightarrow \text{products} \tag{R 16}$$

$$C_2H_6 + O(^1D) \longrightarrow \text{products} \tag{R 17}$$

Products of reaction R 3 include BrO and OH, which both enter catalytic cycles, previously described in reaction R 9, and CH_3 which will be further oxidized. The reactions R 3, R 16 and R 17 will get competition from corresponding reactions with OH:

$$CH_3Br + OH \longrightarrow \text{products} \tag{R 2}$$

$$CH_4 + OH \longrightarrow H_2O + CH_3 \tag{R 15}$$

$$C_2H_6 + OH \longrightarrow H_2O + C_2H_5 \tag{R 18}$$

Determinations of the rate constants for reactions R 2, R 3, R 15–R 18 found in the literature are listed in Table 3.3.

3.7.3. Kinetic Isotope Effect

To measure the Kinetic Isotope Effects (henceforth sometimes abbreviated as KIE), an analogue method to the relative rate described in section 3.7.1 is used. KIE is defined as:

$$\text{KIE} = \frac{\ln\left(\left[{CH_3}^{79}Br\right]_{t=0} \Big/ \left[{CH_3}^{79}Br\right]_t\right)}{\ln\left(\left[{CH_3}^{81}Br\right]_{t=0} \Big/ \left[{CH_3}^{81}Br\right]_t\right)} \tag{3.8}$$

where $\left[{CH_3}^{79}Br\right]_{t=0}$, $\left[{CH_3}^{79}Br\right]_t$, $\left[{CH_3}^{81}Br\right]_{t=0}$ and $\left[{CH_3}^{81}Br\right]_t$ are the concentrations of the isotopes at times $t = 0$ and t, k_{obj}. A straight line is fitted to a $\ln\left(\frac{\left[{CH_3}^{79}Br\right]_{t=0}}{\left[{CH_3}^{79}Br\right]_t}\right)$ versus

$\ln\left(\frac{[CH_3{}^{81}Br]_{t=0}}{[CH_3{}^{81}Br]_t}\right)$ plot points using a linear weighted total least squares fit procedure (Krystek and Anton, 2007). The slope of the curve will then correspond to the KIE. Before applying (3.8) to experiment results, the stability and photolysis tests have to be examined for any KIE effects, since wall effect et cetera may treat isotopes differently. Like in section 3.7.1, the KIE is in fact a linear combination of contributions from both reactions R 2 and R 3. Equation (3.9) is analogue to equation (3.7):

$$\mathrm{KIE}_{\mathrm{meas}} = c \times \mathrm{KIE}_{(\mathrm{R}\,2)} + (1-c) \times \mathrm{KIE}_{(\mathrm{R}\,3)}. \tag{3.9}$$

3.8. Simulation

To simulate the chemical kinetic systems, the Kintecus® software is utilized (Ianni, 2010). The input is a set of reactions, based on a model previously used in Nilsson, Andersen, Nielsen and Johnson (n.d.), see Table E.1 in appendix E. The model in Nilsson, Andersen, Nielsen and Johnson (n.d.) includes 56 reactions, involving O_x, HO_x, CO/CO_2 chemistry and oxidation of methane. Reactions describing CH_3Br, chemistry is added. The full model is sensitivity tested such that reactions not affecting the final result are removed. The reduced model is given in Table E.2. The photolysis rates are controlled by setting an initial concentration of a fictive compound that represents a photon. The concentration is then kept constant, since no sink is included in the model. The initial concentration is adjusted so that the model output fits with the measured development of concentrations. Kintecus® is also employed to determine the $k_{(\mathrm{R}\,3)}$. This is done by first adjusting the photolysis rates such that the model fits the measured CH_4 concentrations with accumulated photolysis time on the abscissa (Table C.1). The deviation between the measured and model levels is quantified by:

$$S_A = \frac{\sum_{i=1}^{k} \sqrt{\left([A]_{i,\mathrm{measured}} - [A]_{i,\mathrm{model}}\right)^2}}{\sum_{i=1}^{k} i} \tag{3.10}$$

where i is the data point index and $[A]$ the concentration of the compound of interest. S_{CH_4} is manually minimized by changing the concentration of the "photon"-body in the model. When the photolysis rate is adjusted, (3.10) is again used to minimized S_{CH_3Br} for the CH_3Br levels by changing the $k_{(\mathrm{R}\,3)}$. The obtained $k_{(\mathrm{R}\,3)}$ is taken as the result of the experiment.

3.9. Method: an example

In this section the entire procedure will be explained by focusing on one example experiment only, namely experiment 28. Experiment 28 is OH experiment at 1000 mbar with CH_4 as the reference compound. The time of stabilisation, the time before the first spectrum, with the full mix and the last spectrum before photolysis start is 34 min. The last spectrum before photolysis start, defined as the point at $T = 00:00$, is shown in Figure 3.6a. The last accepted spectrum of the series (point number 12) is shown in Figure 3.6b. An ozone peak is encircled to show ozone concentration change between these to points. The lamps are turned on between following spectra in a pattern described in Table 3.4. The spectra are then analyzed by MALT5 for two regions (Table 3.2): 1270 cm^{-1} – 1390 cm^{-1} (Figure 3.7) and 2140 cm^{-1} – 2300 cm^{-1} to obtain concentration for H_2O, CO_2, O_3, N_2O, CO, CH_3Br ($CH_3{}^{79}Br$ and $CH_3{}^{81}Br$), CH_4 and HNO_3, see Figure 3.8. The CH_3Br and CH_4 concentrations, as the $CH_3{}^{79}Br$ and $CH_3{}^{81}Br$

Table 3.4.: *Number of lamps, and time the lamps are turned on during experiment 28*

Point	Number of lamps	Time (s)	Accumulated photolysis time (lamp × s)
1	0	0	0
2	1	40	40
3	1	40	80
4	1	40	120
5	1	40	160
6	2	40	240
7	2	40	320
8	2	80	480
9	2	80	640
10	2	80	800
11	2	80	960
12	4	80	1280
13	6	300	3080

concentrations, are plotted against each other Figure 3.9. By convention, the form $\ln\left(\frac{[A]_{t=0}}{[A]_t}\right)$ is used. A line is fitted to the data points, including uncertainty estimated by MALT5, and showed as a red line in Figure 3.9. Its slope and automatically estimated uncertainty (Krystek and Anton, 2007) is taken as the k_{RR}, δk_{RR}, k_{KIE} and δk_{KIE} respectively. The concentrations of point 1, determined by MALT5, are used as initial values for the model (appendix E) is partly to check that raection R 2 is dominating over reaction R 3, see Figure 3.10, partly to verify the model, see Figure 3.11.

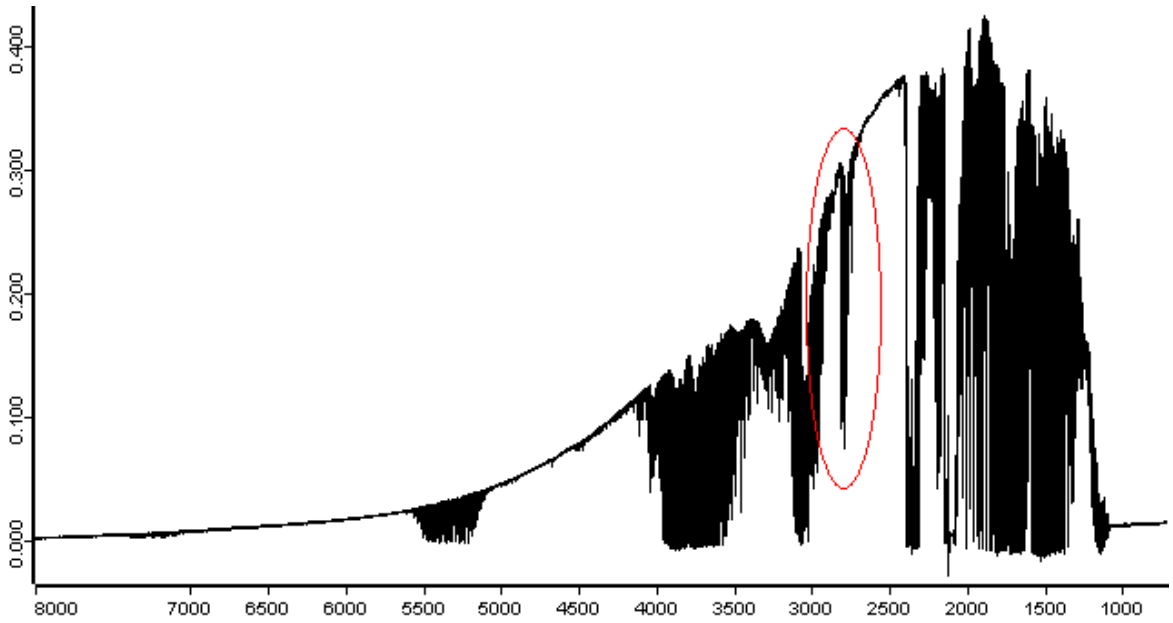

(a) First spectrum in the series

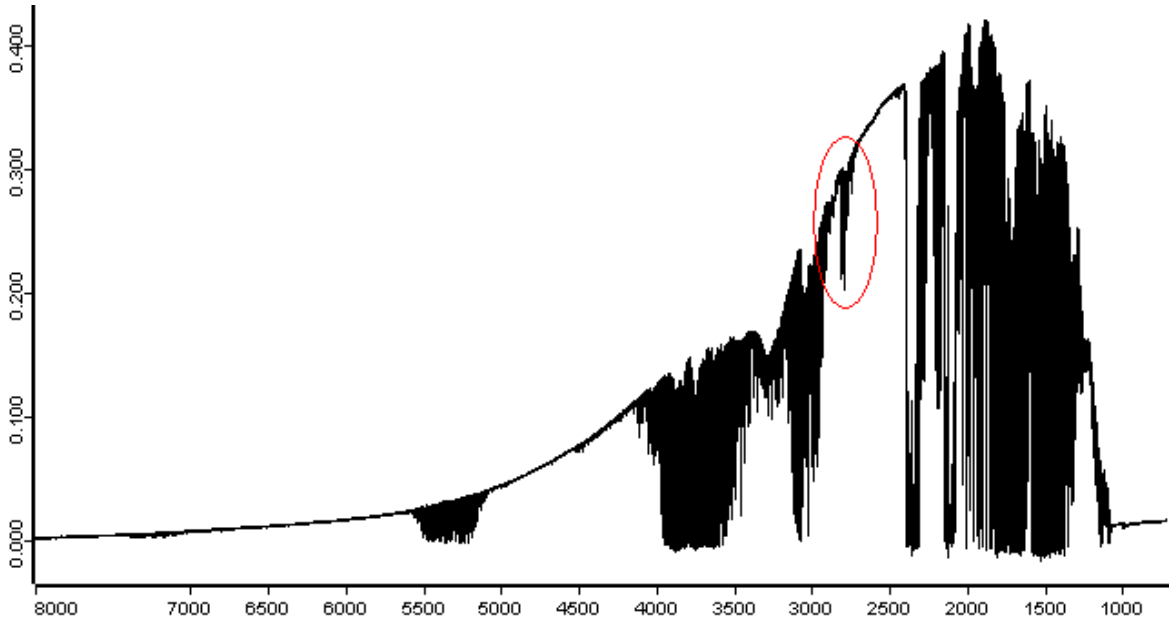

(b) Last accepted spectrum in the series

Figure 3.6.: *Example spectra of experiment 28, ozone part of the spectrum is encircled, intensity of light is drawn on the ordinate, the wave number [cm^{-1}] is drawn on the abscissa*

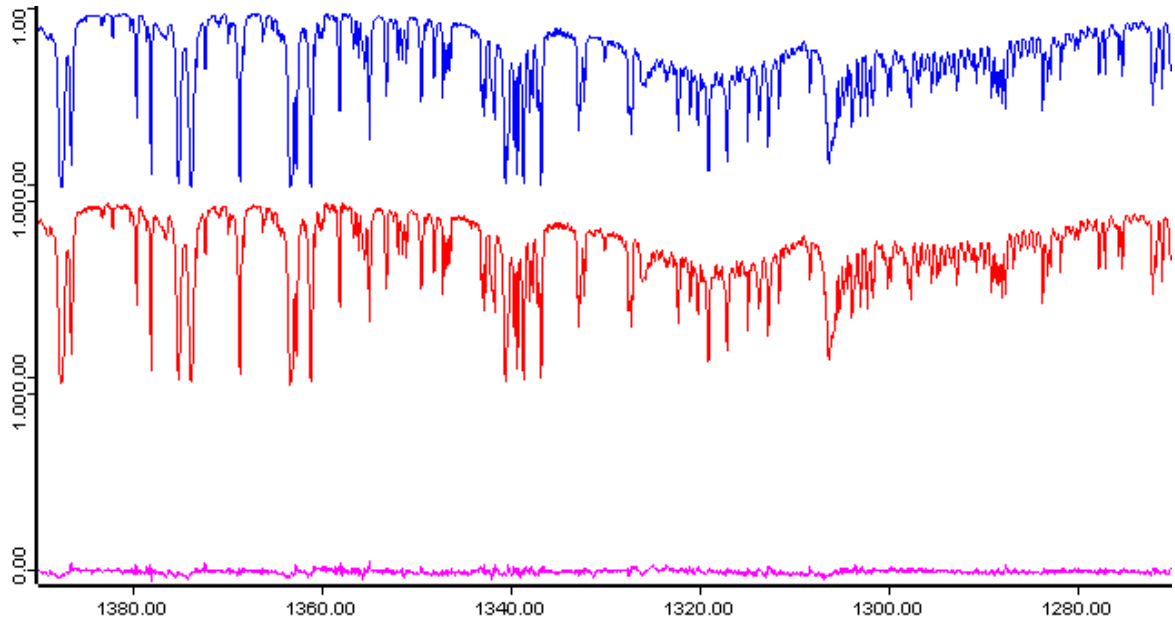

(a) Full spectrum, from top to bottom: blue curve: fitted spectrum, red curve: measured spectrum, pink curve: residual

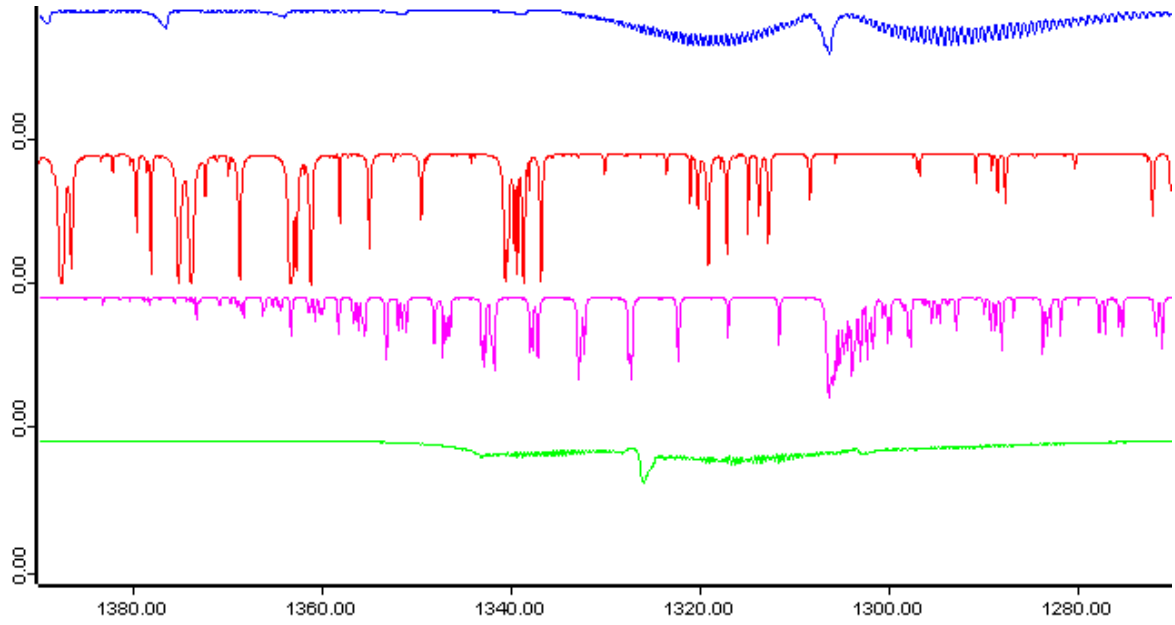

(b) The artificial spectrum broken up in its all contributing compounds, from top to bottom, blue curve: CH_3Br, red curve: H_2O, pink curve: CH_4, green curve HNO_3 (N_2O makes an insignificant contribution only and is therefore left out here)

Figure 3.7.: *Example of MALT5 analysis (spectra 1, experiment 28, 1270–1390 cm^{-1}), artificial spectra of CH_3Br, CH_4, H_2O, N_2O and HNO_3 are combined to synthesizes a spectrum resembling the measured as closely as possible, this IR region is used to obtain concentration of CH_3Br, ($CH_3{}^{79}Br$ and $CH_3{}^{81}Br$) CH_4, H_2O and HNO_3, intensity of light is drawn on the ordinate, the wave number [cm^{-1}] is drawn on the abscissa*

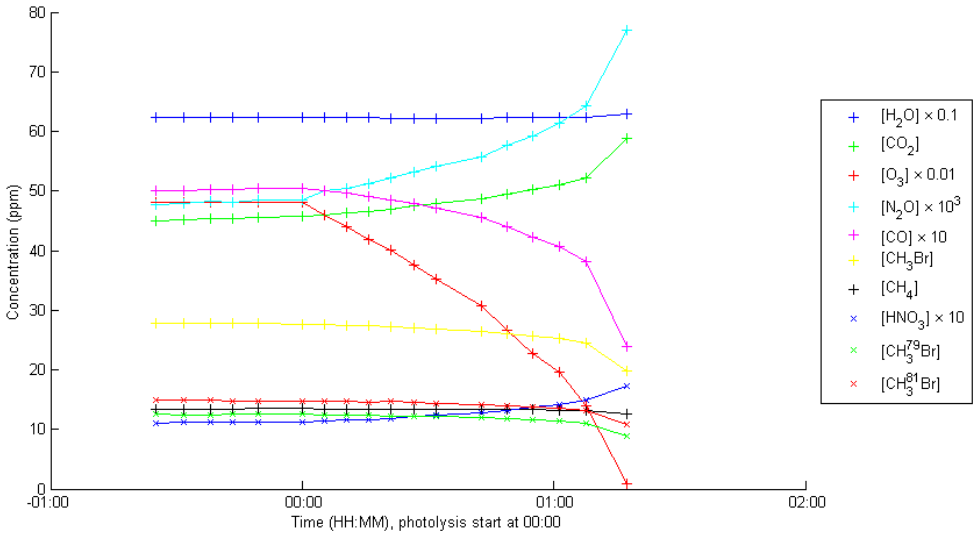

Figure 3.8.: *Example of a MALT5 analysis results, experiment 28 from T=00:00, points prior to T=00:00 defined as stability test 28a*

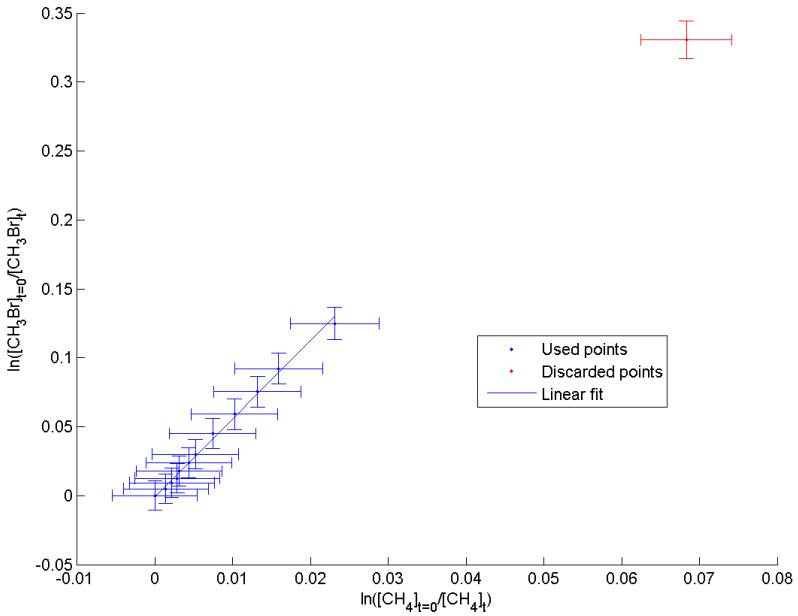

(a) Relative rate

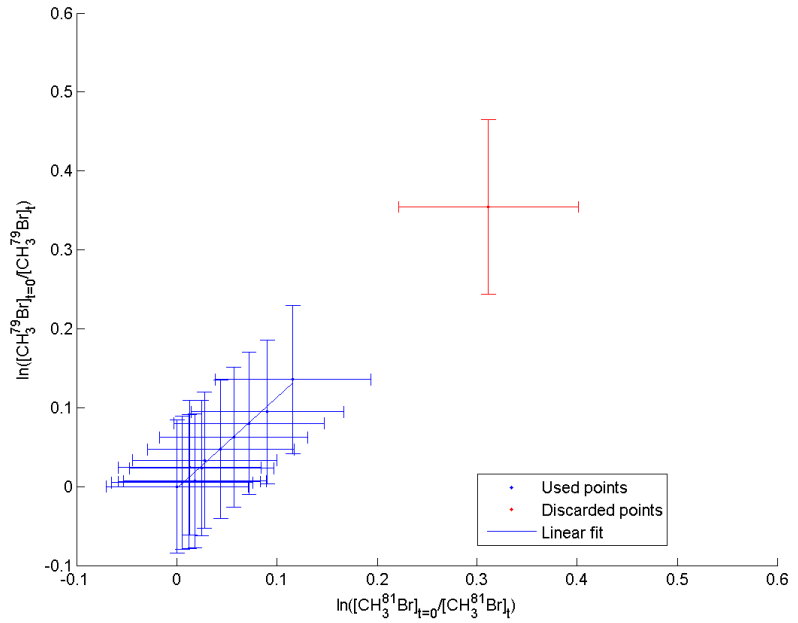

(b) Kinetic Isotope Effect

Figure 3.9.: *Example of results, experiment 28, blue crosses are measured points with uncertainty, red crosses are points discarded due to low ozone concentrations, blue lines are the linear fits*

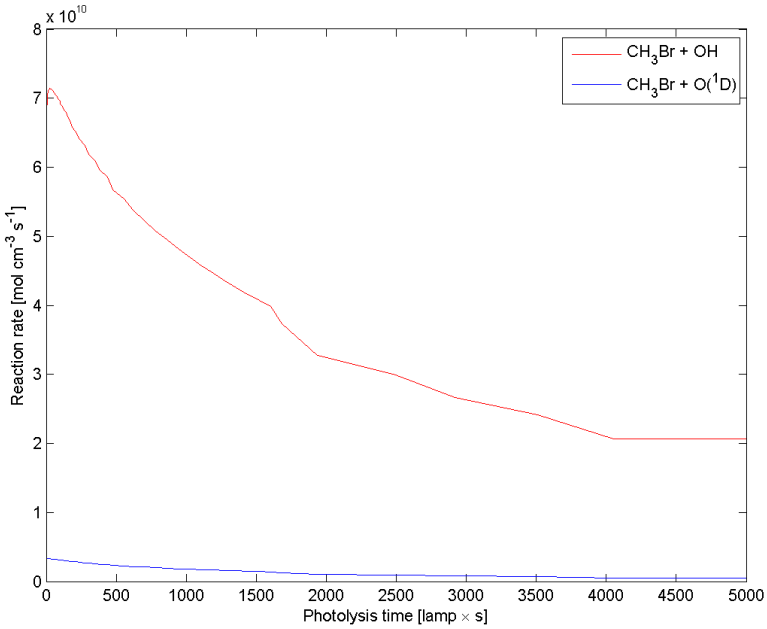

Figure 3.10.: *Example of rate comparison, $CH_3Br + OH \longrightarrow$ products versus $CH_3Br + O(^1D) \longrightarrow$ products rates, experiments 28*

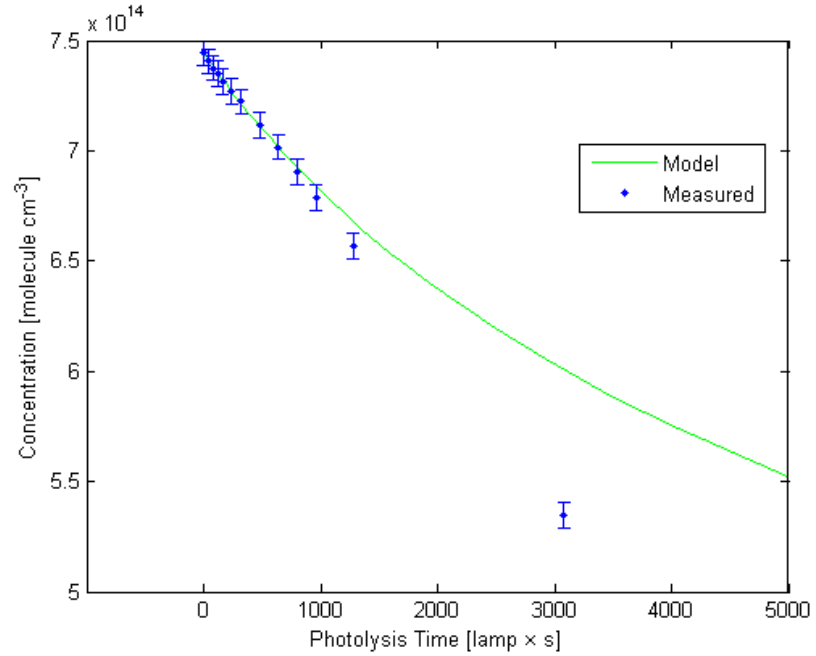

(a) CH_3Br

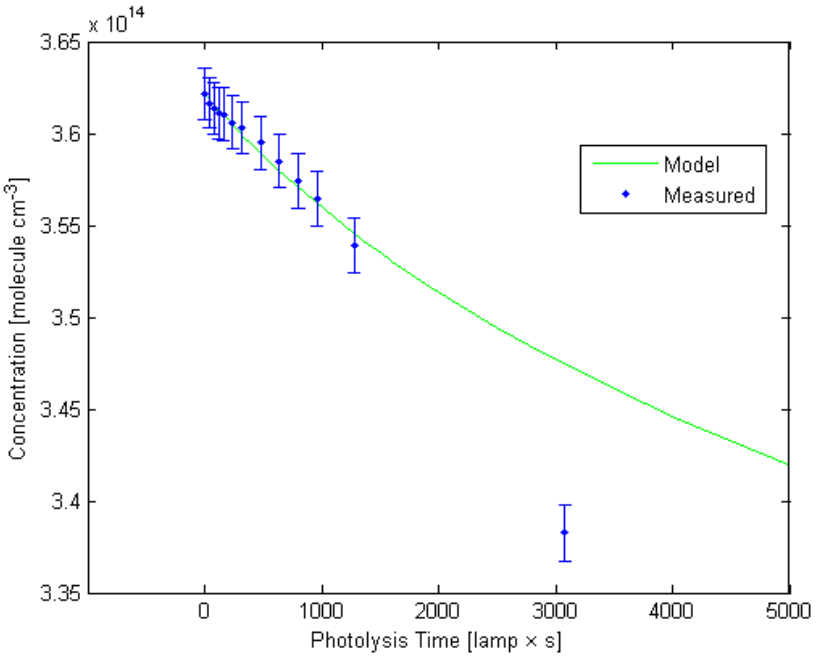

(b) CH_4

Figure 3.11.: *Example of model and measured results, experiment 28*

4. Results

In this chapter the results of this study will be presented. The results of test experiments are fully presented in appendices A and B. Briefly, it should be stated that the stability test show significant instability in all compounds at least for times shorter than 2 h. Complete stability test results are presented in appendix A. Dilution tests results are presented appendix B. All results apply to $T = 298\,\mathrm{K}$.

4.1. Determination of rate constants

4.1.1. Reaction rate constant for the reaction $CH_3Br + OH \rightarrow$ products

$$CH_3Br + OH \longrightarrow \text{products} \qquad (R\,2)$$

Four of the OH experiments turned out useful for calculating the relative rates, namely experiments 25, 28 (with CH_4 as reference), 26 and 27 (with C_2H_6 as reference). Experiments 7, 8 and 11 were rejected because equilibrium in CH_3Br and CH_4 concentrations were not achieved before experiment start. The relative rate calculations are performed with some selection of points, see Table C.2. The results from these four experiments including a total weighted average of the four experiment rates. $k_{(R\,2)}$ in Table 4.1 refer to the reaction rate constant of reaction R 2. Experiments 25 and 28 are presented in Figure 4.1a, experiments 26 and 27 are presented in Figure 4.1b, both along with total weighted averages. In these results uncorrected data are used, since the suggested linear corrections (see Figures A.3–A.6) are all small, except perhaps the CH_4-concentrations in experiment 25 (see Figure A.3b). In that case, the instability prior to the kinetic experiment is not satisfyingly expressed as a linear development. The problem is instead solved by discarding the first part where the instability is still apparent; CH_4 is even increasing for these points. The final result $k_{(R\,2)} = (3.53 \pm 0.23) \times 10^{-14}\,\mathrm{cm^3/molecule\,s}$ is higher than $k_{(R\,2)} = 3.0 \times 10^{-14}\,\mathrm{cm^3/molecule\,s}$ stated in Sander et al. (2011), and lower than values $k_{(R\,2)} = (4.9 \pm 0.5) \times 10^{-14}\,\mathrm{cm^3/molecule\,s}$ determined by Nilsson, Joelsson, Johnson and Nielsen (n.d.). To verify the result, model runs of the experiments along with the measured data are presented in Figure D.1 and Figure D.2. To make sure that the reaction R 2 is dominating over reaction R 3, the rates of the these two reactions computed by the model is shown in Figure D.5. The model is run with $k_{(R\,3)}$ from Sander et al. (2006). The complete uncorrected, unselected relative rate plots are presented in Figures D.3.

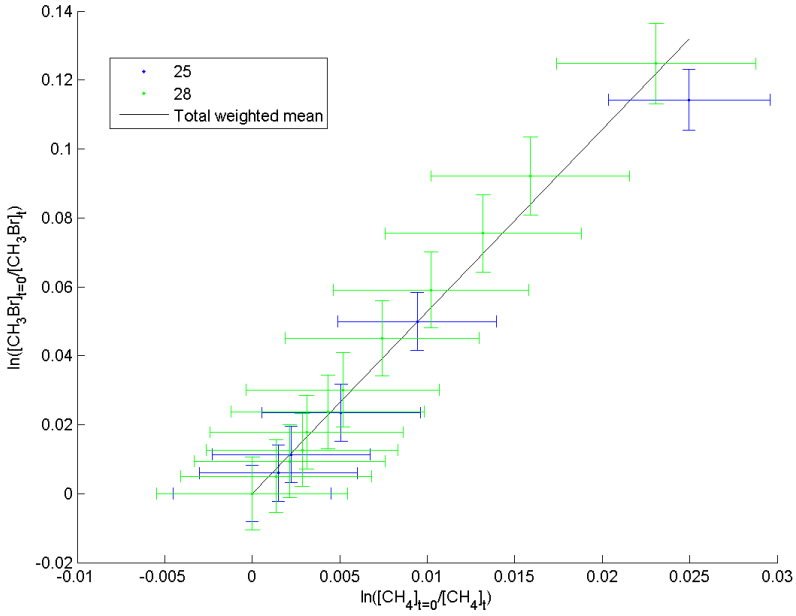

(a) CH_4

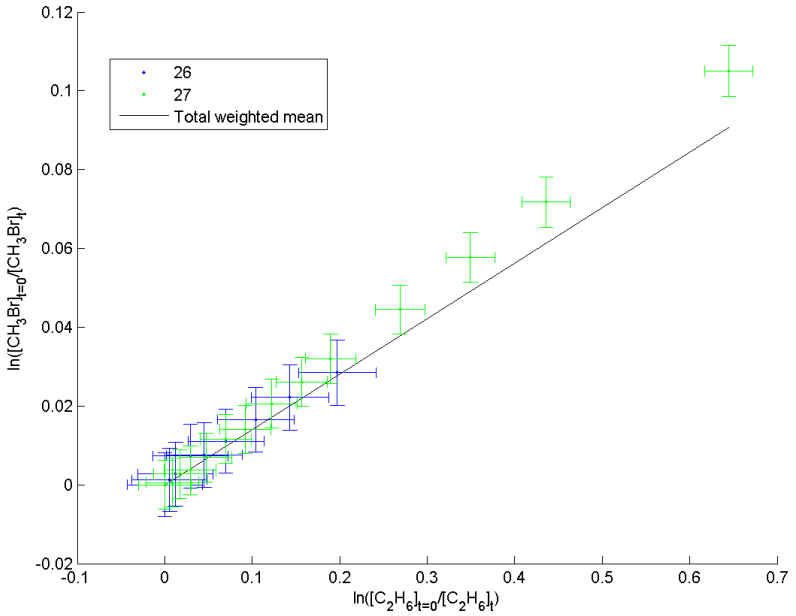

(b) C_2H_6

Figure 4.1.: *Relative rate result of combined experiments: $CH_3Br + OH$, selected data*

Table 4.1.: *Relative rate results: OH, selected data, uncertainties are obtained from the output of the linear fits, with MALT5 analysis uncertainties as input*[a]

Reference reaction	k_{ref} $\left(\mathrm{cm^3/molecule\,s}\right)$	Experiment	$k_{(\mathrm{R}\,2)}/k_{\mathrm{ref}}$	$k_{(\mathrm{R}\,2)}$ $\left(10^{-14}\,\mathrm{cm^3/molecule\,s}\right)$
$CH_4 + OH \longrightarrow$	(6.3 ± 0.6)	25	4.6 ± 1.1	2.90 ± 0.75
$\longrightarrow CH_3 + H_2O$	$\times 10^{-15}$ [b]	28	5.7 ± 1.5	3.6 ± 1.0
$C_2H_6 + OH \longrightarrow$	(2.5 ± 0.2)	26	0.1340 ± 0.0056	3.35 ± 0.30
$\longrightarrow C_2H_5 + H_2O$	$\times 10^{-13}$ [b]	27	0.165 ± 0.012	4.13 ± 0.45
Average[c]				3.53 ± 0.23

[a] All k-values are given at $T = 298\,\mathrm{K}$

[b] Sander et al. (2011)

[c] The weighted mean (as defined in (3.6)) of the the four measured values

Table 4.2.: *Ratio of CH_3Br loss by OH to total loss of CH_3Br, defined as c in (3.7), average over accepted points (Table C.2), only experiments with CH_4 as reference compound are listed, discarded tests are left out*

Experiment	c
9	0.51
10	0.28
12	0.57
25	0.95
28	0.96
29	0.67
30	0.63
31	0.60

4.1.2. Reaction rate constant for the reaction $CH_3Br + O(^1D) \rightarrow$ products

$$CH_3Br + O(^1D) \longrightarrow \text{products} \qquad (R\,3)$$

Since reaction R 3 is not dominating over reaction R 2 in any of the $O(^1D)$-experiments (see Table 4.2), the relative rate method is not suitable for calculating the rate constant $k_{(R\,3)}$. Instead the model (appendix E) is used. The results are tabulated in Table 4.3 and presented visually in Figures 4.2–4.4. Stabilities prior to experiments 9, 10 and 12 were not monitored nor were no time of stabilization given to the gas mix. These results are therefore considered less trustworthy and discarded. Discarded results (experiments 9, 10 and 12) are presented in Table C.3 and Figures D.7–D.9. The linearly corrected data did not give more uniform results than the uncorrected data and are thus considered irrelevant. Results with linear corrections are presented in Table C.4 and Figures D.10–D.12. The value $k_{(R\,3)}$ ranges, with a standard uncertainty estimate of 3%, from 2.47×10^{-10} to $5.36 \times 10^{-10}{}^{\mathrm{cm}^3}/_{\mathrm{molecules}}$, which are all higher than the literature value $k_{(R\,3)} = (1.8 \pm 0.27) \times 10^{-10}{}^{\mathrm{cm}^3}/_{\mathrm{molecules}}$ (Sander et al., 2011). Experiment 29 and 30 are both closer to the literature value and to each other than the value obtained by experiment 31. The two are also more alike compared to experiment 31 in the manor they were conducted with a stabilisation time around 1.5 h. The gas mix in experiment 31, including O_3, was left for almost 20 h. The rate of change due to instability is though comparable for all the three preparatory stability tests Table A.3. For experiments 29 and 30, for both CH_3Br and CH_4, the measured loss rate is increasing with time while the modeled loss rate is rather decreasing with time. For experiment 31, the loss rates of both CH_3Br and CH_4, both measured and modeled are decreasing. The model result resembles the measured data more closely in experiment 31 than in experiments 29 and 30. This notion is confirmed by the values of S_{CH_3Br} and S_{CH_4} which both are lowest for experiment 31.

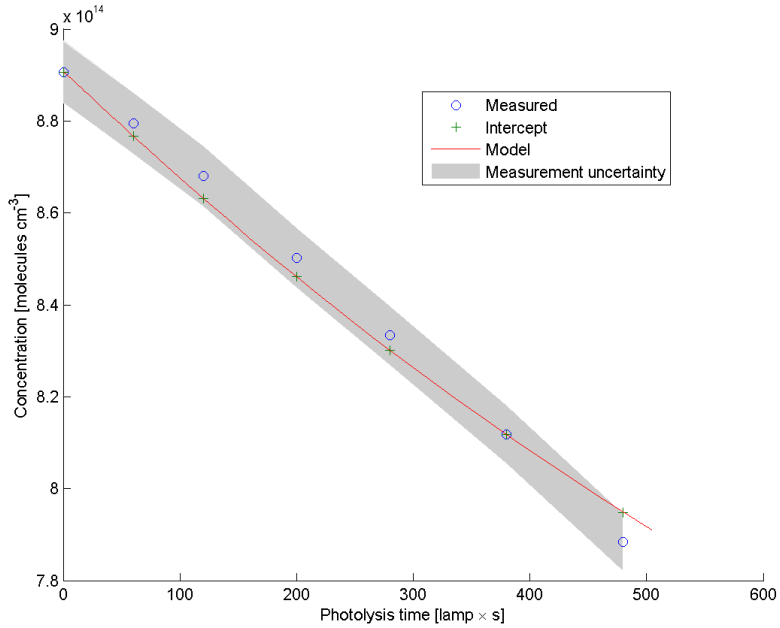

(a) CH_3Br

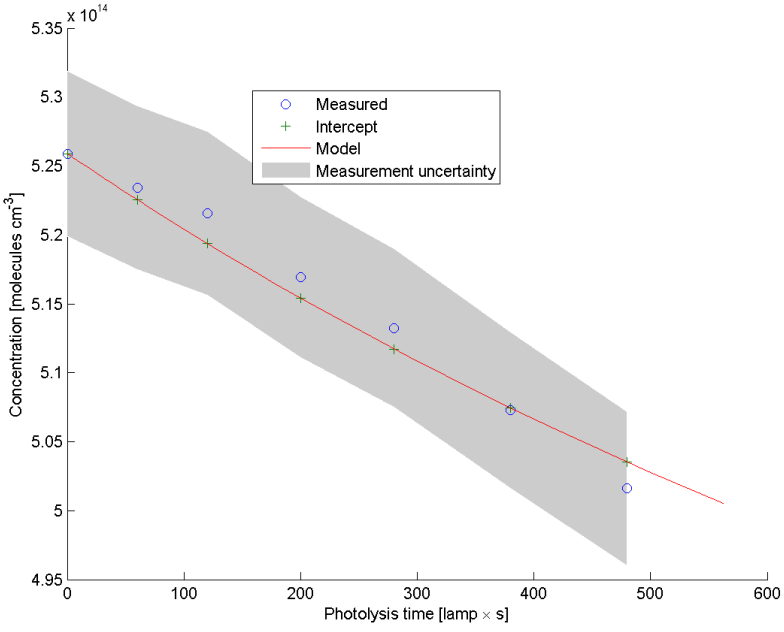

(b) CH_4

Figure 4.2.: *Model and measured results, experiment 29, uncorrected data*

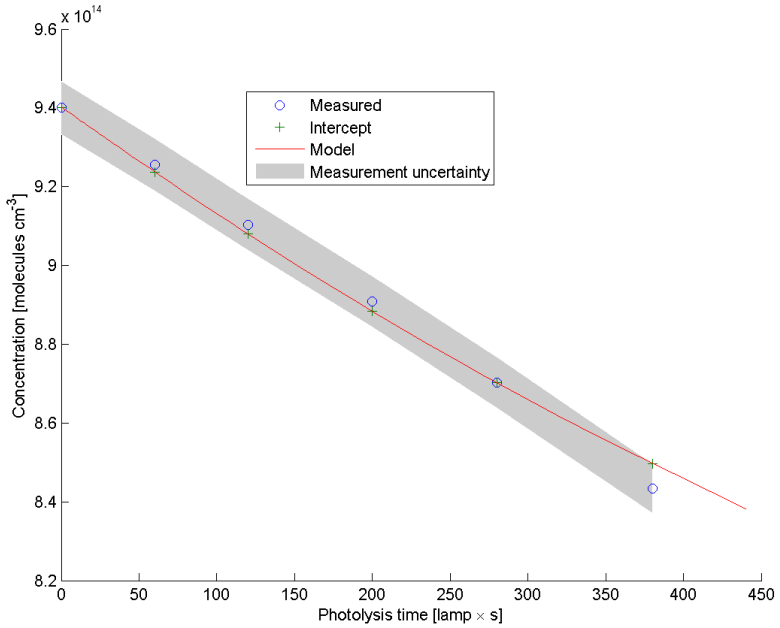

(a) CH_3Br

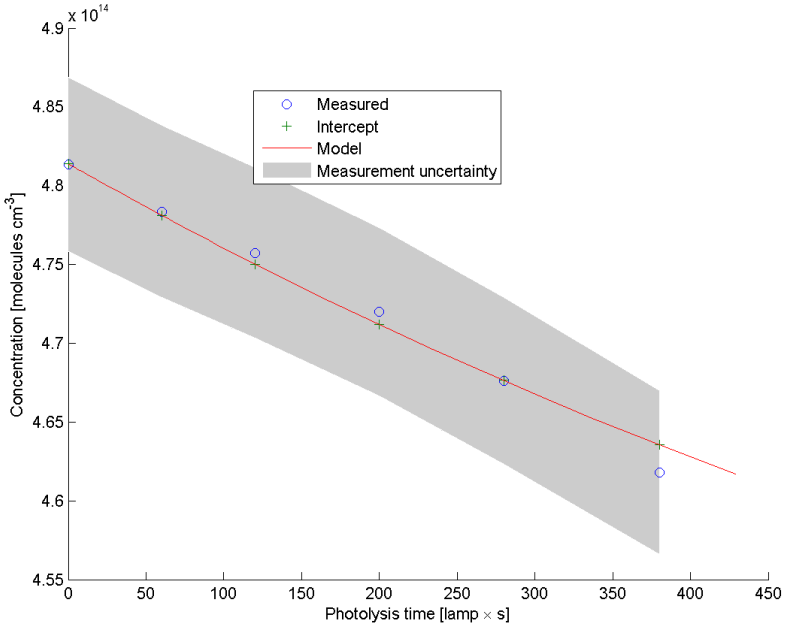

(b) CH_4

Figure 4.3.: *Model and measured results, uncorrected data, experiment 30*

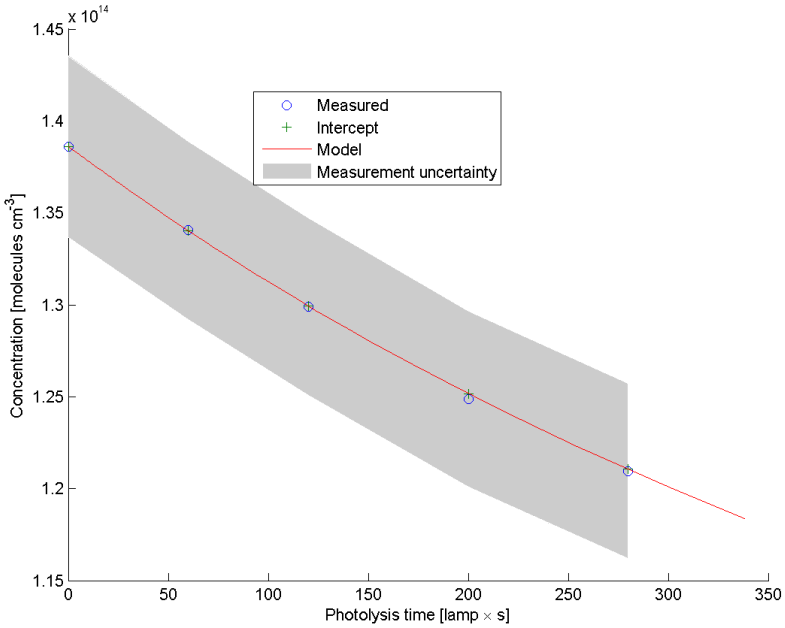

(a) CH_3Br

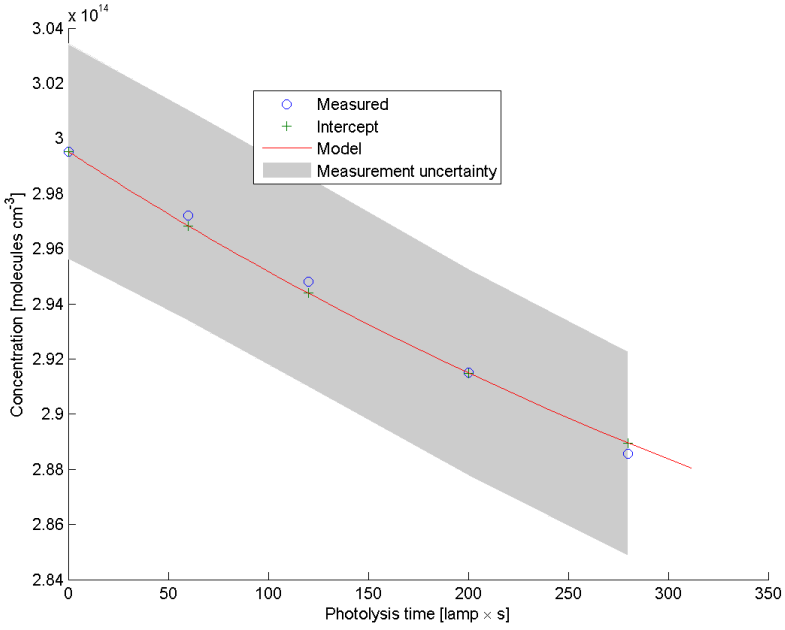

(b) CH_4

Figure 4.4.: *Model and measured results, experiment 31, uncorrected data*

Table 4.3.: *Results: $CH_3Br + O(^1D) \longrightarrow$ products, reference reaction: $CH_4 + O(^1D) \longrightarrow$ products, uncorrected data, data adjusted to model*[a]

Experiment	Time of stabilisation (HH:MM)	$k_{(\mathrm{R}\,3)}$ $\left(\mathrm{cm}^3/\mathrm{molecule\,s}\right)$	$S_{\mathrm{CH_3Br}}$	$S_{\mathrm{CH_4}}$
29	01:23	2.55×10^{-10}	0.0036	0.0023
30	01:29	2.88×10^{-10}	0.0024	0.0013
31	19:29	5.20×10^{-10}	0.0005	0.0008

[a] All k-values are given at $T = 298\,\mathrm{K}$

Table 4.4.: *Kinetic Isotope Effect results: OH, KIE defined as* (3.8)*, uncertainties are obtained from the output of the linear fits, with MALT5 analysis uncertainties as input*

Experiment	KIE
25	1.01 ± 0.93
27	1.14 ± 0.70
28	1.2 ± 1.0
Average	1.12 ± 0.49

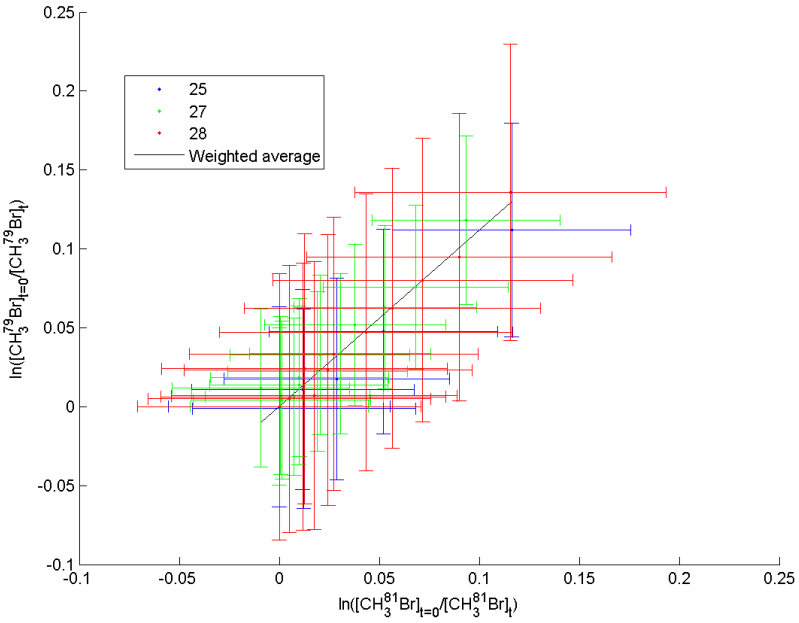

Figure 4.5.: *Kinetic isotope effect of combined experiments*

4.2. Determination of the Kinetic Isotope Effect

4.2.1. Kinetic Isotope Effect for the reaction $CH_3Br + OH \rightarrow$ products

As in section 4.1.1, experiments 7, 8, 11 are discarded. Again as in section 4.1.1, only selected points are used (see Table C.2). In experiment 26, a shorter photolysis time span of the test was used: 300 lamp × s part, which can be compared with 1240, 1220 and 1280 lamp × s for experiment 25, 27, 28 respectively. This time is too short to make a meaningful value of the KIE. Therefore also experiment 26 is rejected. The full results are presented in Table C.5 and in Figure D.13. These selected results are tabulated in Table 4.4 along with the weighted average, defined as (3.6). The weighted average is visualized as a linear slope along with all the data points in Figure D.13. The uncertainty estimates by MALT5 seem to be overestimated (by comparison with Figure D.13). Instead, a 3% standard uncertainty estimate is being added such that the final range of result is: $\mathrm{KIE}_{(\mathrm{R}\,2)} = 0.98 : 1.24$ with average of 1.12. Reaction R 2 is most likely to be faster for the lighter isotopologue $CH_3{}^{79}Br$ than for $CH_3{}^{81}Br$.

Table 4.5.: *Results: Kinetic Isotope Effect, $CH_3Br + O(^1D) \longrightarrow$ products; c is the ratio of CH_3Br loss by OH to total CH_3Br loss, uncertainties are obtained from the output of the linear fits, with MALT5 analysis uncertainties as input*

Experiment	c	KIE_{meas}
9	0.51	0.90 ± 1.1
10	0.28	1.00 ± 0.47
12	0.57	0.96 ± 0.83
29	0.67	0.95 ± 0.31
30	0.63	0.93 ± 0.35
31	0.60	0.7 ± 1.2

4.2.2. Kinetic Isotope Effect for the reaction $CH_3Br + O(^1D) \rightarrow$ products

A Kinetic Isotope Effect for $CH_3Br + O(^1D) \longrightarrow$ products is difficult to quantify, since the influence of OH chemistry still is significant (c not close to zero). The measured combined values, named KIE_{meas}, are all close to or even slightly below unity. No clear connection is between the ratio of OH-chemistry c and KIE_{meas}. According to equation (3.9), if $KIE_{(R\,2)}$ are indeed higher than unity as suggested in section 4.2.1, and KIE_{meas} is less than one, $KIE_{(R\,3)}$ must also be less than one.

5. Discussion

The value of reaction rate constant $k_{(R\,3)} = (3.53 \pm 0.23) \times 10^{-14}\,\mathrm{cm^3/molecules}$ derived in the present work is in the middle of the range of values $2.8\,\mathrm{cm^3/molecules}$ – $4.9\,\mathrm{cm^3/molecules}$ listed in the literature. The recommended value $k_{(R\,2)} = (3.0 \pm 0.3) \times 10^{-14}\,\mathrm{cm^3/molecules}$ (Sander et al., 2011) is based on three different studies (Hsu and Demore, 1994; Zhang et al., 1992; Chichinin et al., 1994), where Hsu and Demore (1994) is, like the present study, a relative rate study, but with HFC152a as a reference compound. The values do therefore depend on the quality of the current recommendations (Sander et al., 2011). Many of the early experiments (up to and including experiment 12) had to be discarded due to instability problems in the cell. The reasons for these problems are not understood beyond the usual effects of initial mixing. This posed problems to the studies, where the only solution was to let the mix reside in the cell for some time. Ozone is very reactive, and is thus problematic to leave in the cell. To add ozone at the end of the stabilization might also be problematic since this have to be done before finally filling the cell to atmospheric pressure and the equilibrium of the reactants which was achieved within the stabilization time might be become askew. To get better result, this problem must be solved. Introduction of ozone into the cell was always accompanied with radically increased concentrations of water vapour in the cell. The conclusion drawn from this is that the ozone generator was leaking. Some attempts were made to run the ozone through a cold trap, decreasing the water content in the cell, but unfortunately also causing ozone loss. From Figure D.6, OH chemistry had less influence in the two experiments at lowest pressure (experiment 9 and 10), indicating that a low pressure (2 mbar) might be preferable for further studies. The analysis of CH_4 by MALT5 gave large uncertainties. In order to improve the results, the analysis of CH_4 could be refined. Perhaps also other references could be considered. CH_3OH was tried for a couple of tests, but proved even more difficult to analyze. Analysis of C_2H_6 gave relatively small uncertainties and the relative rate experiments showed a linear propagation between object and reference compound for experiments 27 and in the beginning of experiment 26. About halfway through the experiment, there is a clear unexpected shift in the loss rate. Despite this, C_2H_6 is a good complementary reference compound for OH experiments. In the case of $O(^1D)$, only one reference compound is used, where at least two reference compounds would be preferable. A common reference compound beside CH_4 is N_2O. N_2O has the advantages that it is relatively easy to analyze and that the loss rate to OH is low at atmospheric temperatures (in the order of $10^{-16}\,\mathrm{cm^3/molecules}$) (Atkinson et al., 1976). A few experiments were conducted during the course of this study with N_2O. Since so much OH was present in the systems, a model had to be used to obtain a value for $k_{(R\,3)}$. No model has thus far been developed for N_2O. Two of the three accepted $O(^1D)$-experiments (29, 30) gave results around 2.5×10^{-10}, while the last experiment (31) gives about twice that number. There is no satisfying argument to prefer either of the two values and the discrepancy is difficult to understand. The model can, however, more closely reproduce the results of experiment 31. Under gun point, this value would therefore be my guess, even though this value farthest from the recommended value $k_{(R\,3)} = (1.8 \pm 0.27) \times 10^{-10}\mathrm{cm^3/molecules}$ (Sander et al., 2011). Analysis of the separate isotopologues $CH_3{}^{79}Br$ and $CH_3{}^{81}Br$ brings large uncertainties, especially

compared to the analysis for the total CH_3Br; this also affects the uncertainty output of the total weighted least squares procedure. The uncertainty estimate is larger than what is intuitive by examining Figure D.13. To get a better value of KIE, perhaps an alternative method (f.x. mass spectroscopy) is more suitable. From the results of the present study, we cannot exclude $KIE_{(R\,2)} = 1$. The $O(^1D)$ system all have different rates of influence by OH-chemistry. There is though surprisingly little connection between the combined, measured KIE for these systems and the amount of OH influence (named c), which underlines the uncertainty of the results. The combined KIE are all close to unity; it can therefore be excluded with some certainty that $KIE_{(R\,3)} > 1$.

6. Conclusions

The current studies show that both $k_{(\mathrm{R}\,2)} = (3.53 \pm 0.23) \times 10^{-14}{}^{\mathrm{cm}^3}/_{\mathrm{molecules}}$ and $k_{(\mathrm{R}\,3)} = (2.5 : 5.4) \times 10^{-10}{}^{\mathrm{cm}^3}/_{\mathrm{molecules}}$, are higher than the current literature values. The results imply that the available estimates of atmospheric CH_3Br budgets, which are highly dependent on models, might need to be revised. This might very well have consequences for concentration estimates of Br-containing compounds at different altitudes in the stratosphere. This might in turn have affect for several other species, including ozone. Unexpected instabilities of reactant concentration in the reaction cell caused problems to the analysis and have added uncertainty to the results. Unwanted high concentrations of water vapour in the cell for the systems designed to determine $k_{(\mathrm{R}\,3)}$, probably due to leakage through the ozone generator, shifted the chemistry in the cell toward OH. Thus, a model fitting method was needed to be used instead of the preferred Relative Rate method. The $k_{(\mathrm{R}\,3)}$ results are therefore quite disparate and a range rather than a value is given. More experiments, preferably including test with different reference compounds, f.x. N_2O, with less water vapour in cell must be conducted to obtain a better result. According to the present work $CH_3{}^{79}Br$ is 1–1.2 times more sensitive towards reactions with OH and less sensitive towards reactions with $O(^1D)$ compared to $CH_3{}^{81}Br$. Large estimated uncertainties in the analysis, despite good linear fits, made it less sensible to give one value for $\mathrm{KIE}_{(\mathrm{R}\,2)}$. Could these problems be overcome, a more precise value would be obtained. The high fraction of OH-chemistry in the $O(^1D)$-systems makes it difficult to quantify $\mathrm{KIE}_{(\mathrm{R}\,3)}$. By deduction, however, it can be concluded that $\mathrm{KIE}_{(\mathrm{R}\,3)}$ most likely is below one. Again, more tests in systems with lower concentrations of water vapour is needed to obtain a precise value. A well defined value for $\mathrm{KIE}_{(\mathrm{R}\,2)}$ and $\mathrm{KIE}_{(\mathrm{R}\,3)}$ might help to pinpoint atmospheric sources of Br-reservoirs.

Bibliography

Air Liquide Gas Encyclopedia (2009).
URL: *http://encyclopedia.airliquide.com*

Aranda, A., Daele, V., Le Bras, G. and Poulet, G. (1998), 'Kinetics of the reactions of CH_3O with Br and BrO at 298 k', *International Journal of Chemical Kinetics* **30**(4), 249–255. Times Cited: 14.

Atkinson, R., Baulch, D. L., Cox, R. A., Crowley, J. N., Hampson, R. F., Hynes, R. G., Jenkin, M. E., Rossi, M. J. and Troe, J. (2006), 'Evaluated kinetic and photochemical data for atmospheric chemistry: Volume II - gas phase reactions of organic species', *Atmospheric Chemistry and Physics* **6**, 3625–4055. ISI Document Delivery No.: 083WT Times Cited: 256 Cited Reference Count: 931 Atkinson, R. Baulch, D. L. Cox, R. A. Crowley, J. N. Hampson, R. F. Hynes, R. G. Jenkin, M. E. Rossi, M. J. Troe, J. COPERNICUS GESELLSCHAFT MBH GOTTINGEN.

Atkinson, R., Perry, R. and Pitts, J.N., J. (1976), 'Kinetics of the reactions of OH radicals with CO and N_2O', *Chem. Phys. Lett.* **44**.

Basu, N., Scheuhammer, A. M., Sonne, C., Letcher, R. J., Born, E. W. and Dietz, R. (2009), 'Is dietary mercury of neurotoxicological concern to wild polar bears (ursus maritimus)?', *Environmental Toxicology and Chemistry* **28**(1), 133–140.
URL: *http://dx.doi.org/10.1897/08-251.1*

Bedjanian, Y., Riffault, V. and Poulet, G. (2001), 'Kinetic study of the reactions of BrO radicals with HO_2 and DO_2', *Journal of Physical Chemistry A* **105**(13), 3167–3175. Times Cited: 10.

Brasseur, G. P. and Holland, E. A. (1995), 'Global changes to atmospheric chemistry', *Bulletin of the Ecological Society of America* **76**(2 SUPPL. PART 2), 28. Annual Meeting of the Ecological Society of America on the Transdisciplinary Nature of Ecology July 30-August 3, 1995 Snowbird, Utah, USA.

Burton, G. (2000), *Salters' Advanced Chemistry: Chemical Storylines*, Heinemann.

Butkovskaya, N. I., Morozov, I., Talrose, V. L. and Vasiliev, E. S. (1983), 'Kinetic-studies of the bromine oxygen system - a new paramagnetic particle, BrO_2', *Chemical Physics* **79**(1), 21–30. Times Cited: 31.

CCME (n.d.), What is smog?, Technical report, Canadian Council of Ministers of the Enviroment, NO_x/VOC Office, 100 Sparks Street, Ottawa, Ontario, Canada.

Chapman, S. (1930), 'On ozone and atomic oxygen in the upper atmosphere', *Philosophical Magazine* **10**(64), 369–383. Times Cited: 86 7TH SERIES.

Chichinin, A., Teton, S., Lebras, G. and Poulet, G. (1994), 'Kinetic investigation of the OH + CH_3Br reaction between 248-K and 390-K', *Journal of Atmospheric Chemistry* **18**(3), 239–245. Times Cited: 6.

Chiorboli, C., Piazza, R., Tosato, M. L. and Carassiti, V. (1993), 'Atmospheric chemistry - rate constants of the gas-phase reactions between haloalkanes of environmental interest and hydroxyl radicals', *Coordination Chemistry Reviews* **125**(1-2), 241–250. Times Cited: 7 INTERNATIONAL SYMP ON PERSPECTIVES IN PHOTOCHEMISTRY OCT 11-14, 1992 FERRARA, ITALY.

Cohen, N. and Benson, S. W. (1987), 'Transition-state-theory calculations for reactions of OH with haloalkanes', *Journal of Physical Chemistry* **91**(1), 162–170. Times Cited: 62.

Cronkhite, J. M. and Wine, P. H. (1998), 'Branching ratios for bro production from reactions of O(D-1) with HBr, CF_3Br, CH_3Br, CF_2ClBr, and CF_2HBr', *International Journal of Chemical Kinetics* **30**(8), 555–563. Times Cited: 8.

Davis, D., Machado, G., Conaway, B., Oh, Y. and Watson, R. (1976), 'A temperature dependent kinetics study of the reaction of OH with CH_3Cl, CH_2Cl_2, $CHCl_3$, and CH_3Br', *J. Chem. Phys.* **65**.

Dietz, R., Born, E. W., Riget, F., Aubail, A., Sonne, C., Drimmie, R. and Basu, N. (2011), 'Temporal trends and future predictions of mercury concentrations in northwest greenland polar bear (ursus maritimus) hair', *Environmental Science & Technology* **45**(4), 1458–1465. Times Cited: 4.

Drougas, E. and Kosmas, A. M. (2004), 'Ab initio molecular orbital and rrkm calculations of the thermal decomposition of CH_2BrO radical', *Chemical Physics* **300**(1-3), 233–238. Times Cited: 3.

Ebinghaus, R., Temme, C., Lindberg, S. E. and Scott, K. J. (2004), 'Springtime accumulation of atmospheric mercury in polar ecosystems', *Journal De Physique Iv* **121**, 195–208. Times Cited: 2 European Research Course on Atmospheres 2004 Grenoble, FRANCE Univ Joseph Fourier; CNRS; LGGE.

Egan, C. and Kemp, J. (1938), 'Methyl bromide. the heat capacity, vapor pressure, heats of trans- ition, fusion and vaporization. entropy and density of the gas', *J. Am. Chem. Soc.* **60**, 2097.

Eskola, A., Wojcik-Pastuszka, D., Ratajczak, E. and Timonen, R. (2006), 'Kinetics of the reactions of CH_2Br and CH_2I radicals with molecular oxygen at atmospheric temperatures', *Phys. Chem. Chem. Phys.* **8**, 1416–1424.

Fahey, D. and Hegglin, M. (2011), *Twenty Questions and Answers About the Ozone Layer: 2010 Update, Scientific Assessment of Ozone Depletion: 2010, Pursuant to Article 6 of the Montreal Protocol on Substances that Deplete the Ozone Layer*, World Meteorological Organization, Geneva, Switzerland.

Griffith, D. (2008), *MALT5 User guide, Version 5*, University of Wollongong, Wollongong, NSW 2522, Australia.

Howard, C. J. and Evenson, K. M. (1976), 'Rate constants for reactions of OH with CH_4 and fluorine, chlorine, and bromine substituted methanes at 296-K', *Journal of Chemical Physics* **64**(1), 197–202. Times Cited: 129.

Hsu, K. J. and Demore, W. B. (1994), 'Rate constants for the reactions of OH with CH_3Cl, CH_2Cl_2, $CHCl_3$, and CH_3Br', *Geophysical Research Letters* **21**(9), 805–808. ISI Document Delivery No.: NK051 Times Cited: 19 Cited Reference Count: 23 HSU, KJ DEMORE, WB AMER GEOPHYSICAL UNION WASHINGTON.

Ianni, J. C. (2010), *Kintecus*.

Ko, M. K. W., Sze, N. D., Scott, C., Rodríguez, J. M., Weisenstein, D. K. and Sander, S. P. (1998), 'Ozone depletion potential of CH_3Br', *J. Geophys. Res.* **103**(D21), 28187–28195. **URL:** *http://dx.doi.org/10.1029/98JD02537*

Krystek, M. and Anton, M. (2007), 'A weighted total least-squares algorithm for fitting a straight line', *Measurement Science & Technology* **18**(11), 3438–3442. ISI Document Delivery No.: 221AT Times Cited: 38 Cited Reference Count: 23 Krystek, Michael Anton, Mathias IOP PUBLISHING LTD BRISTOL.

Kunzli, N., McConnell, R., Bates, D., Bastain, T., Hricko, A., Lurmann, F., Avol, E., Gilliland, F. and Peters, J. (2003), 'Breathless in Los Angeles: The exhausting search for clean air', *American Journal of Public Health* **93**(9), 1494–1499. Times Cited: 35.

Li, Z. J., Jeong, G. R. and Person, E. (2002), 'Kinetics of reactions of OBrO with NO,O-3, OClO, and ClO at 240-350 k', *International Journal of Chemical Kinetics* **34**(7), 430–437. Times Cited: 5.

Lorkovic, I. M., Sun, S., Gadewar, S., Breed, A., Macala, G. S., Sardar, A., Cross, S. E., Sherman, J. H., Stucky, G. D. and Ford, P. C. (2006), 'Alkane bromination revisited: "reproportionation" in gas-phase methane bromination leads to higher selectivity for CH_3Br at moderate temperatures', *Journal of Physical Chemistry A* **110**(28), 8695–8700. Times Cited: 11.

Manney, G. L., Santee, M. L., Rex, M., Livesey, N. J., Pitts, M. C., Veefkind, P., Nash, E. R., Wohltmann, I., Lehmann, R., Froidevaux, L., Poole, L. R., Schoeberl, M. R., Haffner, D. P., Davies, J., Dorokhov, V., Gernandt, H., Johnson, B., Kivi, R., Kyro, E., Larsen, N., Levelt, P. F., Makshtas, A., McElroy, C. T., Nakajima, H., Concepcion Parrondo, M., Tarasick, D. W., von der Gathen, P., Walker, K. A. and Zinoviev, N. S. (2011), 'Unprecedented arctic ozone loss in 2011', *Nature* **478**(7370), 469–U65. Times Cited: 6.

McGivern, W. S., Kim, H. J., Francisco, J. S. and North, S. W. (2004), 'Investigation of the atmospheric oxidation pathways of bromoform and dibromomethane: Initiation via UV photolysis and hydrogen abstraction', *Journal of Physical Chemistry A* **108**(35), 7247–7252. Times Cited: 9.

Mellouki, A., Talukdar, R. K., Schmoltner, A. M., Gierczak, T., Mills, M. J., Solomon, S. and Ravishankara, A. R. (1992), 'Atmospheric lifetimes and ozone depletion potentials of methyl-bromide (CH_3Br) and dibromomethane (CH_2Br_2)', *Geophysical Research Letters* **19**(20), 2059–2062. Times Cited: 88.

Montzka, S. and Reimann, S. (2011), *Ozone-Depleting Substances (ODSs) and Related Chemicals, Scientific Assessment of ozone Depletion: 2010, Pursuant to Article 6 of the Montreal Protocol on Substances that Deplete the Ozone Layer*, number 52, World Meteorological Organization, Geneva, Switzerland.

National Institute of Standards and Technology (2011), 'NIST standard reference database number 69'.
URL: *http://kinetics.nist.gov/kinetics/*

National Institute of Standards and Technology (2012), 'NIST chemical kinetics database, standard reference database 17, version 7.0 (web version), release 1.6.5'.
URL: *http://kinetics.nist.gov/kinetics/*

Nilsson, E. J. K., Andersen, V. F., Nielsen, O. J. and Johnson, M. S. (n.d.), 'Reaction rates of CH_2F_2, $CHClF_2$, CH_2FCF_3 and CH_3CCl_3 with $O(^1D)$ at 298 K'. Submitted for publication in Atmospheric Chemistry and Physics.

Nilsson, E. J. K., Eskebjerg, C. and Johnson, M. S. (2009), 'A photochemical reactor for studies of atmospheric chemistry', *Atmospheric Environment* **43**(18), 3029–3033. Times Cited: 4.

Nilsson, E. J. K., Joelsson, M., Johnson, M. S. and Nielsen, O. J. (n.d.), Temperature dependence of the reaction $CH_3Br + OH$ in the range 298 - 373 K. Unpublished.

Papayannis, D., Kosmas, A. M. and Melissas, V. S. (1999), 'Ab initio calculations for $(BrO)_2$ system and quasiclassical dynamics study of BrO self-reaction', *Chemical Physics* **243**(3), 249–262. Times Cited: 11.

Research Chemicals Catalog (1990), Farchan Laboratories, Gainesville, FL.

Rothman, L. S. (2012), 'The HITRAN database'.
URL: *http://www.cfa.harvard.edu/hitran/*

Sander, S., Friedl, R. R., Barker, J. R., Golden, D. M., Kurylo, M. J., Wine, P. H., Abbatt, J. P. D., Burkholder, J. B., Kolb, C. E., Moortgat, G. K., Huie, R. E. and Orkin, V. L. (2011), *Chemical Kinetics and Photochemical Data for Use in Atmospheric Studies Evaluation Number 17*, 17 edn, Jet Propulsion Laboratory, California Institute of Technology Pasadena, California.

Sander, S., Friedl, R. R., Ravishankara, A. R. and Golden, D. M. (2006), *Chemical Kinetics and Photochemical Data for Use in Atmospheric Studies Evaluation Number 15*, 15 edn, Jet Propulsion Laboratory, California Institute of Technology Pasadena, California.

Schroeder, W. H., Anlauf, K. G., Barrie, L. A., Lu, J. Y., Steffen, A., Schneeberger, D. R. and Berg, T. (1998), 'Arctic springtime depletion of mercury', *Nature* **394**(6691), 331–332. Times Cited: 332.

Seinfeld, J. H. and Pandis, S. N. (2006), *Atmospheric Chemistry and Physics - From Air Pollution to Climate Change (2nd Edition)*, John Wiley & Sons.

Solomon, S., Qin, D., Manning, M., Chen, Z., Marquis, M., Averyt, K., Tignor, M. and Miller, H., eds (2007), *Contribution of Working Group I to the Fourth Assessment Report of the*

Intergovernmental Panel on Climate Change, Cambridge University Press, Cambridge, United Kingdom and New York, NY, USA.

Sonne, C., Dietz, R., Leifsson, P. S., Asmund, G., Born, E. W. and Kirkegaard, M. (2007), 'Are liver and renal lesions in east greenland polar bears (ursus maritimus) associated with high mercury levels?', *Environmental Health* **6**. Times Cited: 18.

Thompson, J. E. and Ravishankara, A. R. (1993), 'Kinetics of $O(^1D)$ reactions with bromocarbons', *International Journal of Chemical Kinetics* **25**(6), 479–487. ISI Document Delivery No.: LD490 Times Cited: 16 Cited Reference Count: 17 THOMPSON, JE RAVISHANKARA, AR JOHN WILEY & SONS INC NEW YORK.

UNEP (2000), *The Montreal Protocol on Substances that Deplete the Ozone Layer*, 6 edn, Ozone Secretariat United Nations Environment Programme, United Nations Environment Programme PO Box 30552 Nairobi Kenya.

Wayne, R. P. (1990), 'Atmospheric chemistry', *Science Progress* **74**(296), 379–409. ISI Document Delivery No.: GB538 Times Cited: 5 Cited Reference Count: 30 WAYNE, RP BLACKWELL SCIENCE LTD OXFORD Part 4.

Zhang, Q. Z., Wang, S. K. and Gu, Y. S. (2002), 'Direct ab initio and kinetic calculation for the abstraction reaction of atomic O (P-3) with CH_3Br', *Chemical Physics Letters* **352**(5-6), 521–528. Times Cited: 7.

Zhang, Z. Y., Saini, R. D., Kurylo, M. J. and Huie, R. E. (1992), 'A temperature-dependent kinetic-study of the reaction of the hydroxyl radical with CH_3Br', *Geophysical Research Letters* **19**(24), 2413–2416. Times Cited: 11.

A. Stability tests

The stability of the object compound alone is tested (experiment 1, 13 in Table A.1), such that any tendency for the molecules to stick to the wall or such is revealed. A concentration of the compound is inserted into the cell along with bath gas to a certain pressure, whereupon IR spectra are taken in the cell with some interval. The experiment extends for at least the same length of time as the kinetics experiments are estimated to last. To make sure the compound does not photodissociate, the UV-C lamps are then turned on for short periods with a following spectrum taken in a pattern resembling that of the kinetic tests (experiment 2, 15, see Table C.1). Also reactivity of CH_3Br towards both the reference compounds and the ozone are checked (experiments 3–4, 17, 19, 22), thus different gas mixes are tested as described above. In addition, photolysis of the reference compounds are investigated (experiment 4, 6, 21, 23). Due to time frames of the laboratory work, some of these experiments are combined. If the concentration of the compound changes during any of these tests, the results of the kinetic experiments will be more difficult to interpret. The results of the stability tests are presented in Table A.2 and in Figures A.1a–A.1h, where the relative change of the compound A is defined as $\frac{[A]_{t=end}-[A]_{t=0}}{[A]_{t=0}}$. Results are obtained using a weighted least square linear fit algorithm, described in Krystek and Anton (2007). The average value is obtained by including points from all stability tests into one fit. There is a substantial instability in all tests for all compounds. The very long stability test 22 (64 h 39 min), has the curious feature that the object compound seems to decrease over time as opposed to every other test where the concentrations rather increases over time. It should be kept in mind here that it is only the first and last point that influence the result in Table A.2. The evolution of concentrations can be more carefully studied in Figure A.1h, where a clear initial increase is visible. Furthermore, the concentrations are given in ppm, such that a significant pressure increase (e.g. due to leakage) could distort the result and imply an apparent concentration decrease. Such a pressure increase is though not noted. This number should in any case be viewed with some caution. The isotope effect, defined as (3.8), is on average non-existing (=1). Because of severe stability problems that occurred in experiments 1–12, stability test were performed prior to each kinetic test 25–31, named 25–31a in Table A.1. From these tests a linear trend of the reference and CH_3Br concentrations are obtained and the corresponding levels in the subsequent kinetic tests could be corrected thereby, see Figures A.3–A.9. The average rate of change is tabulated in Table A.3. The photolysis test plots are presented in Figures A.10a–A.10e. The results are very hard to interpret because of the instability problems. Examining Figure A.10e, where stability was achieved (Figure A.1h), there seems to be some decrease of CH_3Br. The isotope effect is calculated from a weighted total least square fit (Krystek and Anton, 2007) of points from all photolysis test, see Figure A.11, resulting in a value of the isotope effect to be 0.9 ± 0.5. The result covers the expected unity slope and no correction is called for.

Table A.1.: *Stability test setup information (in the order they were conducted): type reference compound pressure and temporal duration*

Experiment	Type	Reference	Total pressure (mbar)	Duration (HH:MM)
1	Stability		1000	01:16
2	Photolysis		1000	00:55
3	Stability	CH_4,CH_3OH,N_2O[a]	1000	01:16
4	Photolysis	CH_4,CH_3OH,N_2O[a]	1000	01:02
5	Stability	(O_3)	1000	00:35
6	Photolysis	(O_3)	1000	00:32
13	Stability		200	02:18
15	Photolysis		200	00:54
16	Stability		200	18:22
17	Stability	CH_4[b]	200	02:40
19	Stability	C_2H_6	200	02:34
21	Photolysis	C_2H_6	200	00:16
22	Stability	CH_4	200	64:39
23	Photolysis	CH_4	200	00:28
25a	Stability	CH_4	1000	01:34
26a	Stability	C_2H_6	1000	15:23[c]
27a	Stability	C_2H_6	1000	01:25
28a	Stability	CH_4	1000	00:34
29a	Stability	CH_4	50	01:23
30a	Stability	CH_4	50	01:29
31a	Stability	CH_4	50	19:29[c]

[a] References N_2O and CH_3OH was used in experiments finally excluded from this report
[b] CH_4 is added to the mix in test 16
[c] Points taken before 2 h prior to start of the kinetic test (photolysis) are not used in the linear trend calculations, since trends on longer timescales are non-linear

Table A.2.: *Stability test results: duration; relative change of object and reference compound concentrations and isotope effect*

Experiment	Reference	Duration (HH:MM)	Relative change, $\frac{\Delta[A]}{[A]_{t=0}}$		Isotope Effect
			CH_3Br	Reference	$\frac{\ln\left(\left[CH_3\,^{79}Br\right]_{t=0}\Big/\left[CH_3\,^{79}Br\right]_t\right)}{\ln\left(\left[CH_3\,^{81}Br\right]_{t=0}\Big/\left[CH_3\,^{81}Br\right]_t\right)}$
1		01:16	0.1123 ± 0.0044		0.79 ± 0.31
3	CH_4	01:16	0.0192 ± 0.007	0.0255 ± 0.0029	1 ± 3.3
	CH_3OH			-0.022 ± 0.014	
	N_2O			0.0910 ± 0	
5	(O_3)	00:35	0.0104 ± 0.0042	0.0201 ± 0.0016	0.3 ± 2.6
13		02:18	0.1789 ± 0.0034		1.028 ± 0.084
16		18:22	0.2642 ± 0.0036		1.003 ± 0.034
17	CH_4	02:40		-0.0207 ± 0.0075	
19	C_2H_6	02:34	0.0785 ± 0.0039	0.158 ± 0.096	1.04 ± 0.2
22	CH_4	64:39	-0.0088 ± 0.0072	0.08 ± 0.0074	1 ± 1.2
Average[a]					1.004 ± 0.031

[a] Weighted average as defined by (3.6)

Table A.3.: *Preparatory stability test results: duration; relative change per hour of object and reference compound concentrations, change defined as percentage of initial value, average over a period from t=end–duration time to t=end*

Experiment	Reference	Duration (HH:MM)	Rate of change, % / h	
			CH_3Br	Reference
25a	CH_4	01:34	−0.5	−1.8
26a	C_2H_6	00:23	0.4	2.1
27a	C_2H_6	01:25	−0.1	−0.3
28a	CH_4	00:34	0.3	−0.3
29a	CH_4	01:23	1.4	−1.2
30a	CH_4	01:29	2.0	−0.6
31a	CH_4	01:13	3.6	−0.2

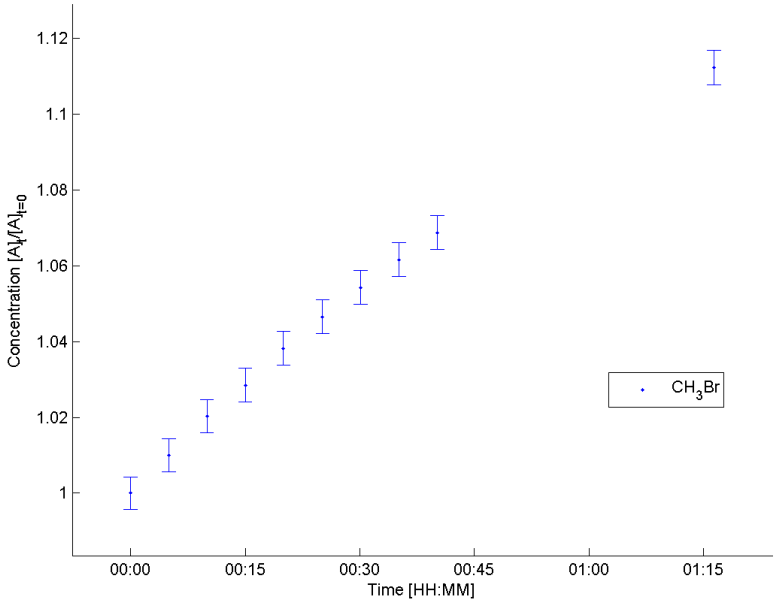

(a) Test 1

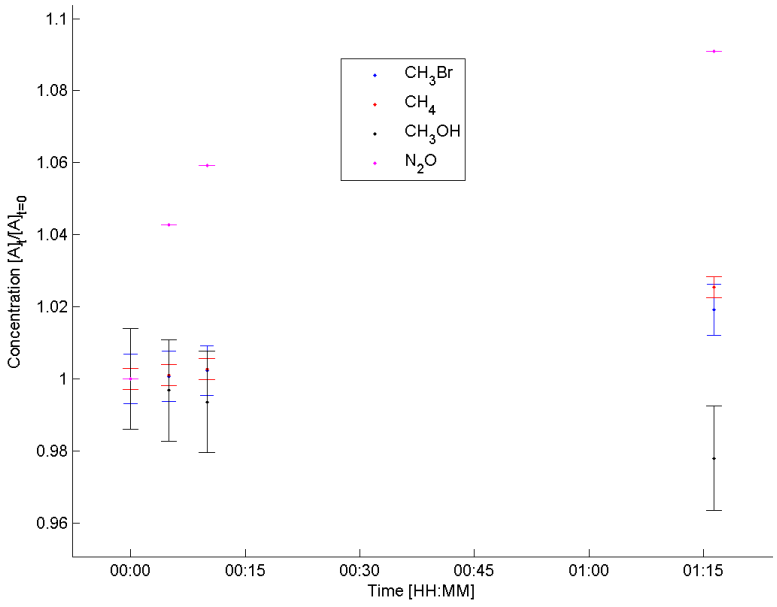

(b) Test: 3, reactions with reference compounds CH_4, CH_3OH and N_2O

Figure A.1.: *Stability tests*

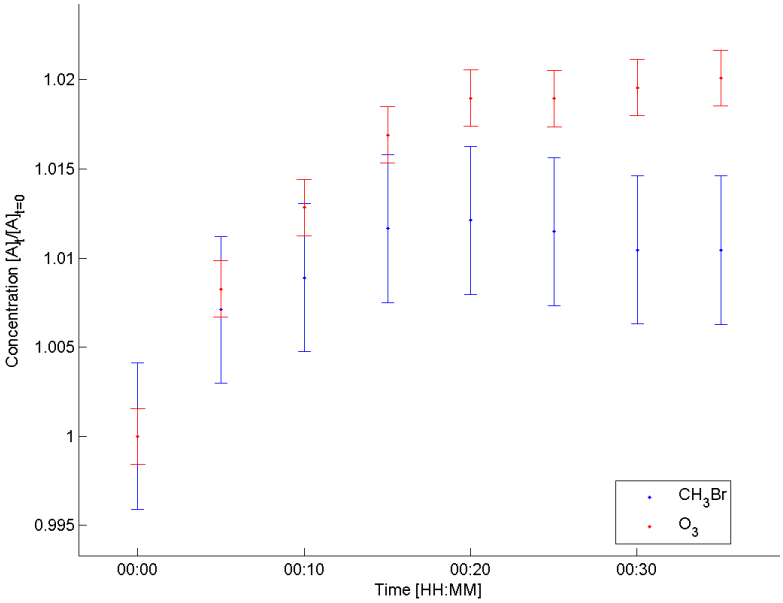

(c) Test: 5, reactions with O_3

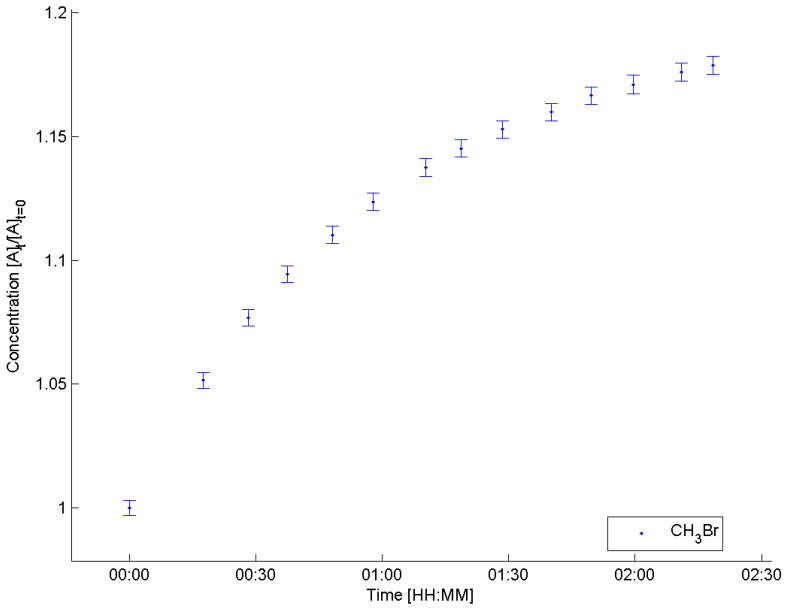

(d) Test: 13

Figure A.1.: *Stability tests, continued from previous page*

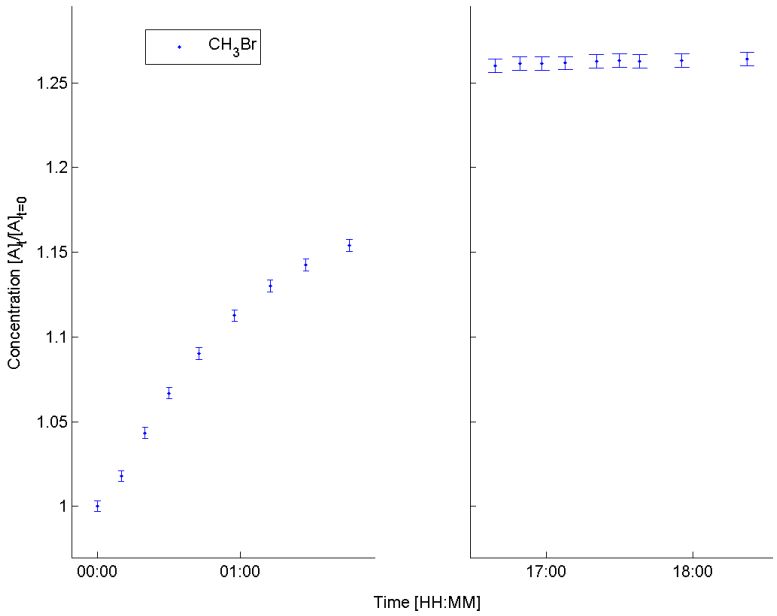

(e) Test: 16

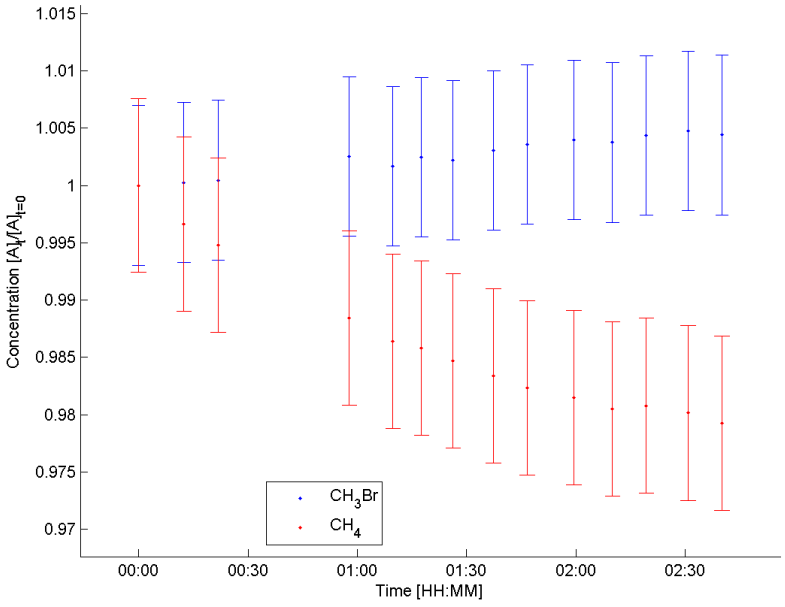

(f) Test: 17, reference compound CH_4 added to 16

Figure A.1.: *Stability tests, continued from previous page*

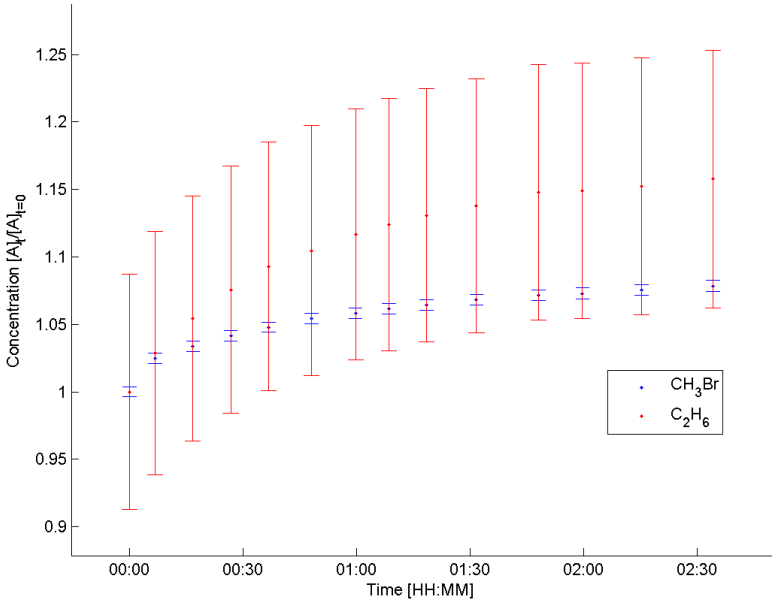

(g) Test: 19, reactions with C_2H_6

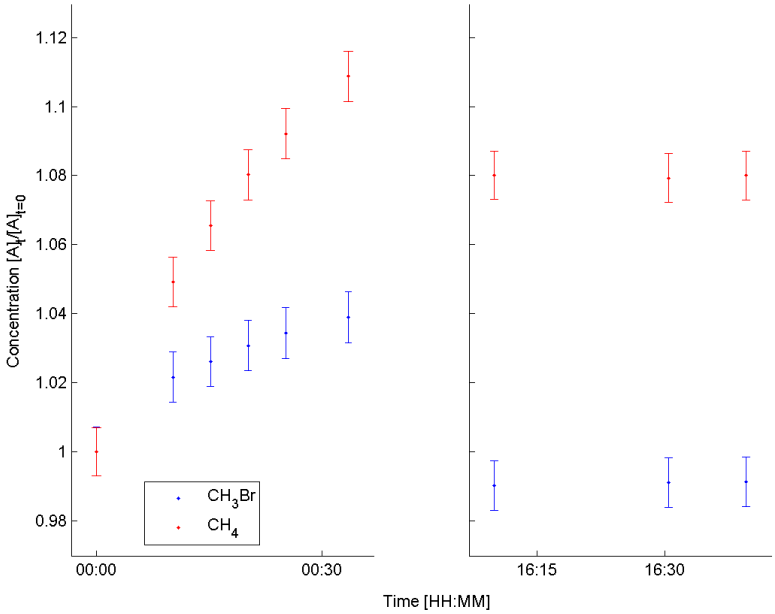

(h) Test: 22, reactions with CH_4

Figure A.1.: *Stability tests, continued from previous page*

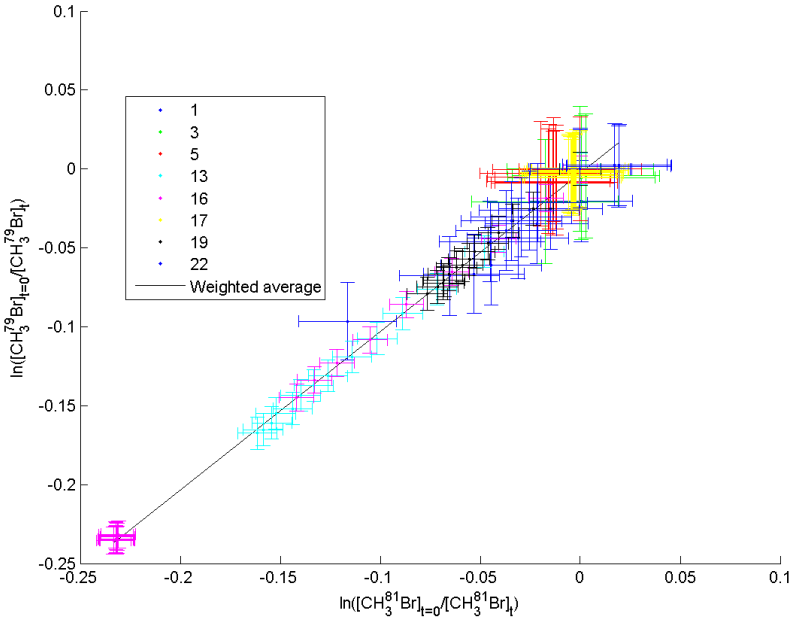

Figure A.2.: *Stability tests: isotope effect, different colours refer to different test named in legend*

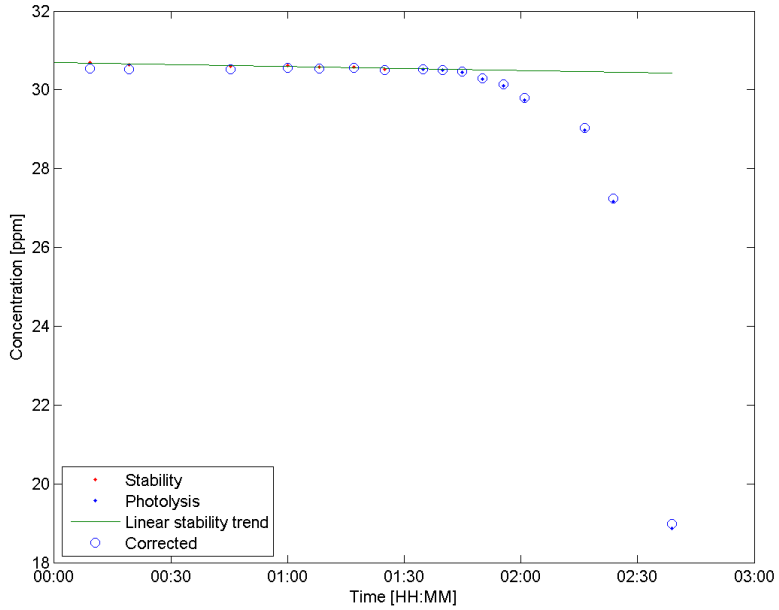

(a) CH_3Br

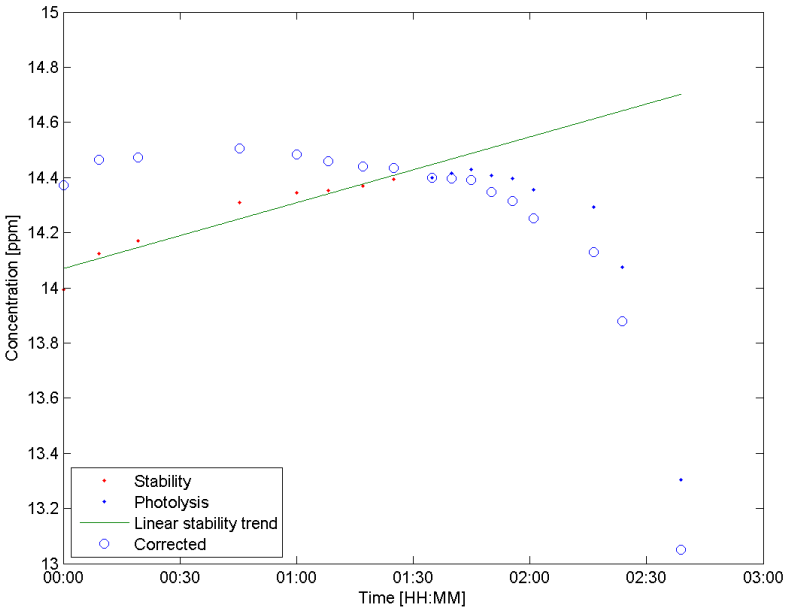

(b) Reference compound CH_4

Figure A.3.: *Correction curve, experiment 25*

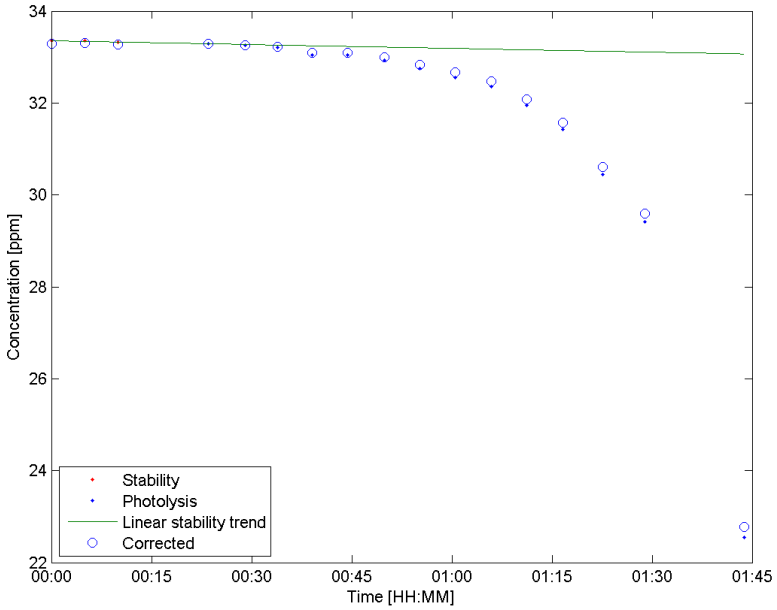

(a) CH_3Br

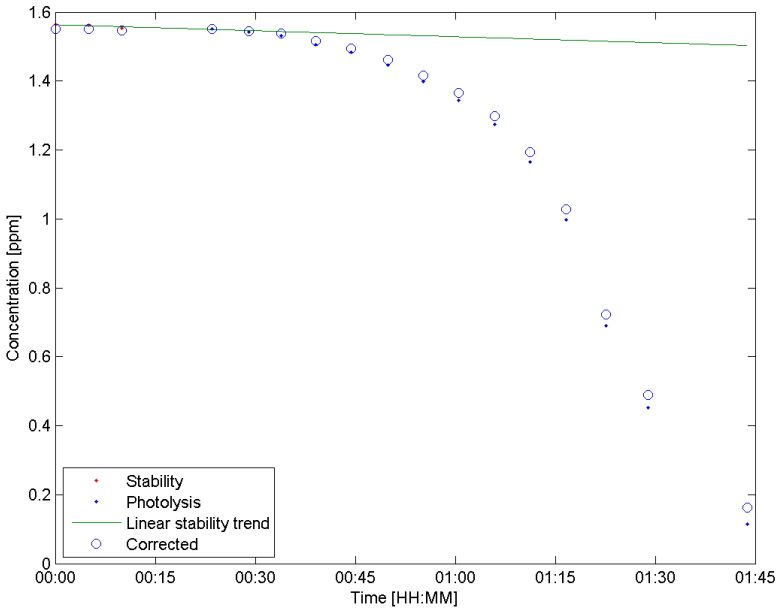

(b) Reference compound C_2H_6

Figure A.4.: *Correction curve, experiment 26*

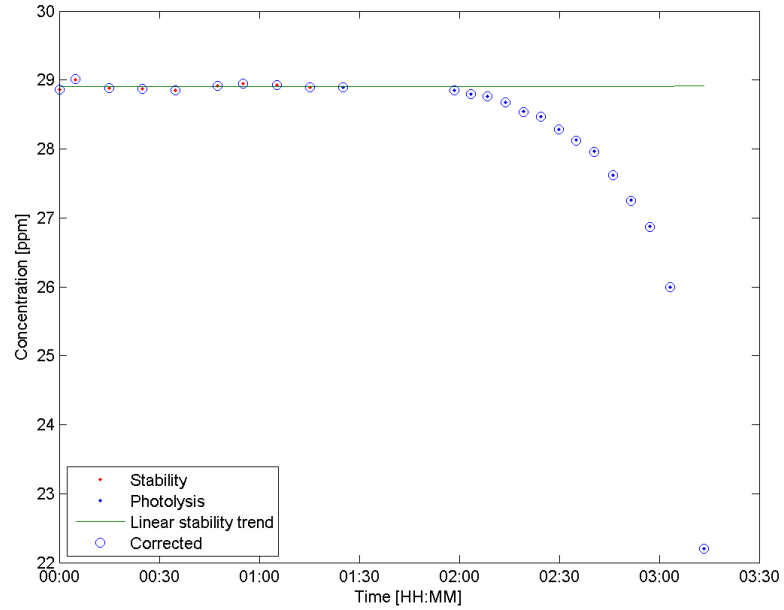

(a) CH_3Br

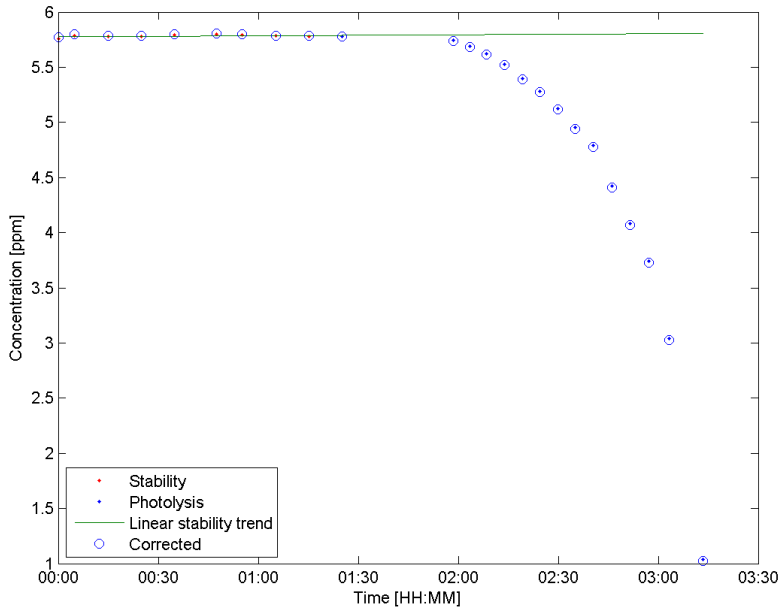

(b) Reference compound C_2H_6

Figure A.5.: *Correction curve, experiment 27*

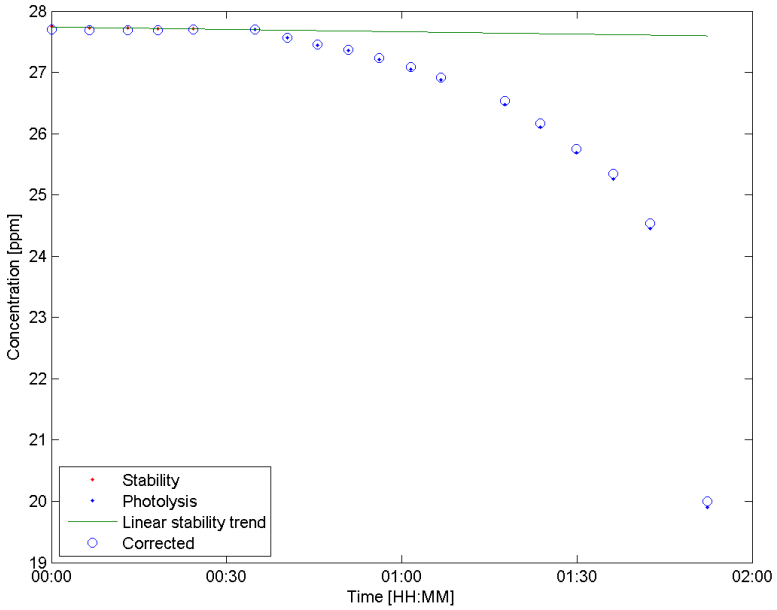

(a) CH_3Br

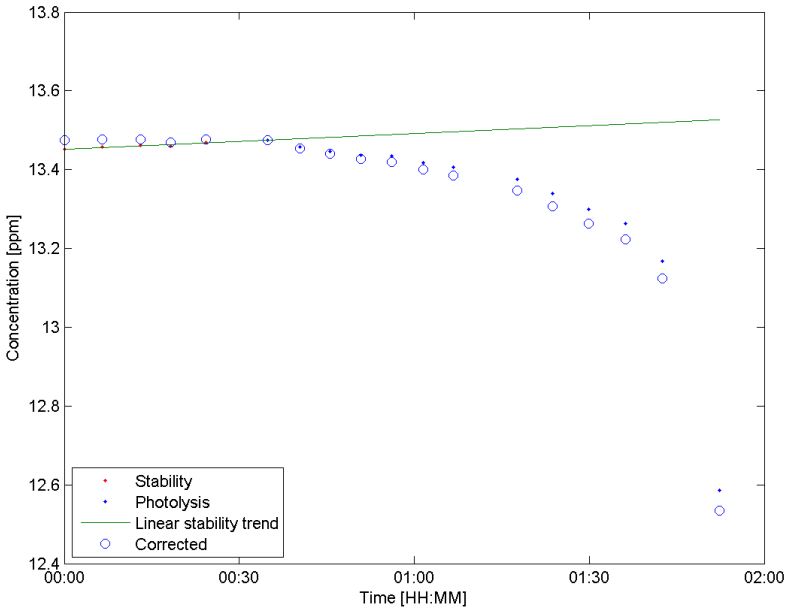

(b) Reference compound CH_4

Figure A.6.: *Correction curve, experiment 28*

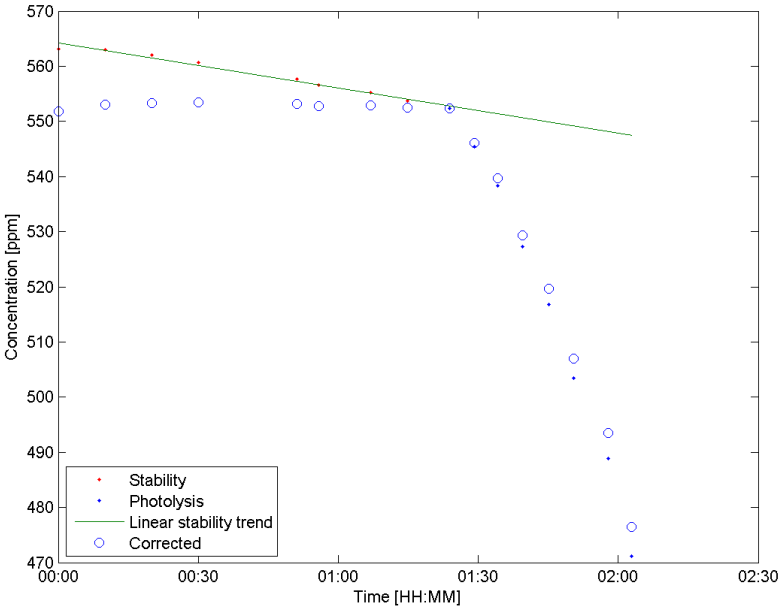

(a) CH_3Br

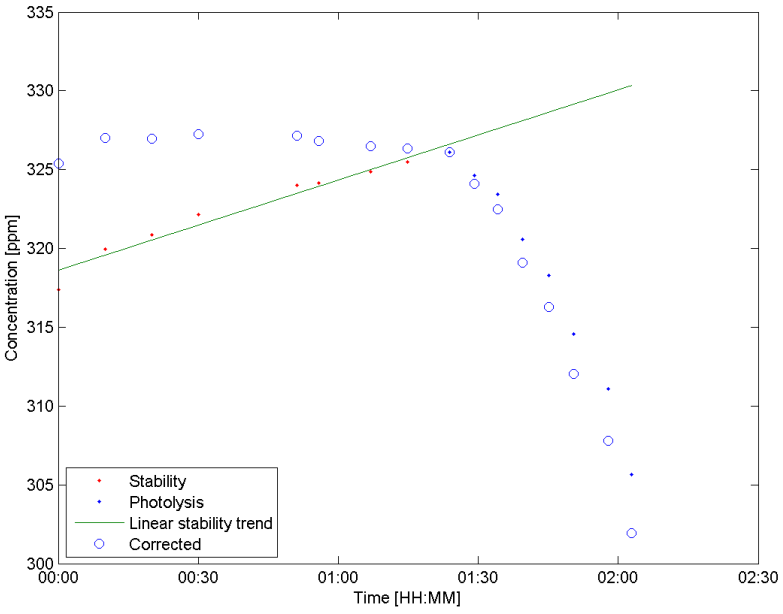

(b) Reference compound CH_4

Figure A.7.: *Correction curve, experiment 29*

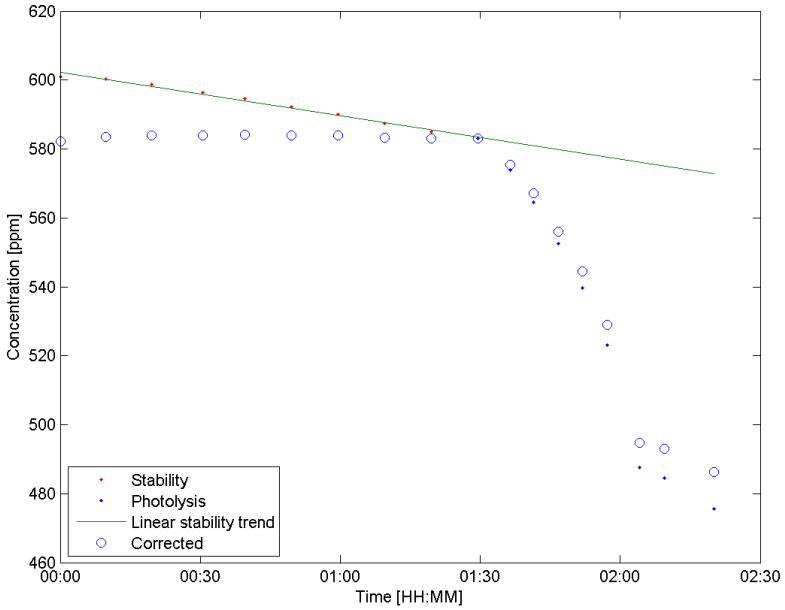

(a) CH_3Br

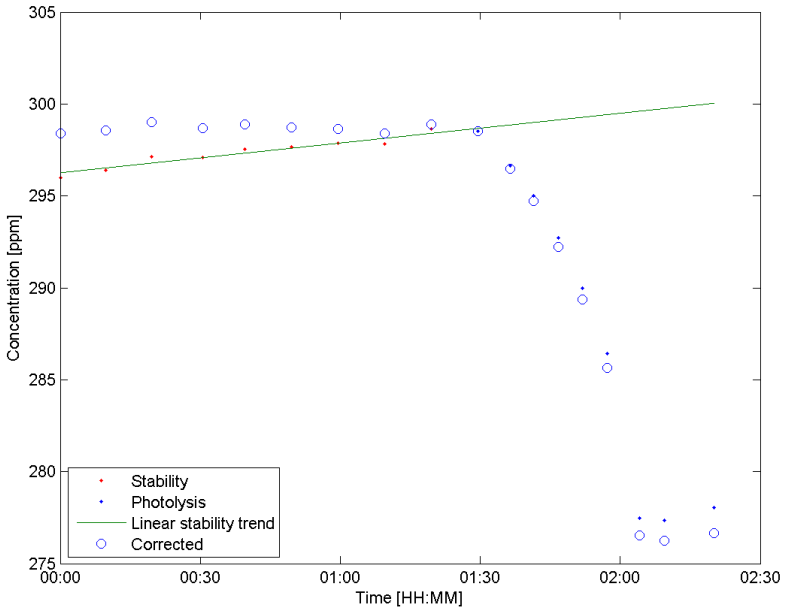

(b) Reference compound CH_4

Figure A.8.: *Correction curve, experiment 30*

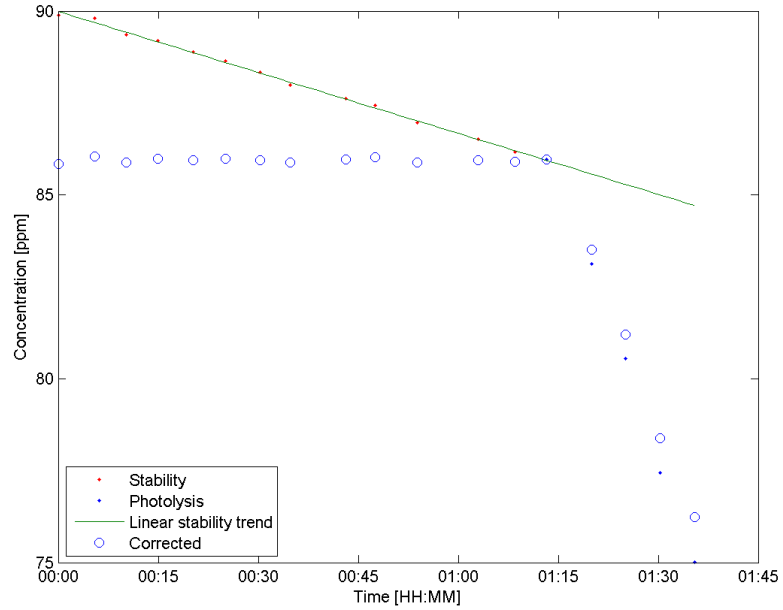

(a) CH_3Br

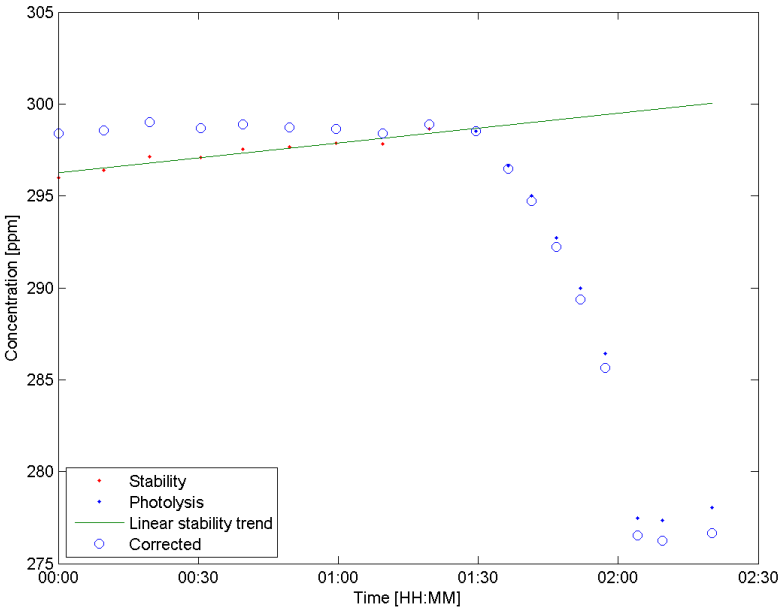

(b) Reference compound CH_4

Figure A.9.: *Correction curve, experiment 31*

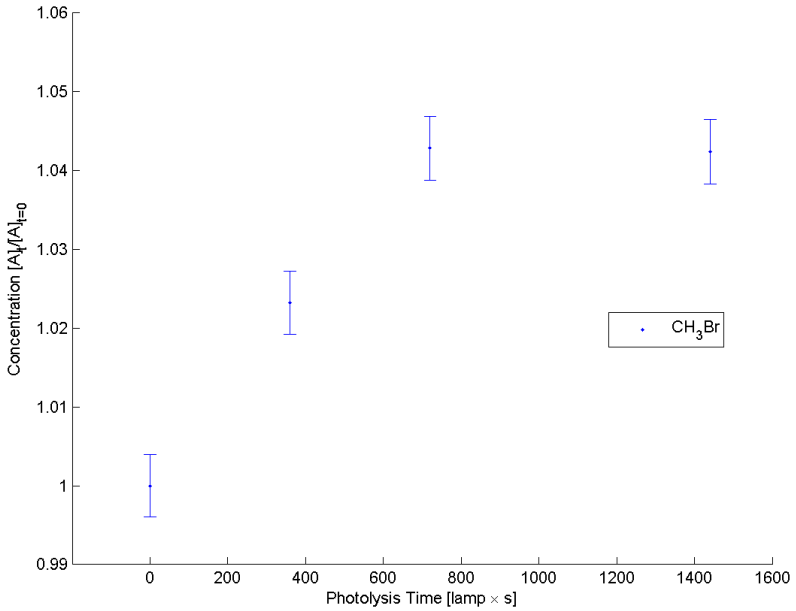

(a) Test: 2

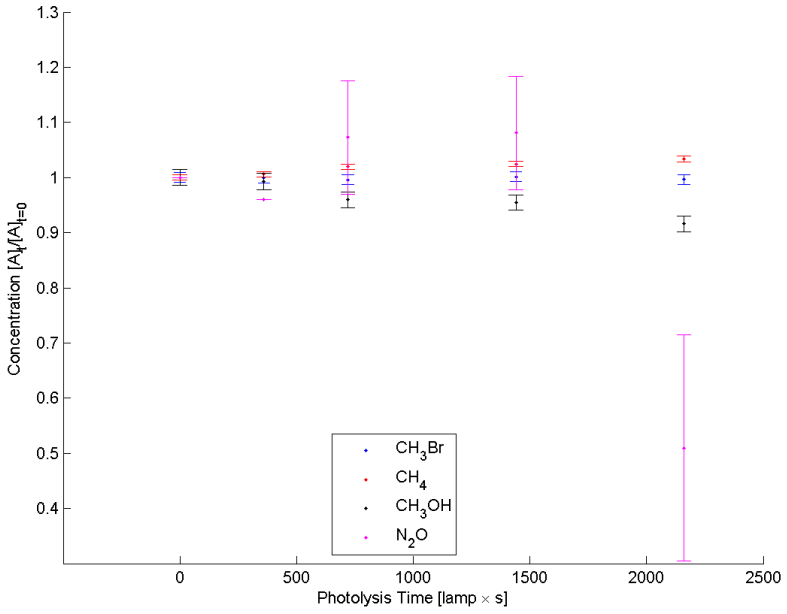

(b) Test: 5, with reference compounds CH_4, CH_3OH and N_2O

Figure A.10.: *Photolysis tests*

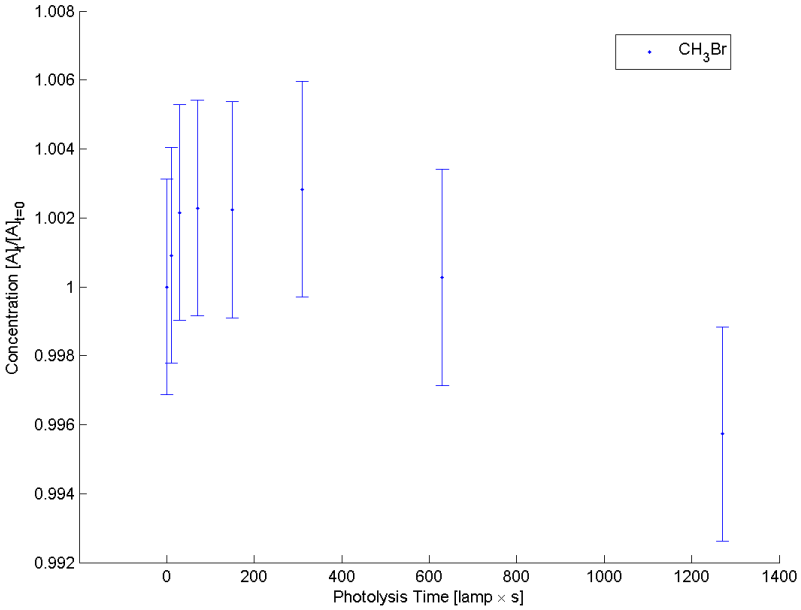

(c) Test: 15

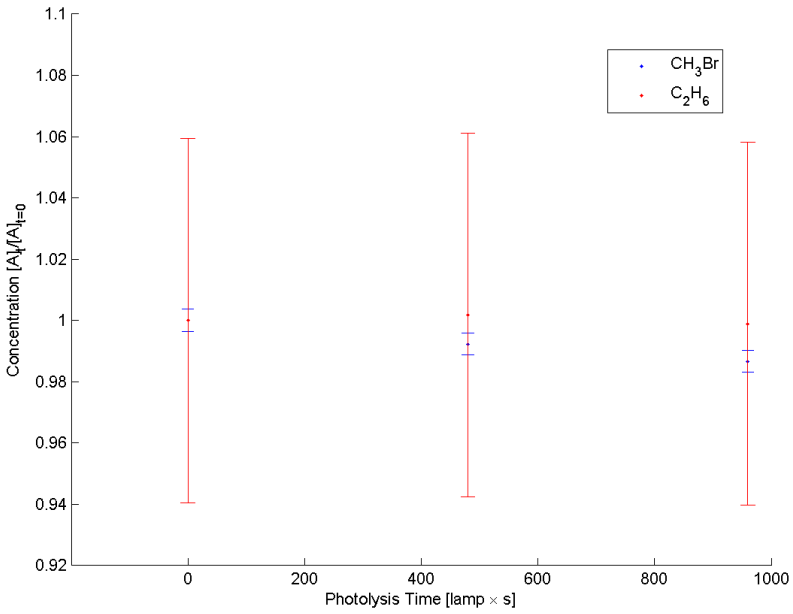

(d) Test: 21, with reference compound C_2H_6

Figure A.10.: *Photolysis tests, continued from previous page*

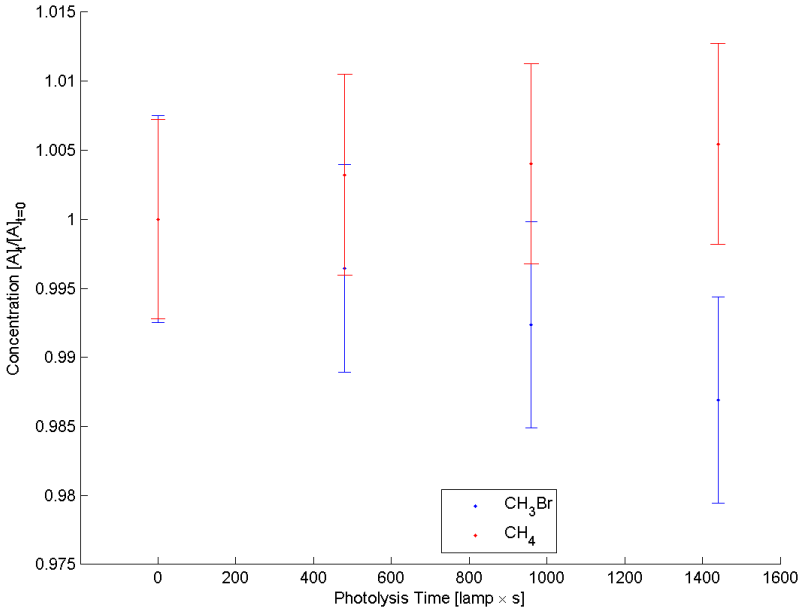

(e) Test: 23, with reference compound CH_4

Figure A.10.: *Photolysis tests, continued from previous page*

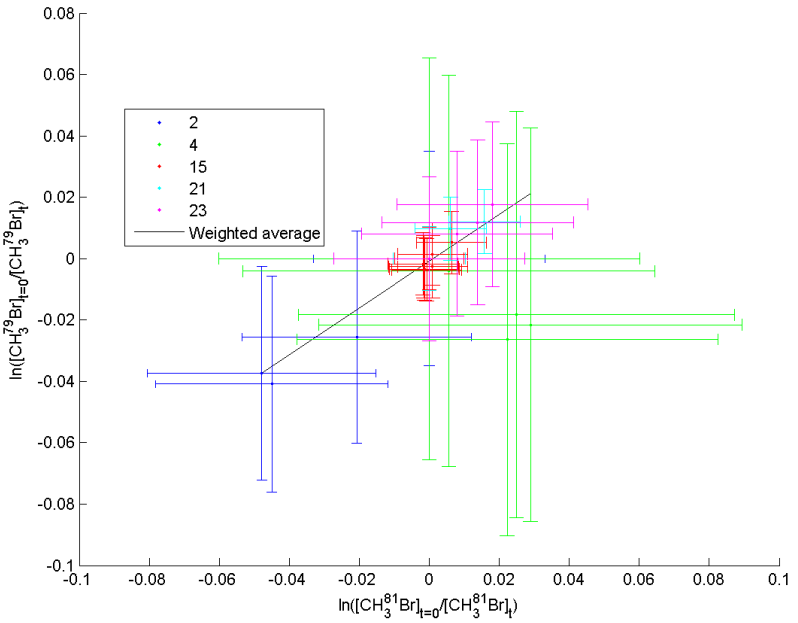

Figure A.11.: *Photolysis tests: isotope effect, different colours refer to different test named in legend*

B. Dilution tests

Gas mix and pressures like those used in kinetics experiments are prepared and a spectrum is taken of the cell. Some volume of the cell is pumped out and the cell is then refilled with bath gas to the initial pressure, whereupon a new spectrum is taken. The procedure is repeated for a number of points. All the species should be diluted in the chamber by the same rate. The analysis can be trusted only if it can reproduce such a development of concentrations. The dilution tests are performed as a reference rate test. N_2O is used as a reference compound because it is relatively easy to analyze. Ideally the relation should be linear with a slope equal to unity. Gas mixes of tests 14 and 20 have resided in the cell less than 3 h each, whereas the other tests have stability times over 16 h (see Table 3.1); tests 14 and 20 are therefore discarded due to instability. Table B.1 show a compound for compound weighted average (see (3.6)). Compounds CH_4 and CH_3Br (including both isotopes) have dilution rates of unity within error margins. The points in Figure B.1a are especially scattered, even disregarding tests 14 and 20, suggesting that H_2O is particularly difficult to analyze. C_2H_6 is present in test 20 only, so its dilution rate is not listed in Table B.1. CO_2 and CO shows minor deviations from unity, indicating that analysis of these compounds are less trustworthy than those of CO_2 and CH_3Br. The deviations are, however, too small and too uncertain to call for any form of calibration.

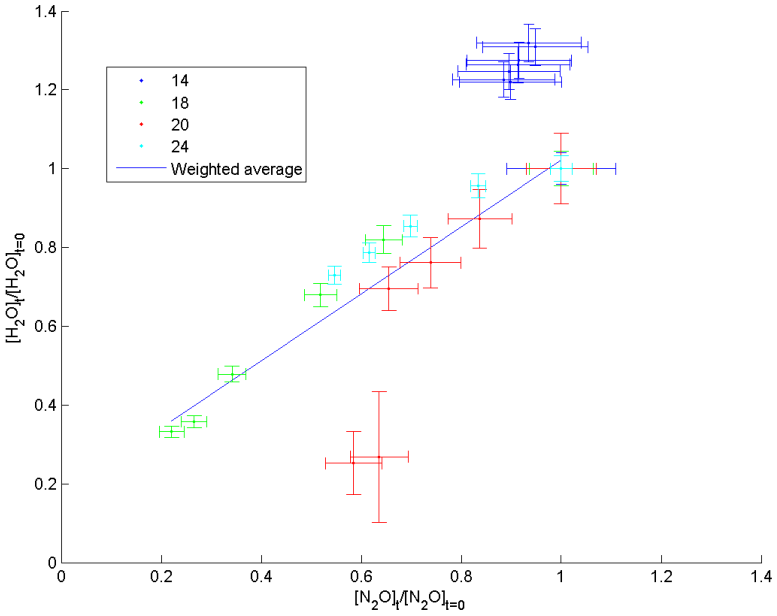

(a) H_2O

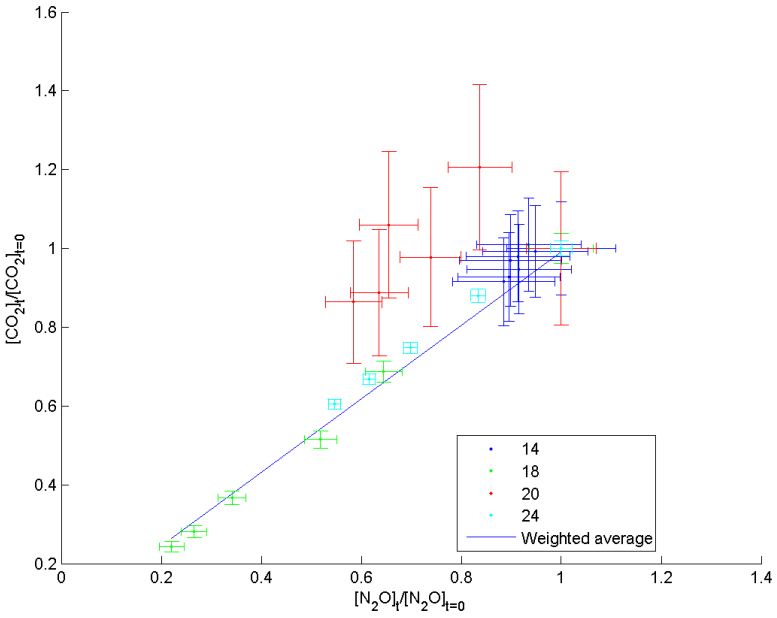

(b) CO_2

Figure B.1.: *Dilution tests, compound by compound*

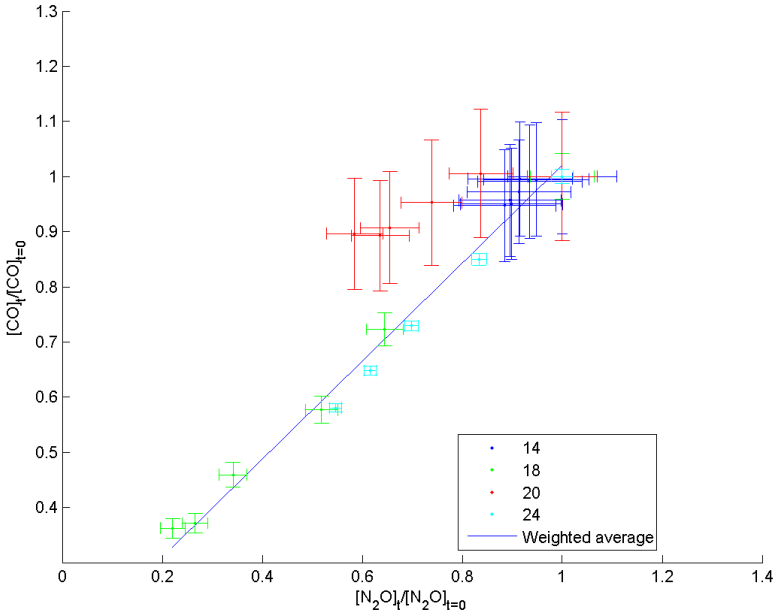

(c) CO

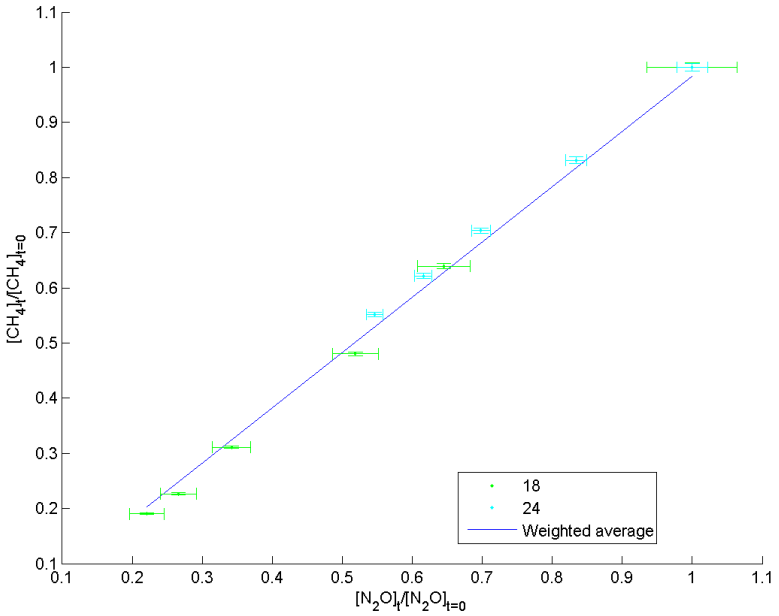

(d) CH_4

Figure B.1.: *Dilution tests, continued from previous page*

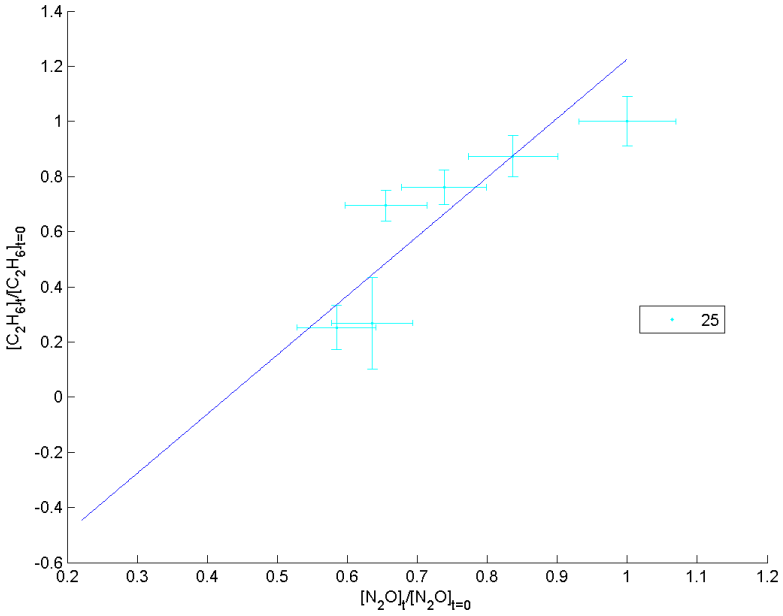

(e) C_2H_6

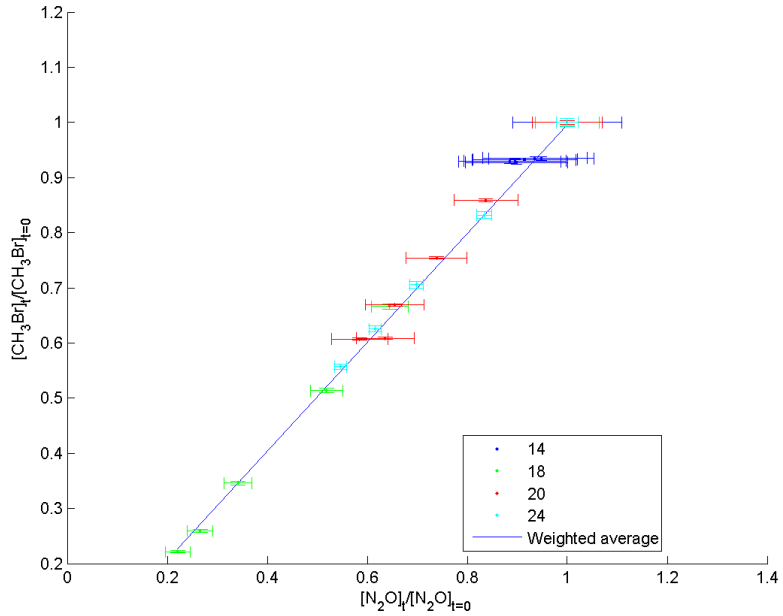

(f) CH_3Br

Figure B.1.: *Dilution tests, continued from previous page*

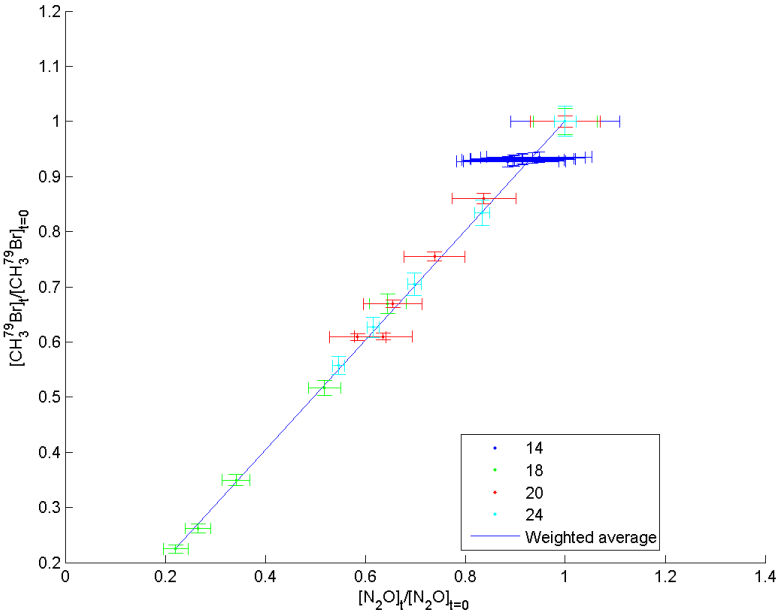

(g) $CH_3^{79}Br$

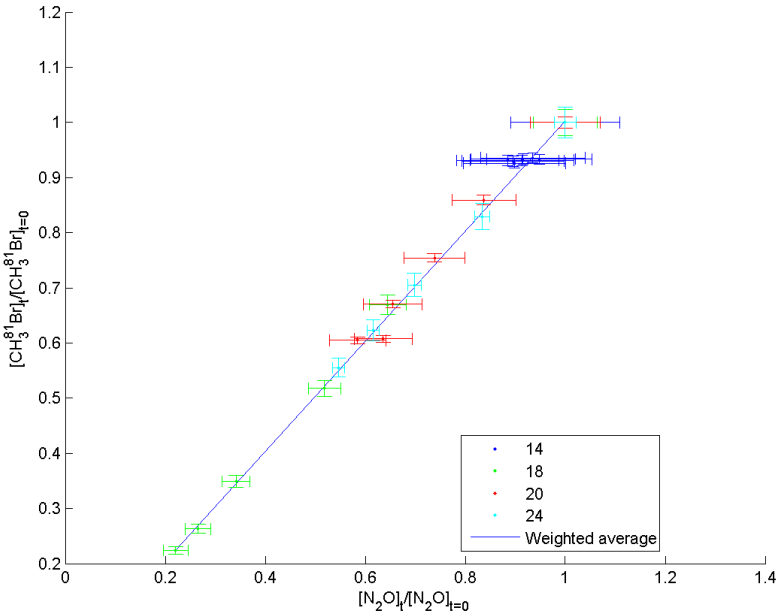

(h) $CH_3^{81}Br$

Figure B.1.: *Dilution tests, continued from previous page*

Table B.1.: *Dilution test results; relative rate of dilution for each compound with N_2O as reference*[a]

Compound (A)	Relative rate $\left(\frac{[A]_t}{[A]_{t=0}} \Big/ \frac{[\mathrm{N_2O}]_t}{[\mathrm{N_2O}]_{t=0}}\right)$
H_2O	0.848 ± 0.061
CO_2	0.932 ± 0.048
CO	0.888 ± 0.042
CH_4	1.002 ± 0.039
CH_3Br	0.986 ± 0.038
$CH_3^{79}Br$	0.996 ± 0.051
$CH_3^{81}Br$	0.998 ± 0.051

[a] Gas mixes of tests 14 and 20 have resided in the cell less than 3 h each, whereas the other tests have stability time over 16 h; tests 14 and 20 are therefore discarded due to instability

C. Tables

Table C.1.: *Photolysis time steps*

Point	**Experiment**, Number of lamps × time [s], Accumulated photolysis time [lamp × s]			
	2	**4**	**6**	**7**
1	$4 \times 90, 360$	$4 \times 90, 360$	$4 \times 120, 480$	$4 \times 120, 480$
2	$4 \times 90, 720$	$4 \times 90, 720$	$4 \times 120, 960$	$4 \times 120, 960$
3	$4 \times 180, 1440$	$4 \times 180, 1440$	$4 \times 120, 1440$	$4 \times 120, 1440$
4	$4 \times 180, 2160$	$4 \times 180, 2160$	$4 \times 120, 1920$	$4 \times 120, 1920$
5			$4 \times 120, 2400$	$4 \times 120, 2400$
6			$4 \times 240, 3360$	$4 \times 240, 3360$
7			$4 \times 240, 4320$	$4 \times 240, 4320$
8			$4 \times 600, 6720$	$6 \times 600, 7920$
	8	**9**	**10**	**11**
1	$4 \times 120, 480$	$1 \times 15, 15$	$1 \times 15, 15$	$1 \times 15, 15$
2	$4 \times 120, 960$	$1 \times 15, 30$	$1 \times 15, 30$	$1 \times 15, 30$
3	$4 \times 60, 1200$	$2 \times 15, 60$	$1 \times 15, 45$	$1 \times 15, 45$
4	$4 \times 60, 1440$	$2 \times 15, 90$	$1 \times 15, 60$	$1 \times 15, 60$
5	$4 \times 60, 1680$	$2 \times 15, 120$	$1 \times 15, 75$	$1 \times 15, 75$
6	$4 \times 120, 2160$	$2 \times 15, 150$	$1 \times 15, 90$	$2 \times 15, 105$
7	$4 \times 300, 3360$	$2 \times 30, 210$	$1 \times 15, 105$	$2 \times 30, 165$
8	$4 \times 600, 5760$	$2 \times 30, 270$	$1 \times 15, 120$	$2 \times 30, 225$
9		$2 \times 30, 330$	$1 \times 15, 135$	$4 \times 30, 345$
10		$2 \times 30, 390$	$6 \times 60, 495$	$4 \times 30, 465$
11		$2 \times 30, 450$		$4 \times 60, 705$
12		$2 \times 30, 510$		$4 \times 60, 945$
13		$2 \times 30, 570$		$4 \times 120, 1425$
14		$2 \times 30, 630$		$6 \times 300, 3225$
15		$2 \times 60, 750$		
16		$2 \times 60, 870$		
17		$6 \times 60, 1230$		

Continued on next page

Table C.1 – *continued from previous page*

Point	**Experiment**, Number of lamps × time [s], Accumulated photolysis time [lamp × s]			
	15	**21**	**23**	**25**
1	$1 \times 10, 10$	$4 \times 120, 480$	$4 \times 120, 480$	$1 \times 10, 10$
2	$1 \times 20, 30$	$4 \times 120, 960$	$4 \times 120, 960$	$1 \times 20, 30$
3	$1 \times 40, 70$		$4 \times 120, 1440$	$1 \times 40, 70$
4	$2 \times 40, 150$			$2 \times 40, 150$
5	$4 \times 40, 310$			$4 \times 40, 310$
6	$4 \times 80, 630$			$4 \times 80, 630$
7	$4 \times 160, 1270$			$4 \times 160, 1270$
8				$6 \times 600, 4870$
	26	**27**	**28**	**29**
1	$1 \times 10, 10$	$1 \times 20, 20$	$1 \times 40, 40$	$2 \times 30, 60$
2	$1 \times 10, 20$	$1 \times 20, 40$	$1 \times 40, 80$	$2 \times 30, 120$
3	$1 \times 20, 40$	$1 \times 20, 60$	$1 \times 40, 120$	$2 \times 40, 200$
4	$1 \times 20, 60$	$1 \times 40, 100$	$1 \times 40, 160$	$2 \times 40, 280$
5	$1 \times 40, 100$	$1 \times 40, 140$	$2 \times 40, 240$	$2 \times 50, 380$
6	$1 \times 40, 140$	$1 \times 40, 180$	$2 \times 40, 320$	$2 \times 50, 480$
7	$2 \times 40, 220$	$2 \times 40, 260$	$2 \times 80, 480$	$4 \times 30, 600$
8	$2 \times 40, 300$	$2 \times 40, 340$	$2 \times 80, 640$	$4 \times 30, 720$
9	$4 \times 40, 460$	$2 \times 40, 420$	$2 \times 80, 800$	$6 \times 300, 2520$
10	$4 \times 40, 620$	$4 \times 40, 580$	$2 \times 80, 960$	
11	$4 \times 80, 940$	$4 \times 40, 740$	$4 \times 80, 1280$	
12	$4 \times 80, 1260$	$4 \times 40, 900$	$6 \times 300, 3080$	
13	$6 \times 600, 4860$	$4 \times 80, 1220$		
14		$6 \times 300, 3020$		
	30	**31**		
1	$2 \times 30, 60$	$2 \times 30, 60$		
2	$2 \times 30, 120$	$2 \times 30, 120$		
3	$2 \times 40, 200$	$2 \times 40, 200$		
4	$2 \times 40, 280$	$2 \times 40, 280$		
5	$2 \times 50, 380$			
6	$2 \times 110, 600$			
7	$4 \times 30, 720$			
8	$6 \times 360, 2880$			
9				
10				
11				
12				

Table C.2.: *Data points discarded in the relative rate calculations*

Experiment	Points	Note
9	1:6	Equilibrium not achieved
	11:17	Ozone levels under 20% of initial value
10	1,2	Equilibrium not achieved
	11	Ozone levels under 20% of initial value
12	1:6	Equilibrium not achieved
	12:14	Ozone levels under 20% of initial value
25	1,2	Equilibrium not achieved
	9	Ozone levels under 20% of initial value
26	10:14	Secondary chemistry
27	15	Ozone levels under 20% of initial value
28	13	Ozone levels under 20% of initial value
29	8	Ozone levels under 20% of initial value
30	7:9	Ozone levels under 20% of initial value

Table C.3.: *Discarded results: $CH_3Br + O(^1D) \longrightarrow$ products, reference reaction: $CH_4 + O(^1D) \longrightarrow$ products, uncorrected data, data adjusted to model*

Experiment	$k_{(\mathrm{R}\,3)}$ $\left(\mathrm{cm}^3/\mathrm{molecule\,s}\right)$	$S_{\mathrm{CH_3Br}}$	$S_{\mathrm{CH_4}}$
9	9.4870×10^{-10}	0.0041	0.0024
10	6.9370×10^{-10}	0.0051	0.0027
12	7.7865×10^{-10}	0.0051	0.0015

Table C.4.: *Results: $CH_3Br + O(^1D) \longrightarrow$ products, reference reaction: $CH_4 + O(^1D) \longrightarrow$ products, corrected data, data adjusted to model*

Experiment	Time of stabilisation (HH:MM)	$k_{(\mathrm{R}\,3)}$ $\left(\mathrm{cm}^3/\mathrm{molecule\,s}\right)$	$S_{\mathrm{CH_3Br}}$	$S_{\mathrm{CH_4}}$
29	01:23	1.4416×10^{-10}	0.0038	0.0026
30	01:29	1.9462×10^{-10}	0.0027	0.0013
31	19:29	4.3248×10^{-10}	0.0006	0.0009

Table C.5.: *Full Kinetic Isotope Effect results: OH, KIE defined as* (3.8)*, all points before 80% of the initial ozone is consumed are used, unless where indicated*

Experiment	KIE
25	0.98 ± 0.82
26	1.08 ± 0.80
26 (selected points)	0.6 ± 2.4
27	1.14 ± 0.70
28	1.2 ± 1.0

D. Figures

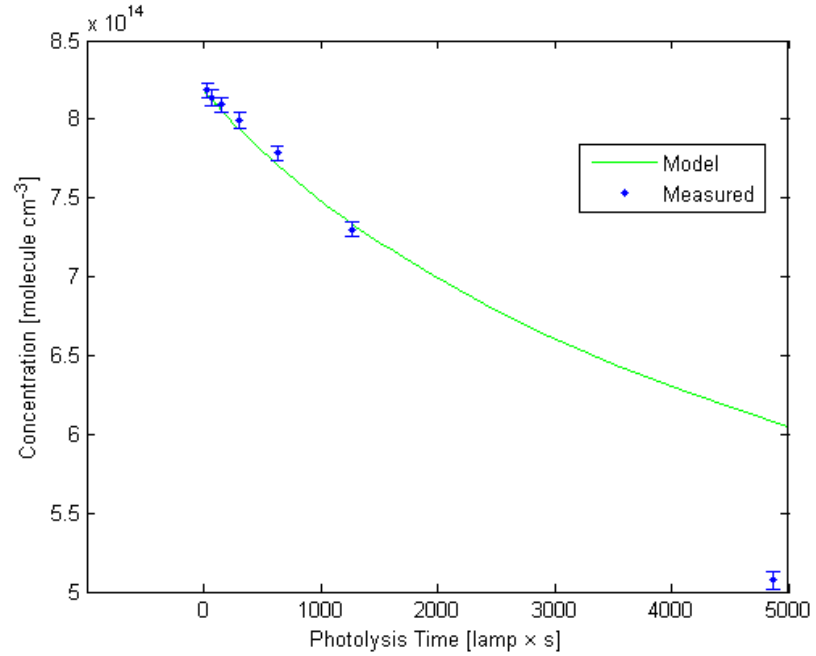

(a) CH_3Br

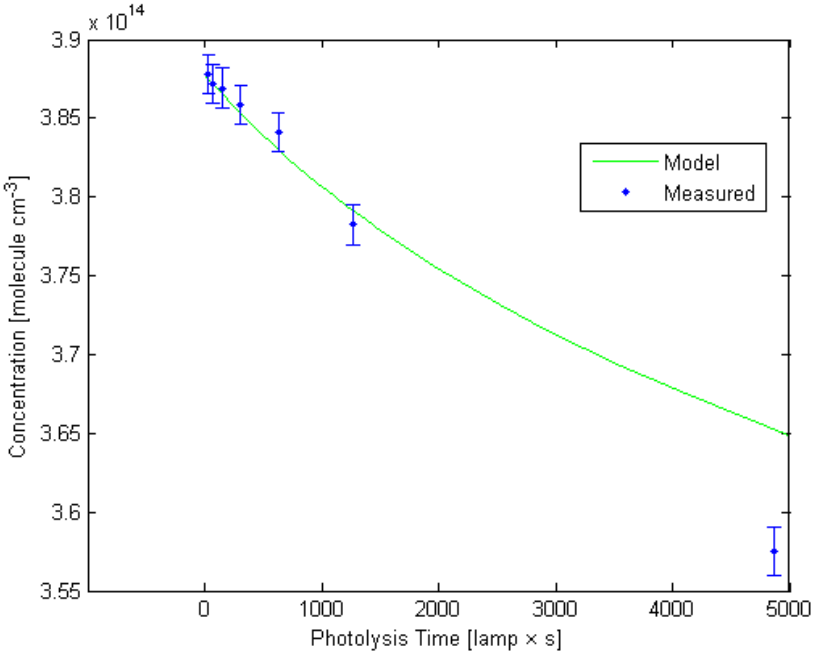

(b) CH_4

Figure D.1.: *Model and measured results, experiment 25*

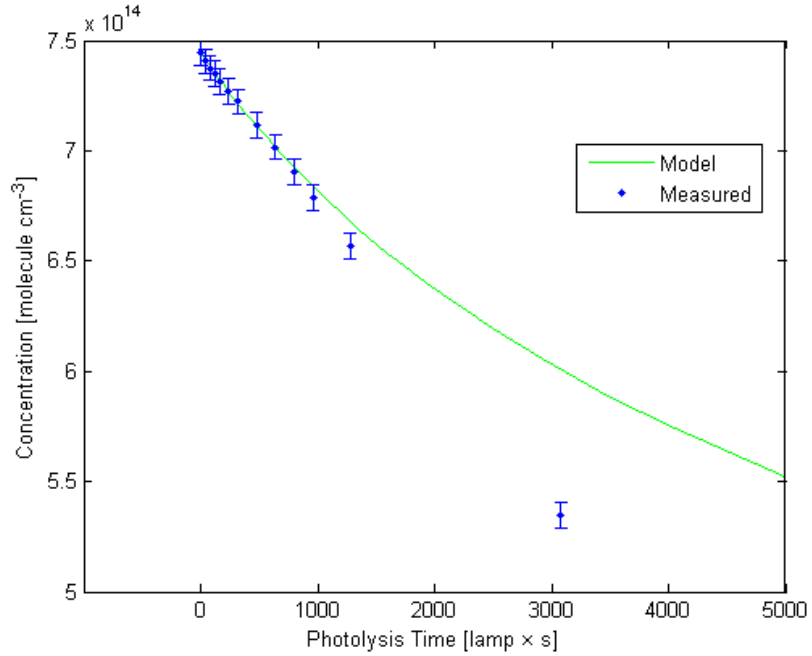

(a) CH_3Br

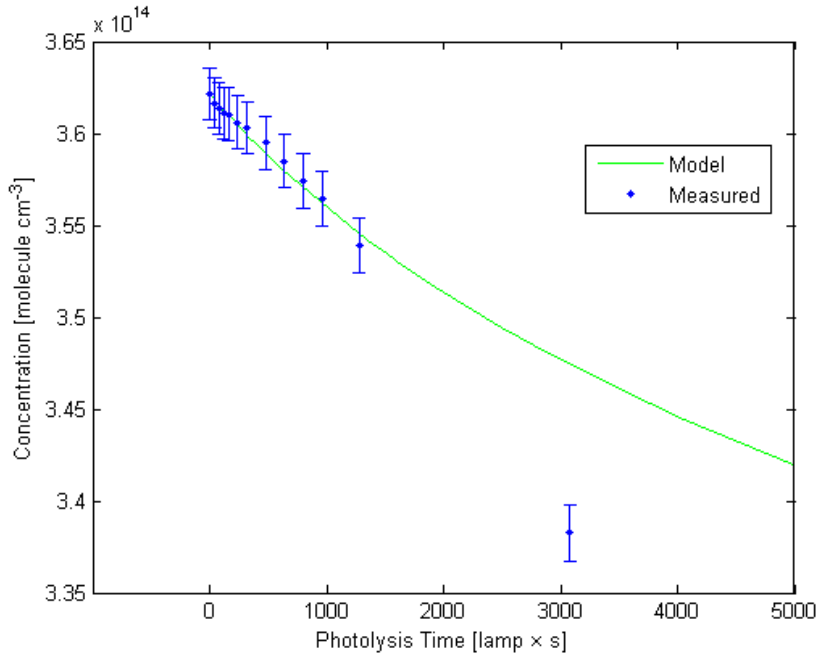

(b) CH_4

Figure D.2.: *Model and measured results, experiment 28*

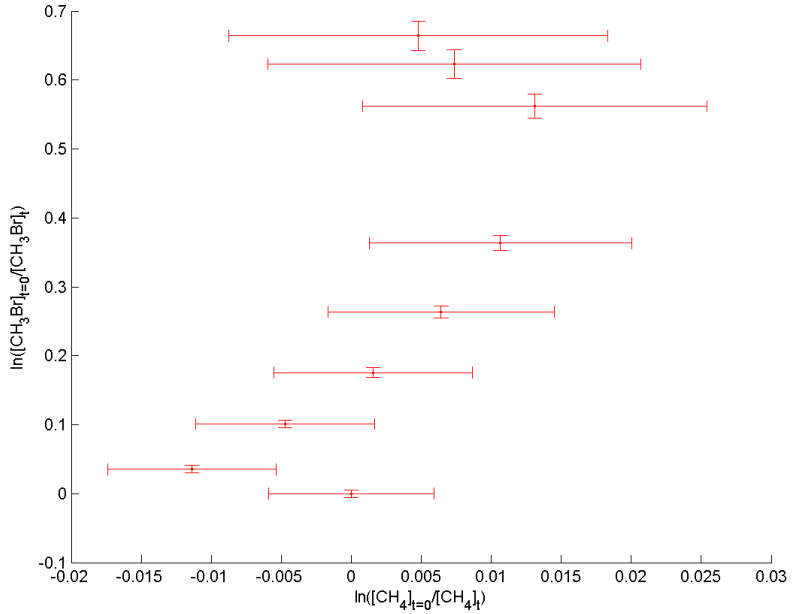

(a) Experiment 7

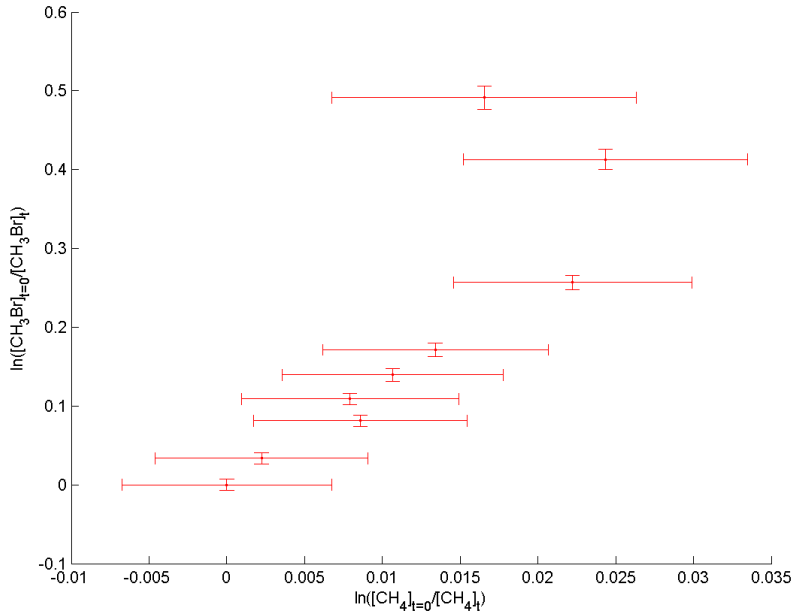

(b) Experiment 8

Figure D.3.: *Relative rate, OH experiments*

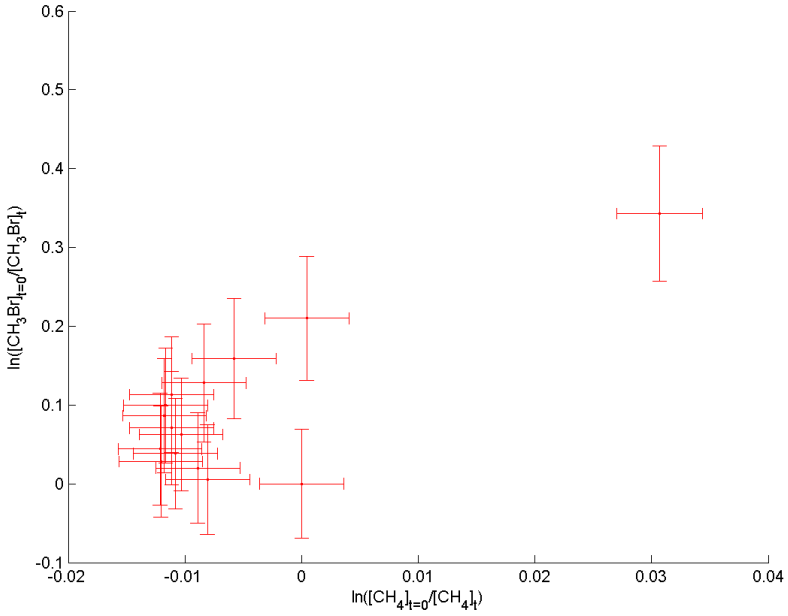

(c) Experiment 11

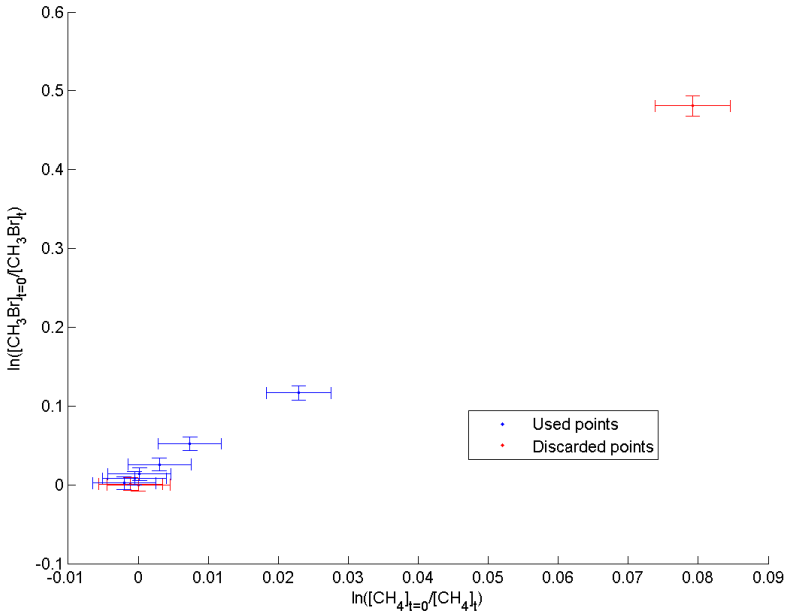

(d) Experiment 25

Figure D.3.: *Relative rate, OH experiments, continued from previous page*

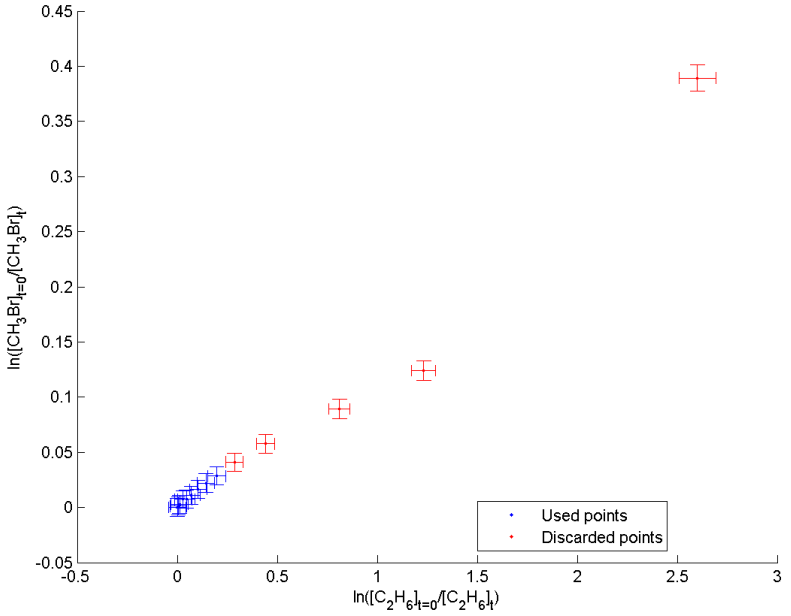

(e) Experiment 26

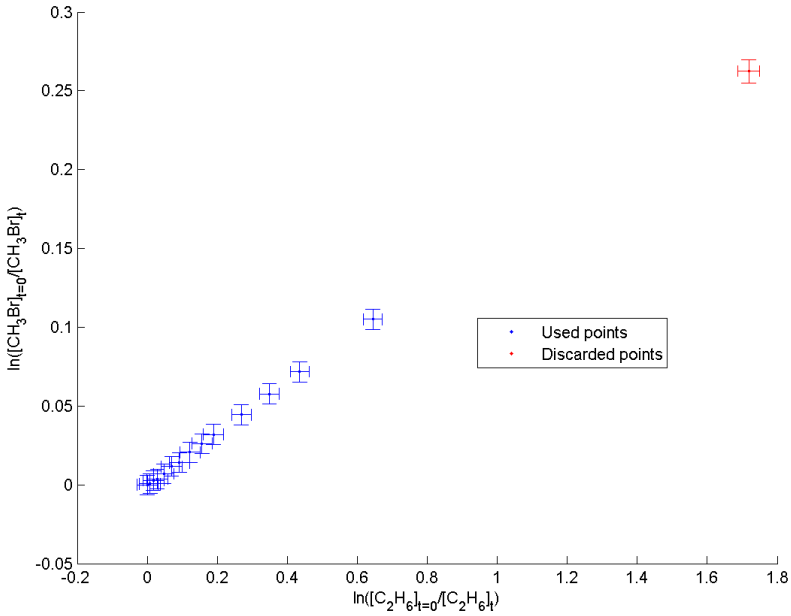

(f) Experiment 27

Figure D.3.: *Relative rate, OH experiments, continued from previous page*

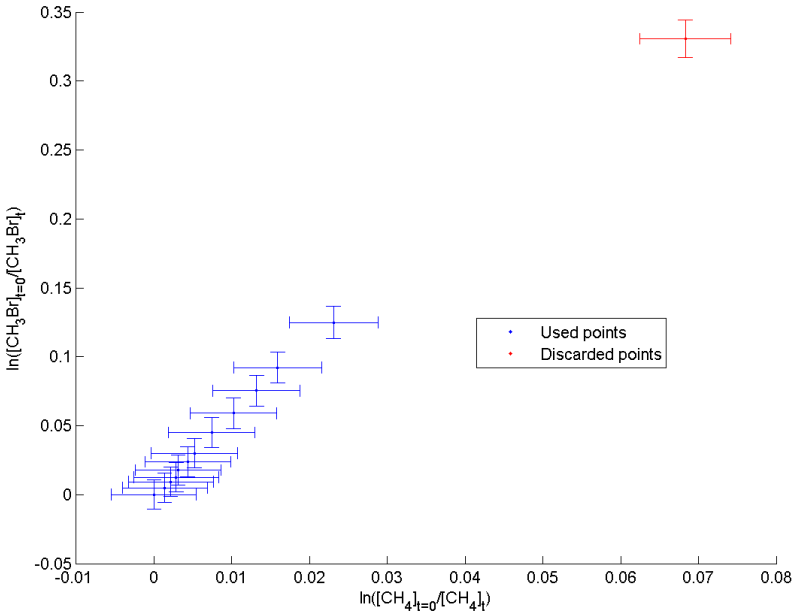

(g) Experiment 28

Figure D.3.: *Relative rate, OH experiments, continued from previous page*

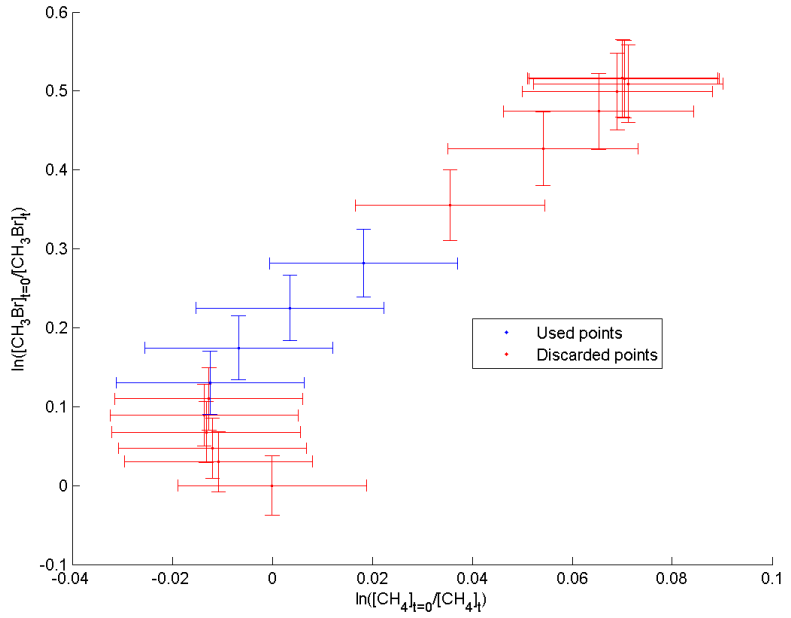

(a) Experiment 9

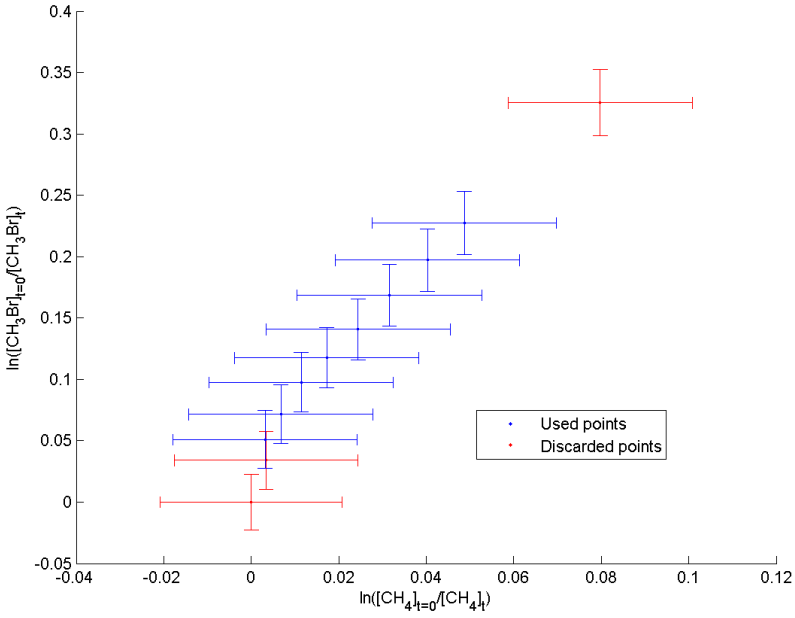

(b) Experiment 10

Figure D.4.: *Relative rate, $O(^1D)$ experiments*

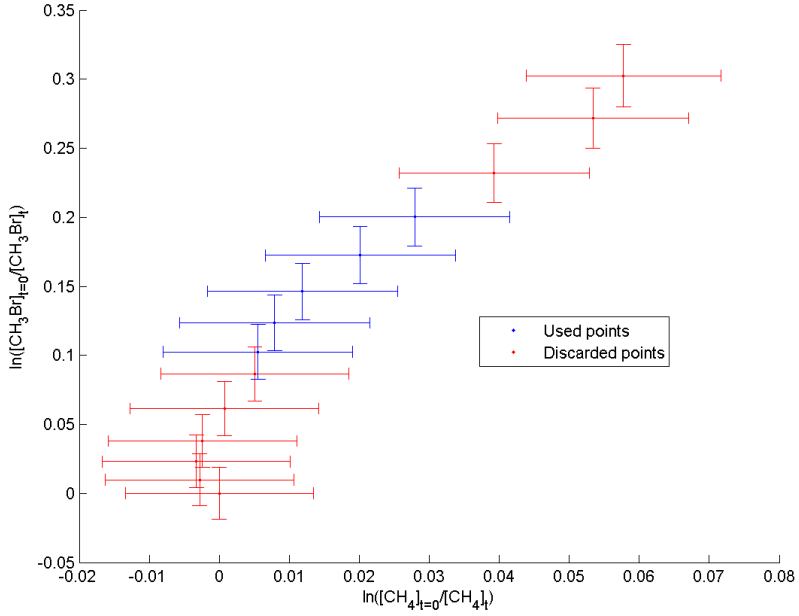

(c) Experiment 12

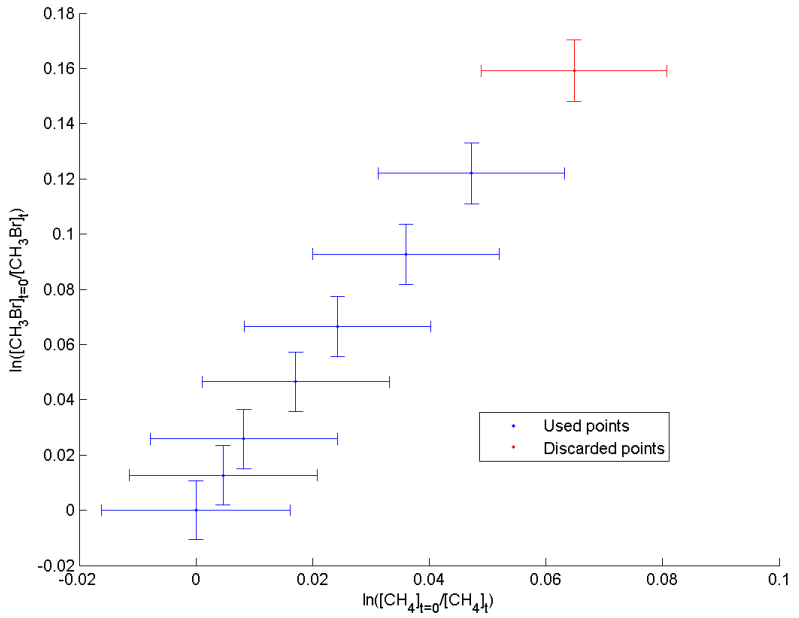

(d) Experiment 29

Figure D.4.: *Relative rate, $O(^1D)$ experiments, continued from previous page*

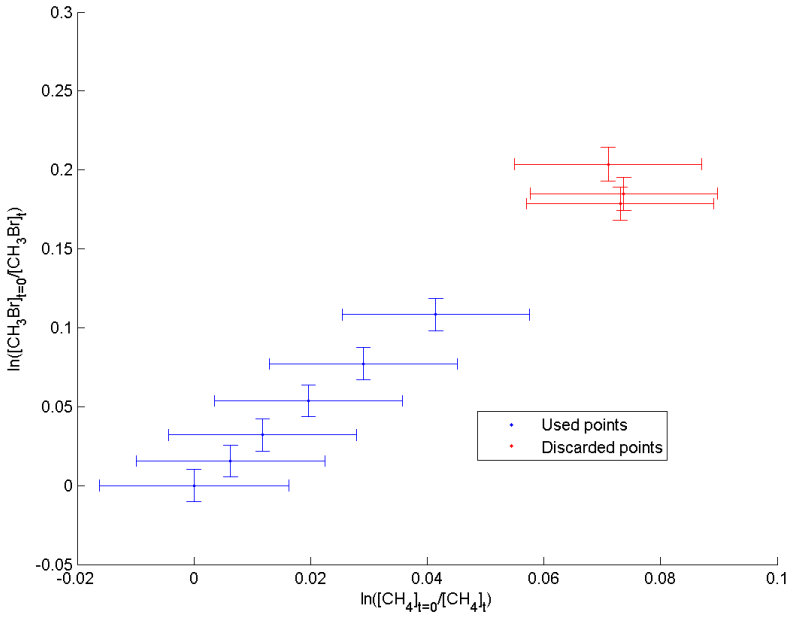

(e) Experiment 30

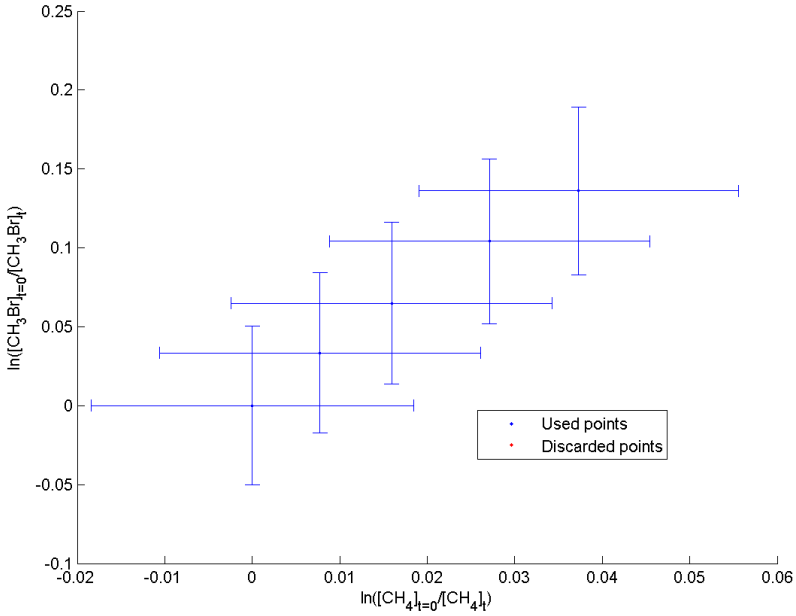

(f) Experiment 31

Figure D.4.: *Relative rate, O(^{1}D) experiments, continued from previous page*

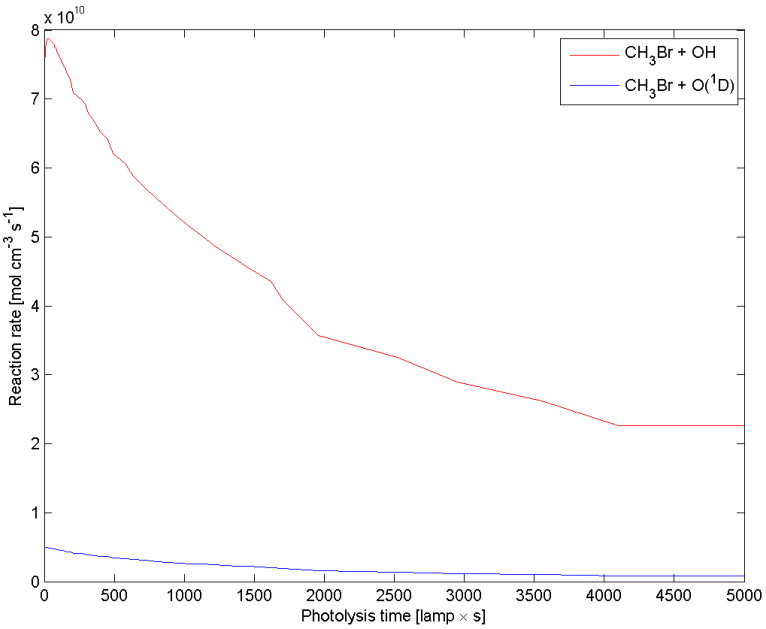

(a) Experiment 25

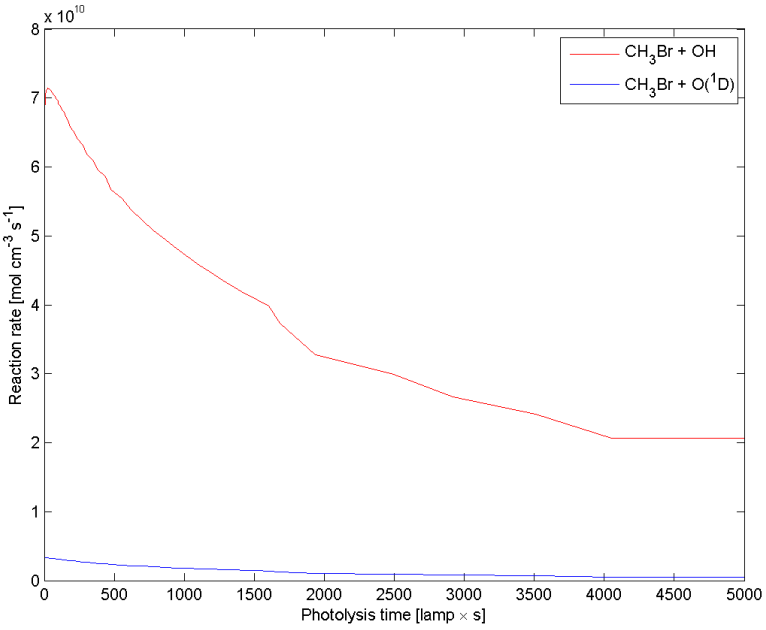

(b) Experiment 28

Figure D.5.: *$CH_3Br + OH \longrightarrow$ products versus $CH_3Br + O(^1D) \longrightarrow$ products rates, OH experiments, $k_{(\mathrm{R}\,3)}$ used in the model are taken from Sander et al. (2006)*

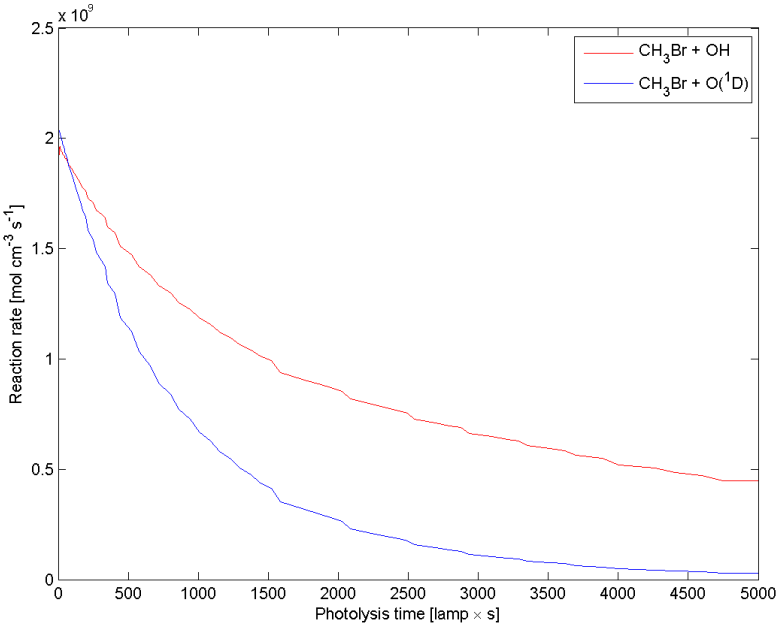

(a) Experiment 9

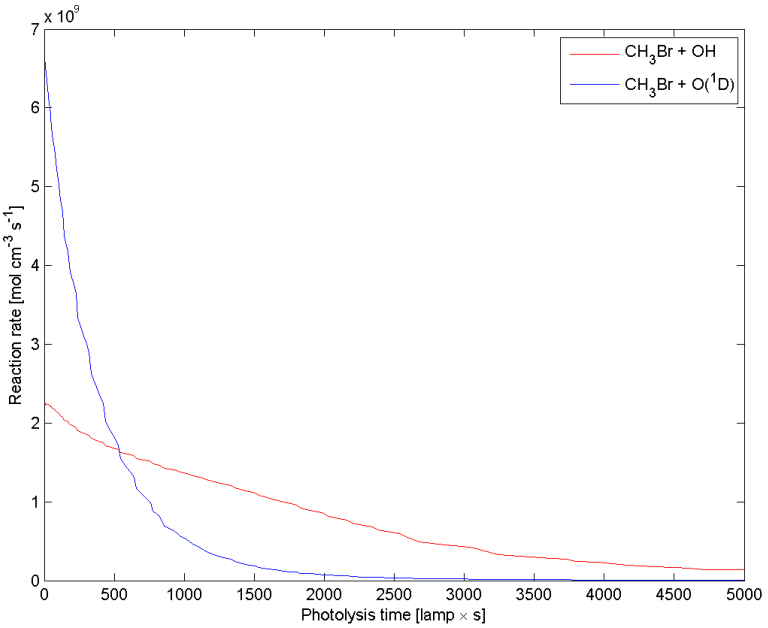

(b) Experiment 10

Figure D.6.: *$CH_3Br + OH \longrightarrow$ products versus $CH_3Br + O(^1D) \longrightarrow$ products rates, $O(^1D)$ experiments, $k_{(\mathrm{R}\,3)}$ used in the model are taken from Sander et al. (2006)*

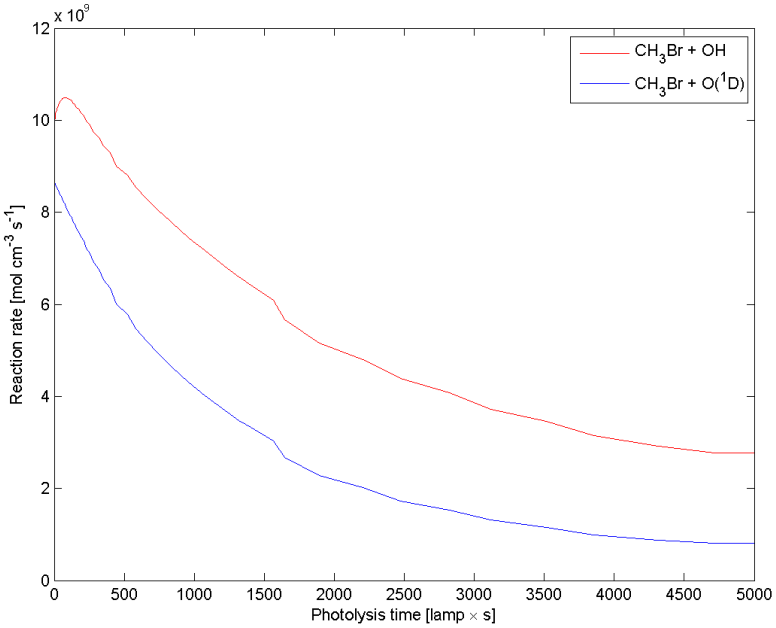

(c) Experiment 12

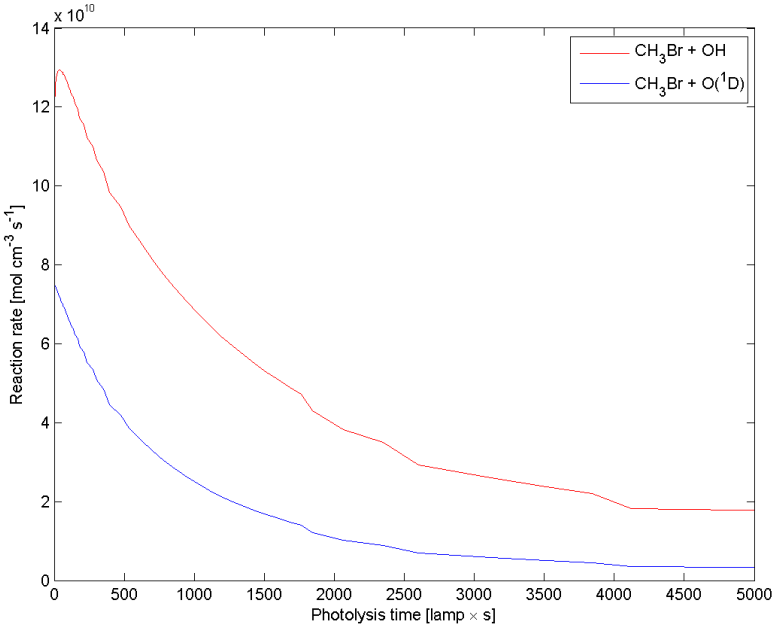

(d) Experiment 29

Figure D.6.: *OH versus O(^{1}D) chemistry, O(^{1}D) experiments, continued from previous page*

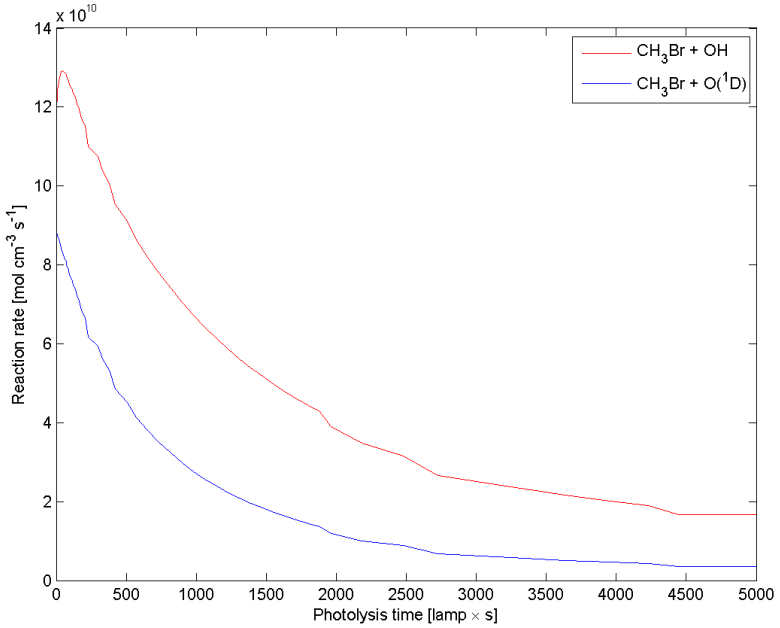

(e) Experiment 30

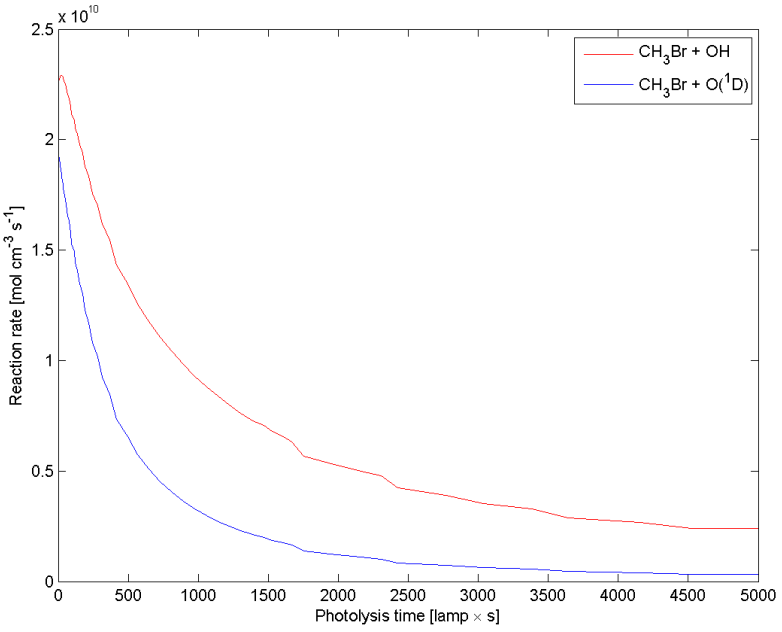

(f) Experiment 31

Figure D.6.: *OH versus O(^{1}D) chemistry, O(^{1}D) experiments, continued from previous page*

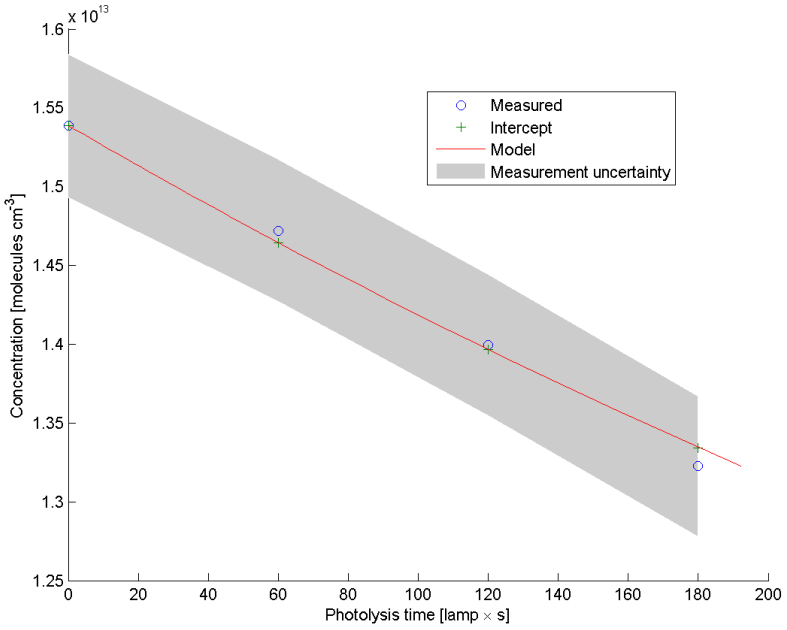

(a) CH_3Br

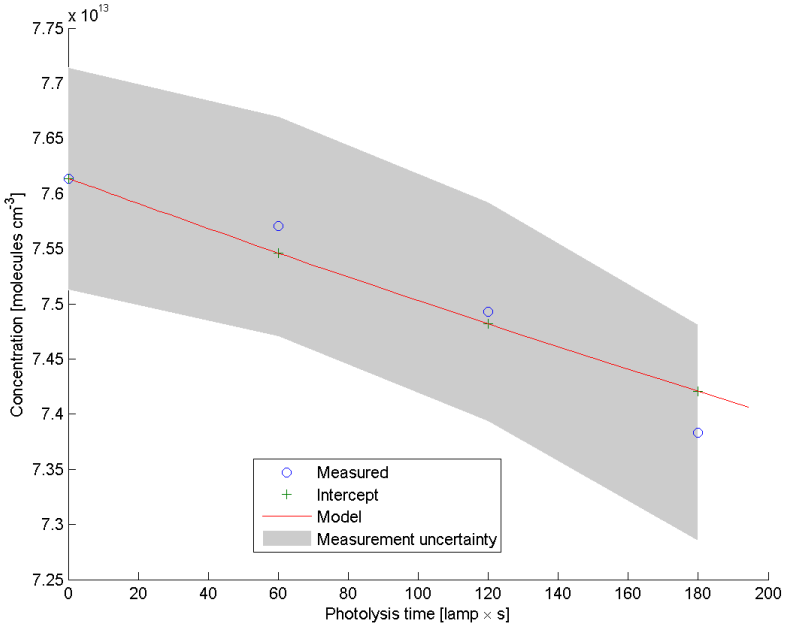

(b) CH_4

Figure D.7.: *Model and measured results, experiment 9, uncorrected data*

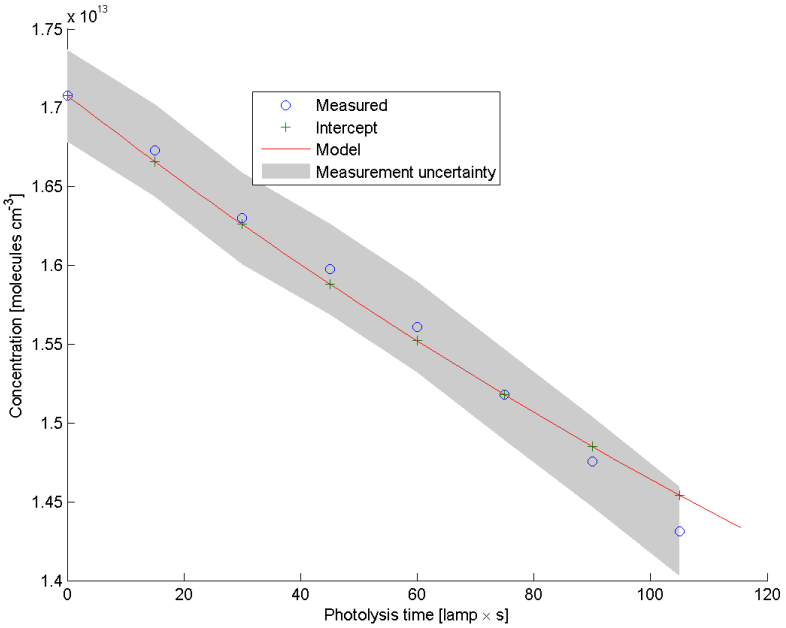

(a) CH_3Br

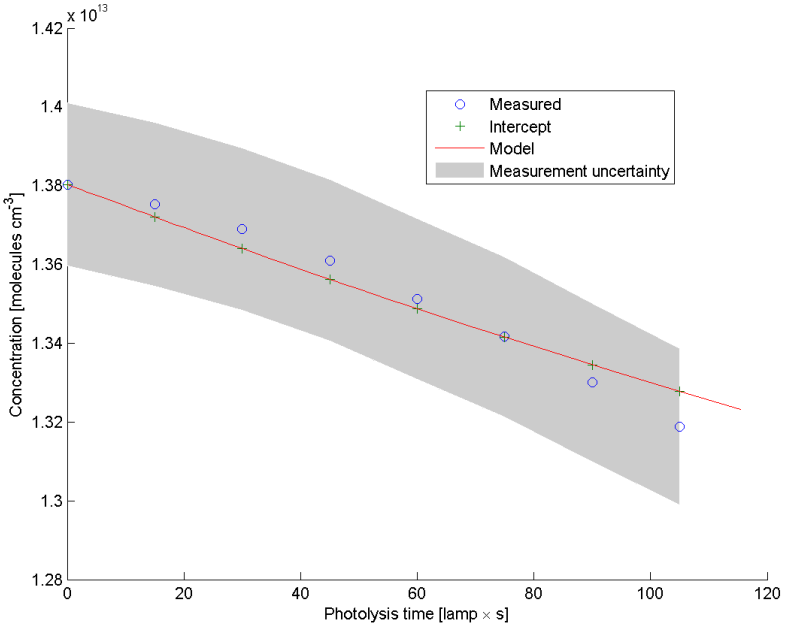

(b) CH_4

Figure D.8.: *Model and measured results, experiment 10, uncorrected data*

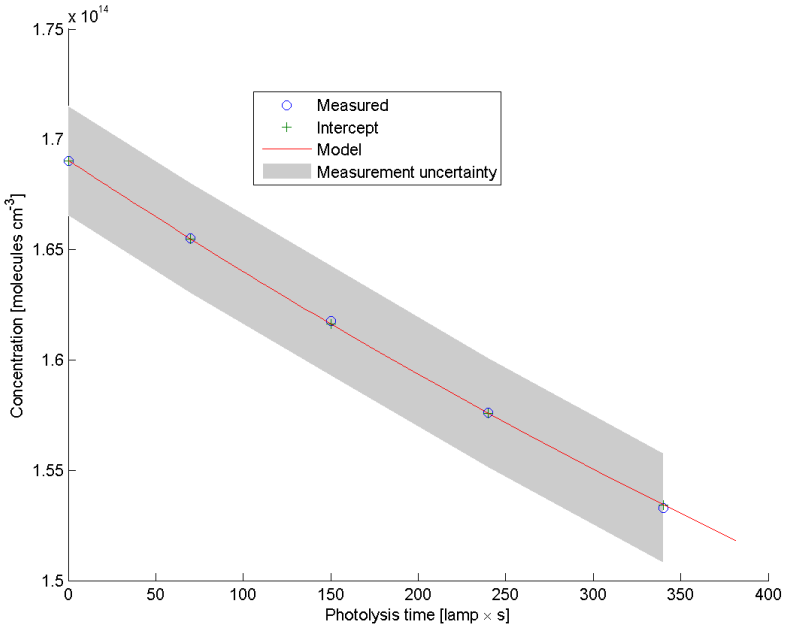

(a) CH_3Br

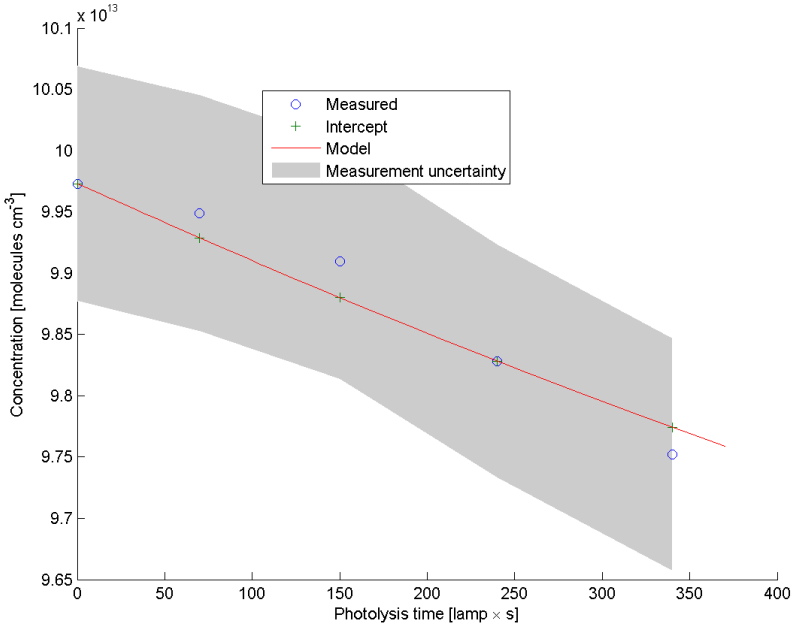

(b) CH_4

Figure D.9.: *Model and measured results, experiment 12, uncorrected data*

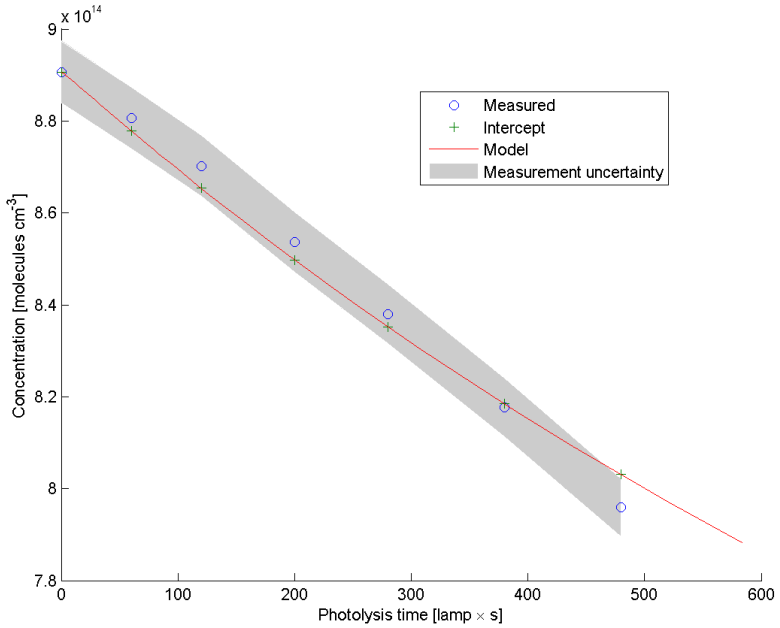

(a) CH_3Br

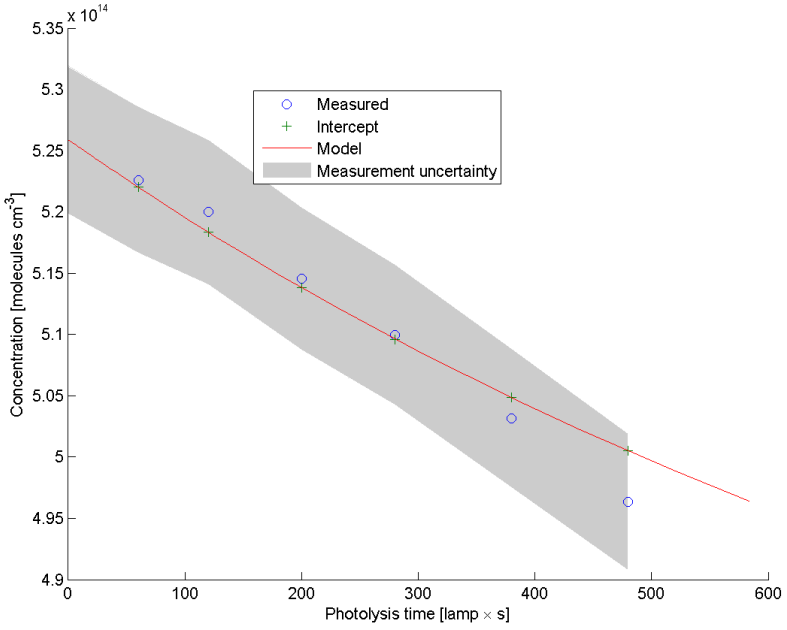

(b) CH_4

Figure D.10.: *Model and measured results, experiment 29, corrected data*

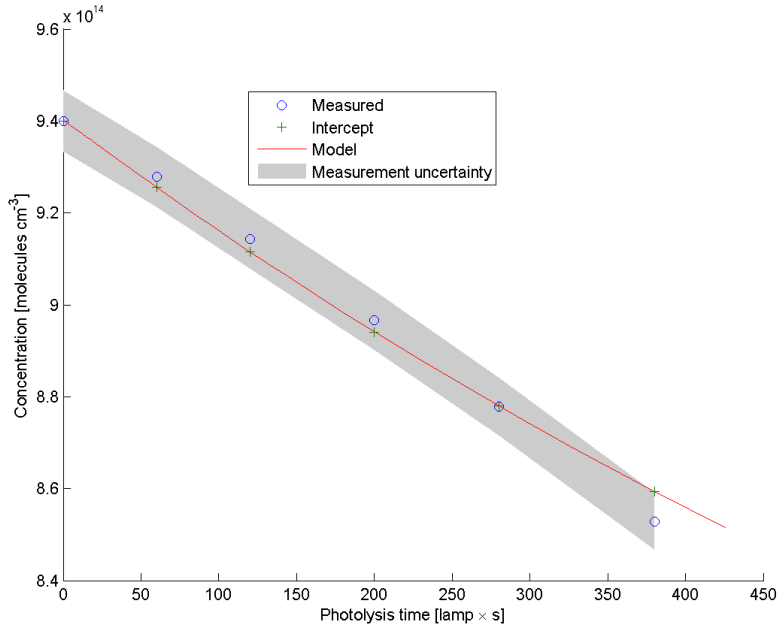

(a) CH_3Br

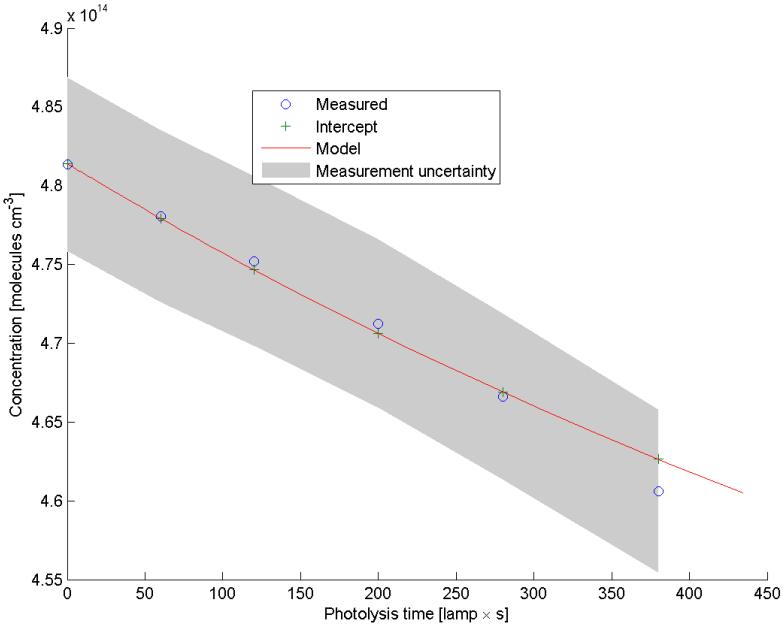

(b) CH_4

Figure D.11.: *Model and measured results, corrected data, experiment 30*

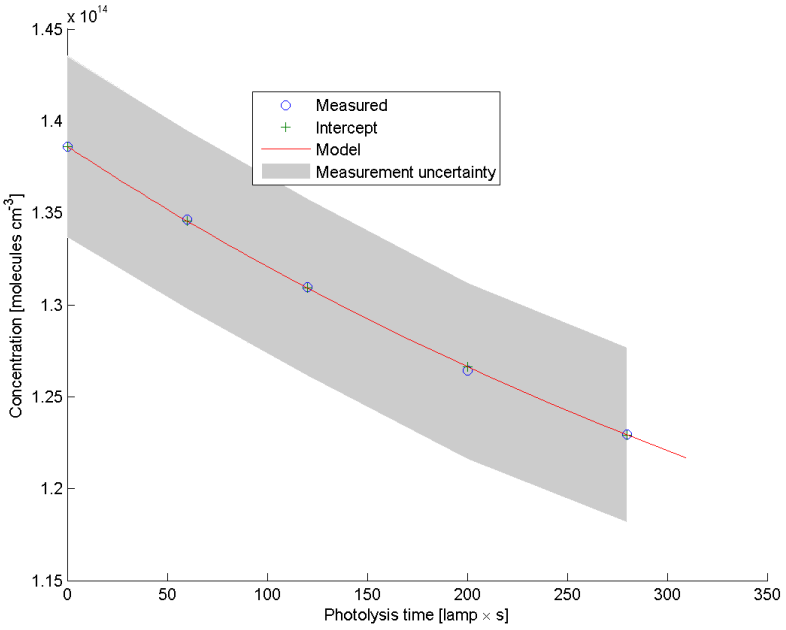

(a) CH_3Br

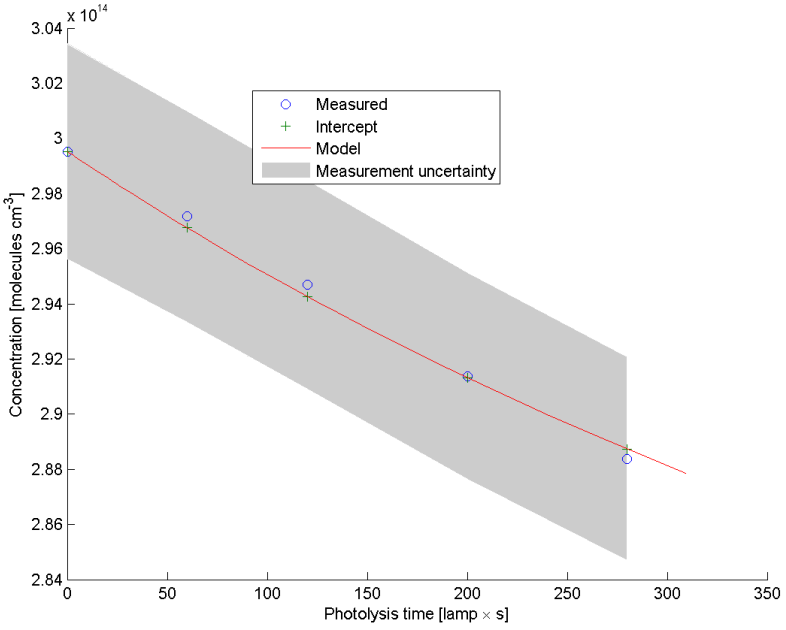

(b) CH_4

Figure D.12.: *Model and measured results, experiment 31, corrected data*

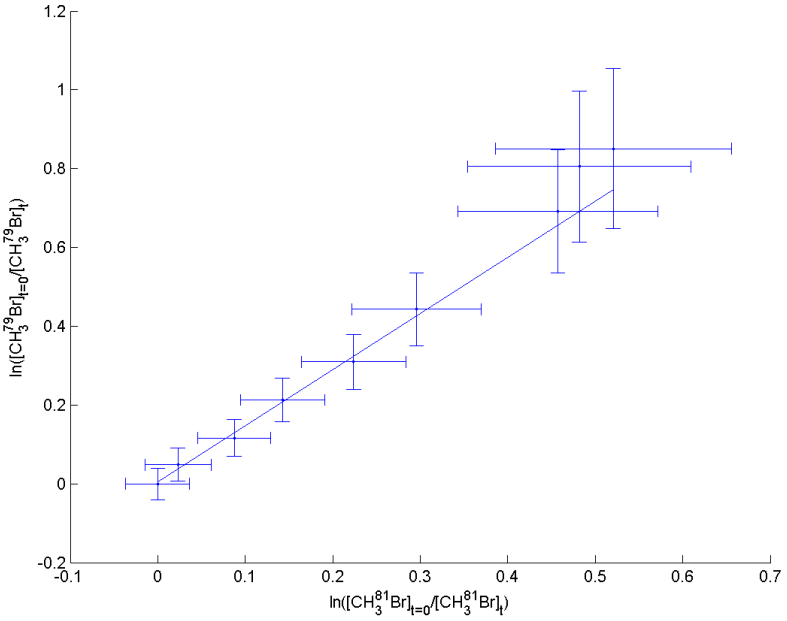

(a) Experiment 7

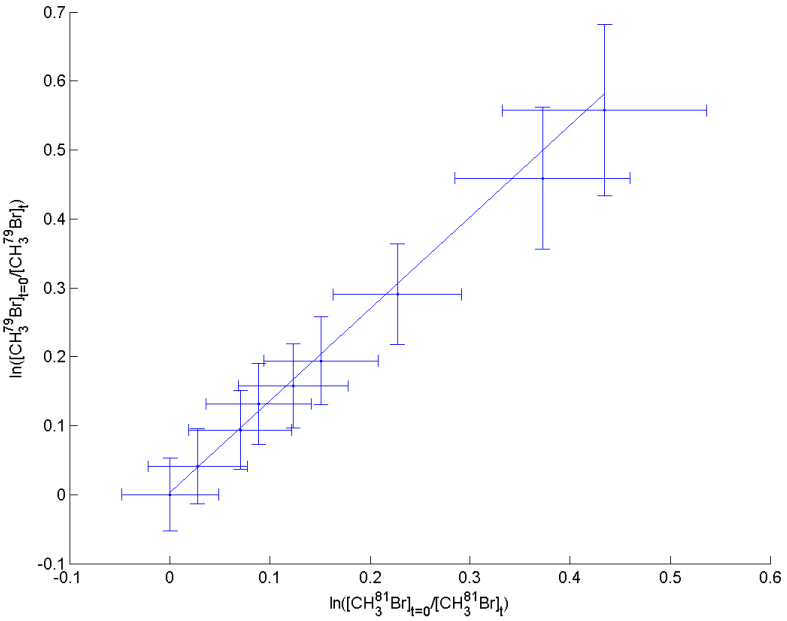

(b) Experiment 8

Figure D.13.: *Kinetic Isotope Effect, OH experiments*

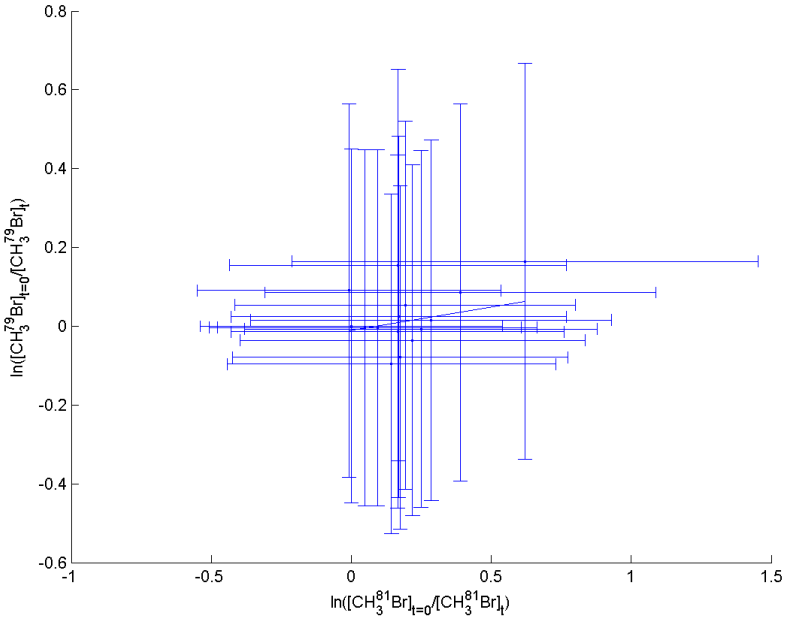

(c) Experiment 11

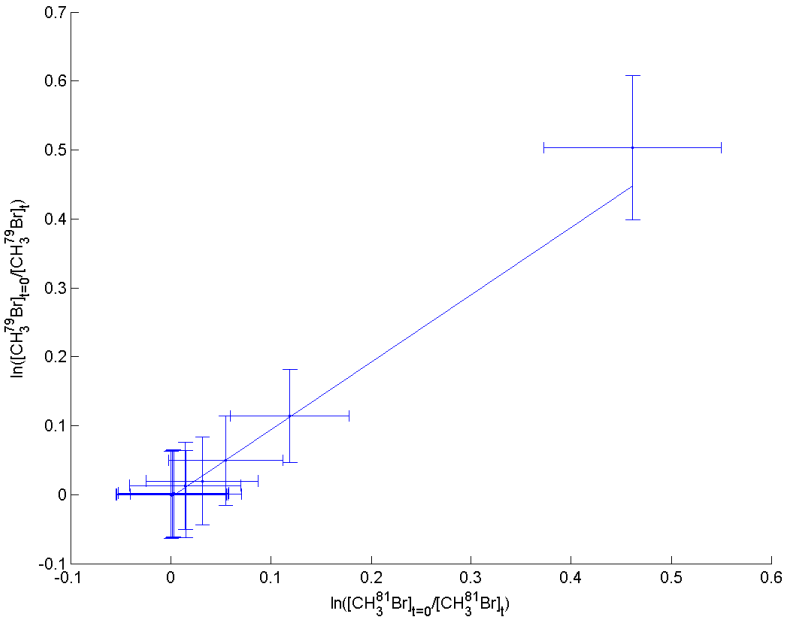

(d) Experiment 25

Figure D.13.: *Kinetic Isotope Effect, OH experiments, continued from previous page*

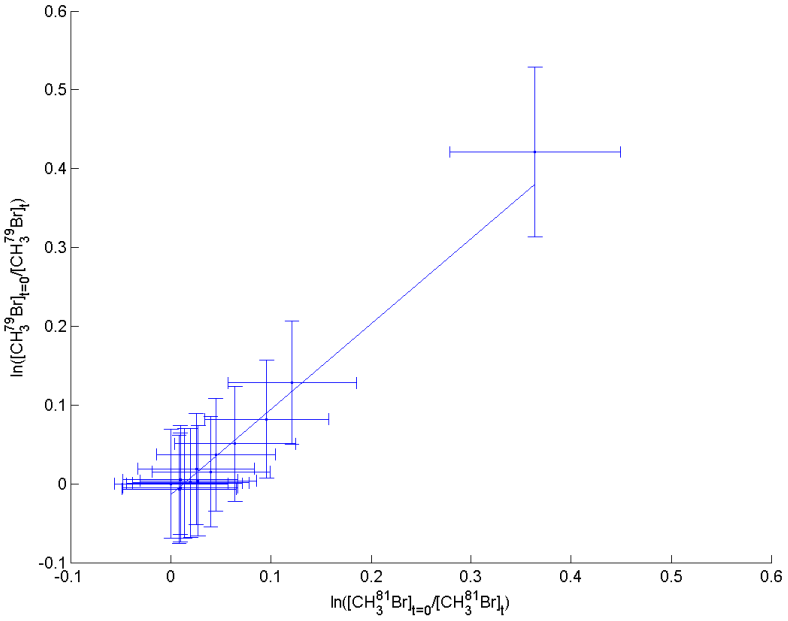

(e) Experiment 26

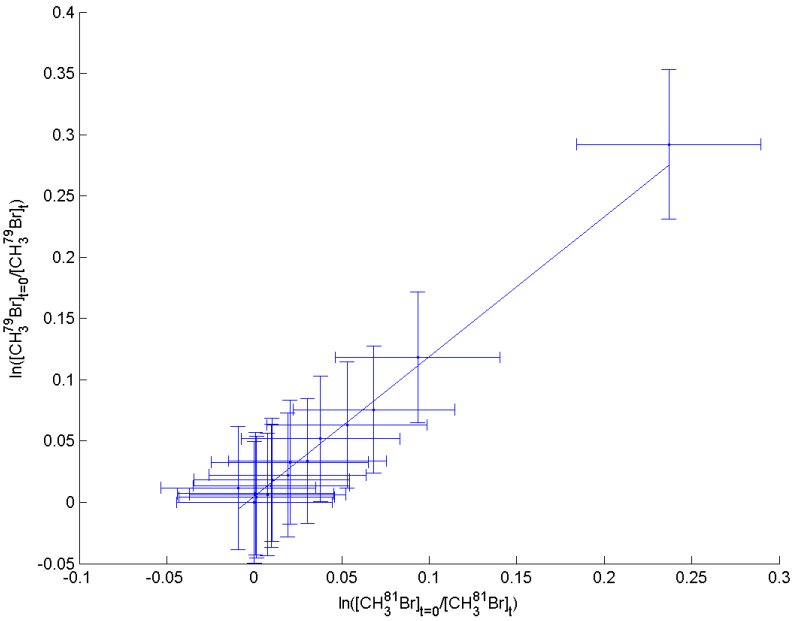

(f) Experiment 27

Figure D.13.: *Kinetic Isotope Effect, OH experiments, continued from previous page*

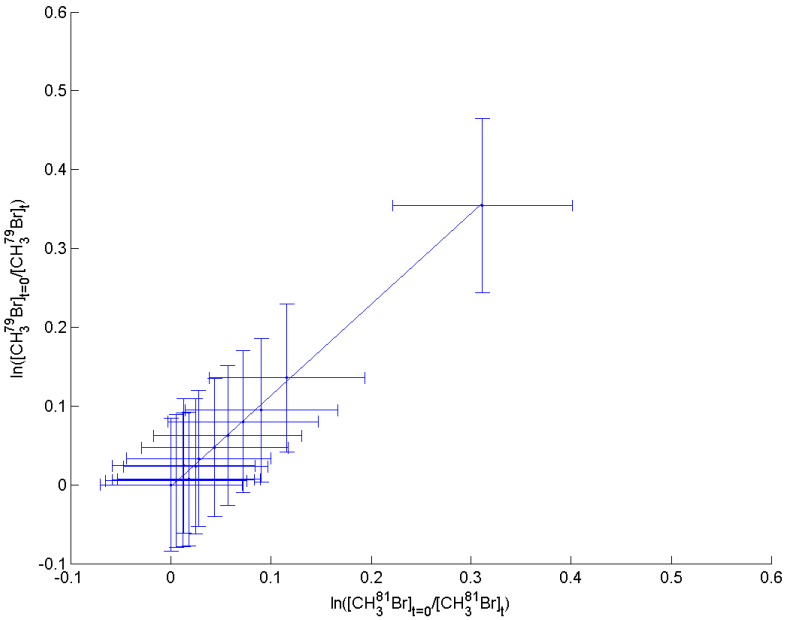

(g) Experiment 28

Figure D.13.: *Kinetic Isotope Effect, OH experiments, continued from previous page*

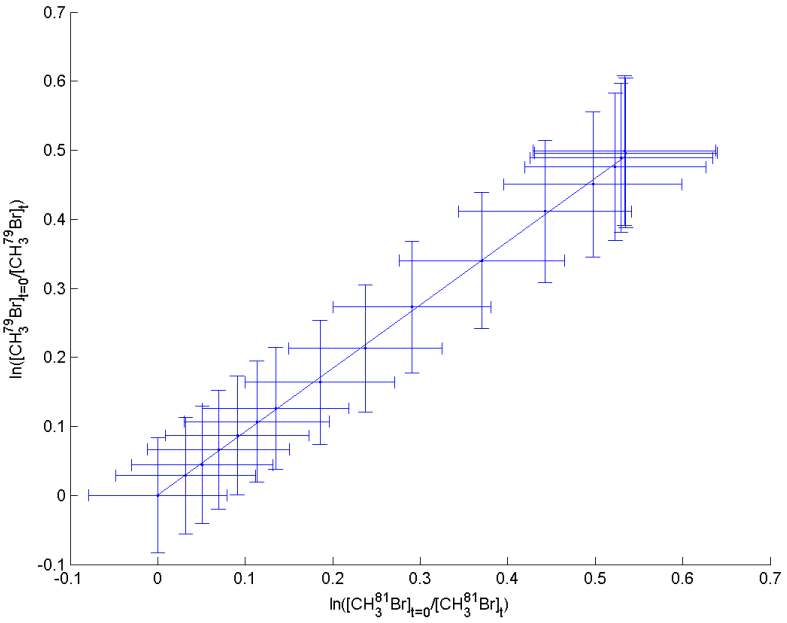

(a) Experiment 9

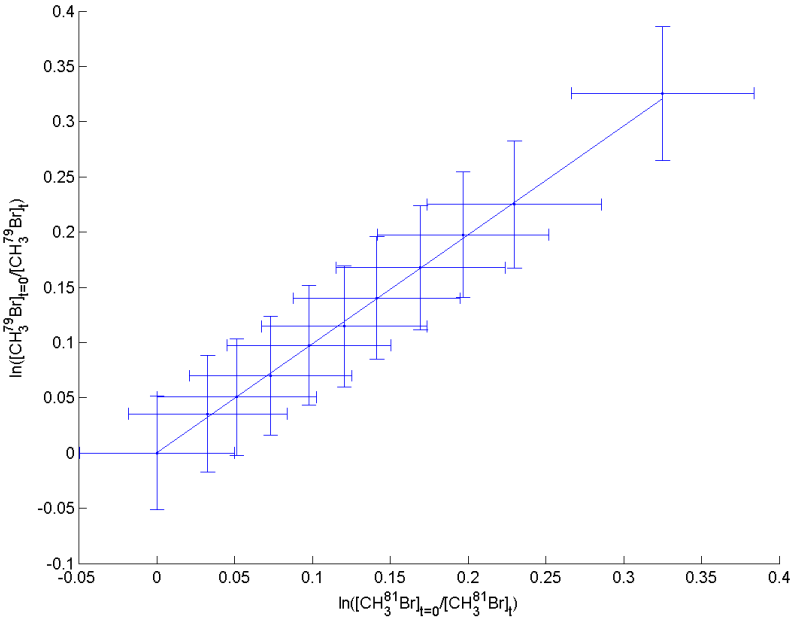

(b) Experiment 10

Figure D.14.: *Kinetic Isotope Effect, $O(^1D)$ experiments*

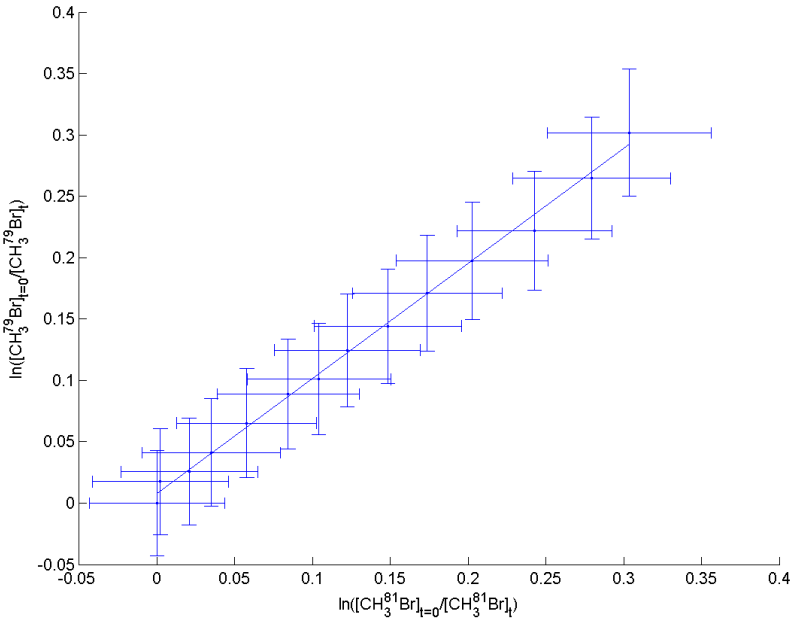

(c) Experiment 12

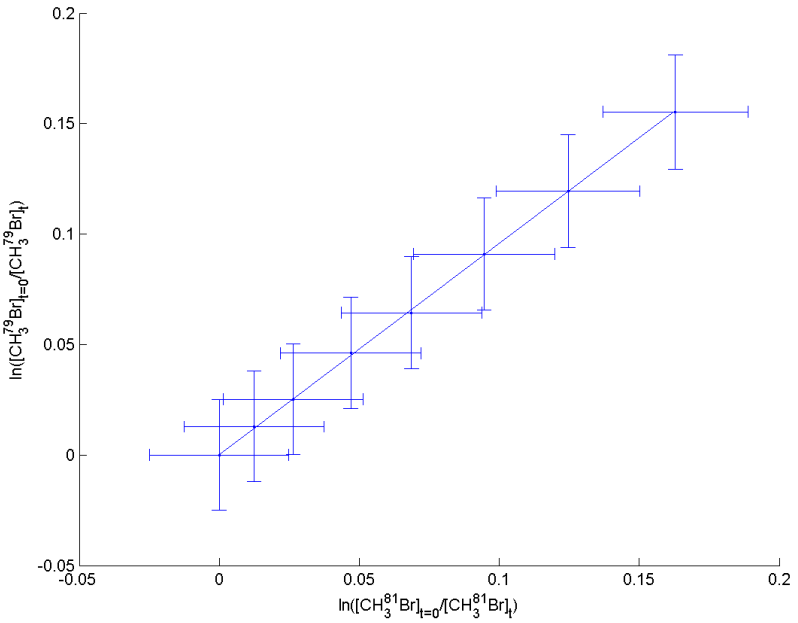

(d) Experiment 29

Figure D.14.: *Kinetic Isotope Effect, $O(^1D)$ experiments, continued from previous page*

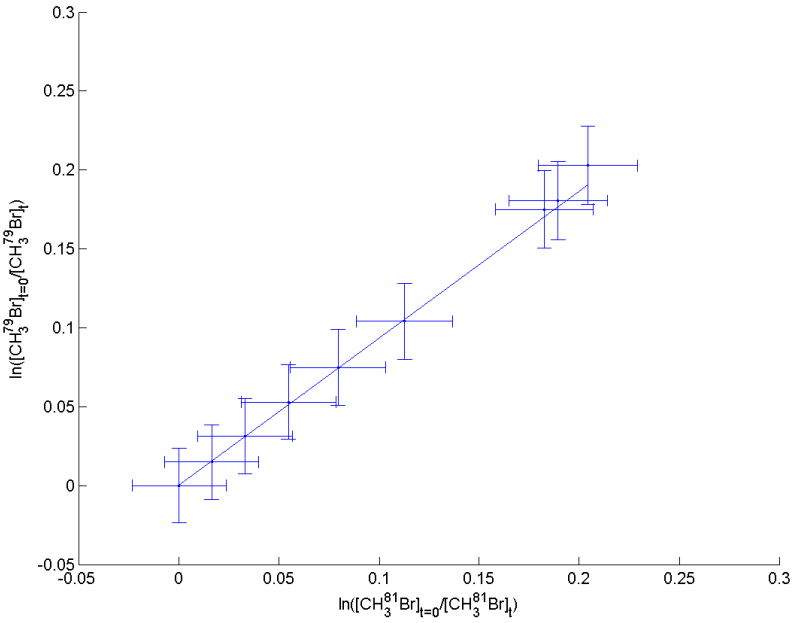

(e) Experiment 30

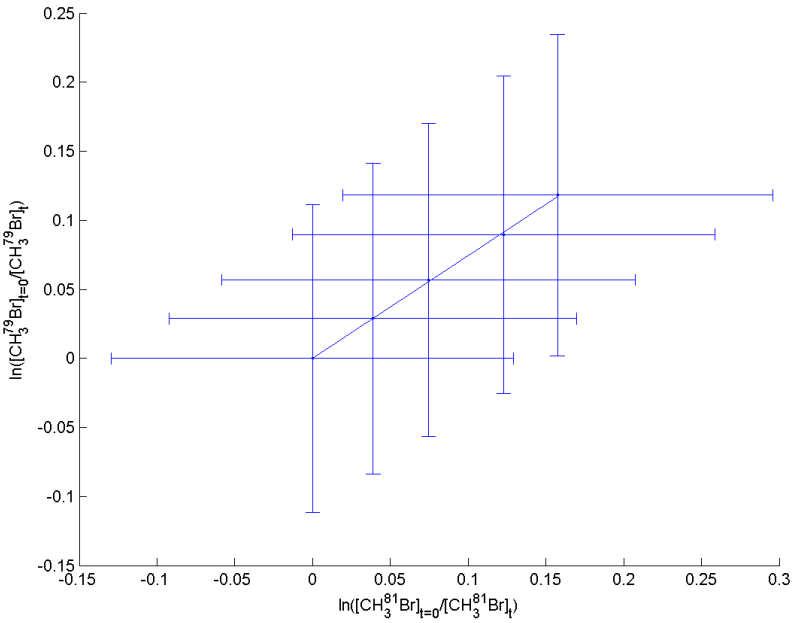

(f) Experiment 31

Figure D.14.: *Kinetic Isotope Effect, $O(^1D)$ experiments, continued from previous page*

E. Model

Table E.1.: *Model for O_x, HO_x, CO/CO_2 chemistry and oxidation of CH_4 as used in Nilsson, Andersen, Nielsen and Johnson (n.d.), units for k is as stated in the header except where noted otherwise, for references see Nilsson, Andersen, Nielsen and Johnson (n.d.)*

Number	Reaction	Rate k [$^{cm^3}/_{molecule\,s}$]
Photolysis		
1	$O_3 + h\nu \longrightarrow O(^1D) + O_2$ [1]	1 s^{-1} [2]
2	$HO_2 + h\nu \longrightarrow OH + O(^1D)$ [1]	0.04405 s^{-1} [2]
O_x chemistry		
3	$O + O_2 + M \longrightarrow O_3 + M$	$6.0 \times 10^{-34} {}^{cm^6}/_{molecule^2 s}$
4	$O + O_3 \longrightarrow O_2 + O_2$	8.0×10^{-15}
$O(^1D)$ chemistry		
5	$O(^1D) + O_2 \longrightarrow O + O_2$	3.95×10^{-11}
6	$O(^1D) + O_3 \longrightarrow O_2 + O_2$	1.2×10^{-10}
7	$O(^1D) + O_3 \longrightarrow O_2 + O + O$	1.2×10^{-10}
8	$O(^1D) + H_2O \longrightarrow OH + OH$	2.0×10^{-10}
9	$O(^1D) + N_2 \longrightarrow O + N_2$	3.10×10^{-11}
10	$O(^1D) + CO_2 \longrightarrow O + CO_2$	1.10×10^{-10}
11	$O(^1D) + N_2 + M \longrightarrow N_2O + M$	$2.80 \times 10^{-36} {}^{cm^6}/_{molecule^2 s}$
12	$O(^1D) + CO \longrightarrow CO_2$	8.00×10^{-11}
13	$O(^1D) + CO \longrightarrow O + CO$	5.80×10^{-11}
HO_x chemistry		
14	$O + OH \longrightarrow O_2 + H$	3.50×10^{-11}
15	$O + HO_2 \longrightarrow OH + O_2$	5.9×10^{-11}
16	$O + H_2O_2 \longrightarrow OH + HO_2$	1.70×10^{-15}
17	$H + O_2 + M \longrightarrow HO_2 + M$	$5.50 \times 10^{-32} {}^{cm^6}/_{molecule^2 s}$
18	$H + O_3 \longrightarrow OH + O_2$	2.9×10^{-11}
19	$OH + O_3 \longrightarrow HO_2 + O_2$	7.3×10^{-14}
20	$OH + OH \longrightarrow H_2O + O$	1.48×10^{-12}

Continued on next page

[1] The photonlysis reactions are run by a fictive molecule representing the photon ($h\nu$), in the model the molecule appears on both sides of the reactions to simulate the constant radiation from the lamps

[2] The photlysis rate is not controlled by the reaction rate parameter, but rather the concentration of a fictive molecule representing the photon, photolysis rates are thus expressed as multiples of the reference reaction $O_3 + h\nu \longrightarrow O(^1D) + O_2$

Table E.1 – *continued from previous page*

Number	Reaction	Rate k [$^{cm^3}/_{molecule\,s}$]
21	$OH + OH + M \longrightarrow H_2O_2 + M$	$6.90 \times 10^{-31} {}^{cm^6}/_{molecule^2 s}$
22	$OH + HO_2 \longrightarrow H_2O + O_2$	1.1×10^{-10}
23	$OH + H_2O_2 \longrightarrow H_2O + HO_2$	1.8×10^{-12}
24	$HO_2 + O_3 \longrightarrow OH + O_2 + O_2$	1.9×10^{-15}
25	$HO_2 + HO_2 \longrightarrow H_2O_2 + O_2$	1.4×10^{-12}
26	$HO_2 + HO_2 + M \longrightarrow H_2O_2 + O_2 + M$	$4.90 \times 10^{-32} {}^{cm^6}/_{molecule^2 s}$
CO/CO_2 chemistry		
27	$HCO + O_2 \longrightarrow CO + HO_2$	5.2×10^{-12}
28	$OH + CO + M \longrightarrow HOCO + M$	$3.43 \times 10^{-33} {}^{cm^6}/_{molecule^2 s}$
29	$O_2 + HOCO \longrightarrow HO_2 + CO_2$	2.09×10^{-12}
30	$OH + CO \longrightarrow CO_2 + H$	1.5×10^{-13}
31	$HCO + HO_2 \longrightarrow CO + OH + OH$	5.0×10^{-11}
32	$HCO + O \longrightarrow CO_2 + H$	5.0×10^{-11}
33	$CO + O + M \longrightarrow CO_2 + M$	$1.7 \times 10^{-33} {}^{cm^6}/_{molecule^2 s}$
Oxidation of CH_4 by OH and $O(^1D)$, and its reaction products		
34	$CH_4 + O(^1D) \longrightarrow CH_3 + OH$	1.31×10^{-10}
35	$CH_4 + O(^1D) \longrightarrow CH_3O + H$	1.75×10^{-11}
36	$CH_4 + O(^1D) \longrightarrow CH_2OH + H$	1.75×10^{-11}
37	$CH_4 + O(^1D) \longrightarrow HCHO + H_2$	9.00×10^{-12}
38	$CH_4 + OH \longrightarrow CH_3 + H_2O$	6.3×10^{-15}
39	$CH_3 + O_2 + M \longrightarrow CH_3O_2 + M$	$4.00 \times 10^{-31} {}^{cm^6}/_{molecule^2 s}$
40	$CH_3O_2 + HO_2 \longrightarrow CH_3OOH + O_2$	4.68×10^{-12}
41	$CH_3O_2 + HO_2 \longrightarrow HCHO + H_2O + O_2$	5.2×10^{-13}
42	$CH_3O + O_2 \longrightarrow HCHO + HO_2$	1.9×10^{-15}
43	$OH + CH_3OOH \longrightarrow CH_3O_2 + H_2O$	6.00×10^{-12}
44	$OH + CH_3OOH \longrightarrow CH_2OOH + H_2O$	4.00×10^{-12}
45	$CH_3 + O_3 \longrightarrow CH_3O + O_2$	2.6×10^{-12}
46	$CH_3O_2 + O_3 \longrightarrow CH_3O + O_2 + O_2$	1.00×10^{-17}
47	$CH_3O_2 + O \longrightarrow CH_3O + O_2$	4.30×10^{-11}
48	$OH + HCHO \longrightarrow H_2O + HCO$	8.50×10^{-12}
49	$O + HCHO \longrightarrow OH + HCO$	1.6×10^{-13}
50	$HO_2 + HCHO \longrightarrow HOCH_2O_2$	5.00×10^{-14}
51	$CH_2OOH \longrightarrow HCHO + OH$	5.00×10^{4}
52	$HOCH_2O_2 + HO_2 \longrightarrow HOCH_2OOH + O_2$	6.00×10^{-12}
53	$HOCH_2O_2 + HO_2 \longrightarrow HOCH_2O + OH + O_2$	2.40×10^{-12}
54	$HOCH_2O_2 + HO_2 \longrightarrow HCOOH + H_2O + O_2$	3.60×10^{-12}
55	$CH_2OH + O_2 \longrightarrow HCHO + HO_2$	9.1×10^{-12}
56	$HOCH_2O_2 \longrightarrow HO_2 + HCHO$	1.5×10^{2}

Table E.2.: *Model, oxidation of* CH_3Br *by* OH *and* $O(^1D)$ *and its reaction products, added for the current work, units for k is as stated in the header except where noted otherwise*

Number	Reaction	Rate k $[^{cm^3}/_{molecule\,s}]$
57	$CH_3Br + OH \longrightarrow H_2O + CH_2Br$	3.75×10^{-14} [a]
58	$CH_3Br + O(^1D) \longrightarrow CH_3 + BrO$	7.88×10^{-11} [b] [c]
59	$CH_3Br + O(^1D) \longrightarrow CH_2Br + OH$	1.00×10^{-10} [d]
60	$CH_3Br + O(^3P) \longrightarrow OH + CH_2Br$	1.36×10^{-16} [e]
61	$CH_2Br + O_2 + M \longrightarrow$ $\longrightarrow CH_2BrO_2 + M$	$1.24 \times 10^{-30} {}^{cm^6}/_{molecule^2 s}$ [f]
62	$BrO + O \longrightarrow BrO_2$	5.0×10^{-11} [g]
63	$BrO + O \longrightarrow O_2 + Br$	4.1×10^{-11} [h]
64	$BrO + BrO \longrightarrow Br + BrO_2$	2.09×10^{-12} [i]
65	$BrO + BrO \longrightarrow O_2 + Br + Br$	2.7×10^{-12} [h]
66	$BrO + BrO \longrightarrow Br_2 + O_2$	4.8×10^{-13} [h]
68	$BrO + HO_2 \longrightarrow HOBr + O_2$	2.1×10^{-11} [j]
69	$BrO + CH_3O \longrightarrow HCHO + HOBr$	3.8×10^{-11} [k]
70	$BrO + OH \longrightarrow Br + HO_2$	3.90×10^{-11} [j]
71	$Br + O_3 \longrightarrow O_2 + BrO$	1.2×10^{-12} [j]
72	$BrO_2 + O \longrightarrow O_2 + BrO$	4.25×10^{-12} [g]
73	$HOBr + O \longrightarrow OH + BrO$	2.8×10^{-11} [h]
74	$Br_2 + O \longrightarrow Br + BrO$	1.4×10^{-11} [h]
75	$CH_2BrO_2 + CH_2BrO_2 \longrightarrow$ $\longrightarrow CH_2BrO + CH_2BrO + O_2$	3.3×10^{-11} [h]
76	$CH_2BrO_2 + CH_2BrO_2 \longrightarrow$ $\longrightarrow CH_2BrO_2CH_2Br + O_2$	3.3×10^{-11} [h]
77	$CH_2BrO_2 + HO_2 \longrightarrow$ $\longrightarrow CH_2BrO + OH + O_2$	4.16×10^{-13} [m] [h]
78	$CH_2BrO \longrightarrow HCHO + Br$	8.095×10^{7} [n]

[a] Present work
[b] Thompson and Ravishankara (1993)
[c] Cronkhite and Wine (1998)
[d] Based on estimation $k_{59} = k_{(R\,3)} - k_{58}, k_{(R\,3)}$ taken from Thompson and Ravishankara (1993)
[e] Zhang et al. (2002)
[f] Eskola et al. (2006)
[g] Butkovskaya et al. (1983)
[h] Atkinson et al. (2006)
[i] Papayannis et al. (1999)
[j] Sander et al. (2006)
[k] Aranda et al. (1998)
[l] Li et al. (2002)
[m] McGivern et al. (2004)
[n] Drougas and Kosmas (2004)